DETECTION OF PORCINE UMBILICAL CORD MATRIX STEM CELLS IN THE INTESTINE AND OTHER ORGANS AFTER ORAL AND INTRAPERITONEAL ADMINISTRATION TO ALLOGENEIC RECIPIENTS

by

KREESON PACKTHONGSUK

D.V.M., Kasetsart University, Bangkok, Thailand, 2002
M.Sc., Kasetsart University, Bangkok, Thailand, 2002

AN ABSTRACT OF A DISSERTATION

submitted in partial fulfillment of the requirements for the degree

DOCTOR OF PHILOSOPHY

Department of Animal Sciences and Industry
College of Agriculture

KANSAS STATE UNIVERSITY
Manhattan, Kansas

2013

Abstract

Umbilical cords matrix stem cells (UCs) have been characterized most thoroughly in humans (HUCs) and are considered to have great promise for regenerative medicine and cell-based therapy. Although UCs were first identified in pigs the description of porcine UCs (PUCs) is limited. Here we reported some standard mesenchymal stem cell characteristics for PUCs. Development of knowledge about PUCs is useful because the pig is a valuable biomedical model for humans and the species is an important human food source. PUCs were isolated from Wharton's jelly using an explant technique. They attached on the plastic and showed fibroblast-like morphology. Immunophenotype analysis showed they are positive for CD44, CD90 and CD105 and negative for CD31, CD45 and SLA-DR. Under specific in vitro conditions, PUCs were differentiated to adipocytes, chondrocytes and osteocytes. The growth curve of PUCs exhibited a lag phase, log phase and doubling time of 24, 60 and 13.8 hour respectively.

Engraftment potential of allogeneic PUCs administered orally and intraperitoneally (IP) was evaluated. Newborn, 1-day, 1-week, 2-week and 3-week old pigs were administered a dose of fluorescently labeled PUCs ($1.1x10^7$ cells/kg body weight) and their tissue incorporation were evaluated using confocal microscopy with confirmation by PCR to detect SRY gene, the Y-chromosome gene of male PUCs in female recipients. One week after PUCs administration, they were found mostly in the gastrointestinal tract and abdominal organs after either oral or intraperitoneal transplantation. The intestinal mucosa layer around the base of villi and intestinal crypts was the main location. PUCs were also detected in thoracic organs, muscle and bone marrow. Additionally, PKH26-labeled fibroblasts labeled were detected in recipient intestine 1 week after IP injection. Donor cells were not found in blood at one week post transplantation. When recipients were sacrificed at 6 h after IP injection PKH26-labeled PUCs were found mostly in omentum and diaphragm by PCR. It is likely these are the primary sites for donor cells in the peritoneal cavity to enter the circulation. Fluorescent in situ hybridization (FISH), using an SRY probe and PCR, demonstrated the PUCs isolated from recipient intestines by enzymatic digestion. Therefore, transplanted PUCs were recovered from the intestinal mucosa and were viable and able to proliferate in vitro.

DETECTION OF PORCINE UMBILICAL CORD MATRIX STEM CELLS IN THE INTESTINE AND OTHER ORGANS AFTER ORAL AND INTRAPERITONEAL ADMINISTRATION TO ALLOGENEIC RECIPIENTS

by

KREESON PACKTHONGSUK

D.V.M., Kasetsart University, Bangkok, Thailand, 2002
M.Sc., Kasetsart University, Bangkok, Thailand, 2002

A DISSERTATION

submitted in partial fulfillment of the requirements for the degree

DOCTOR OF PHILOSOPHY

Department of Animal Sciences and Industry
College of Agriculture

KANSAS STATE UNIVERSITY
Manhattan, Kansas

2013

Approved by:

Major Professor
Duane Davis

Copyright

Abstract

Umbilical cords matrix stem cells (UCs) have been characterized most thoroughly in humans (HUCs) and are considered to have great promise for regenerative medicine and cell-based therapy. Although UCs were first identified in pigs the description of porcine UCs (PUCs) is limited. Here we reported some standard mesenchymal stem cell characteristics for PUCs. Development of knowledge about PUCs is useful because the pig is a valuable biomedical model for humans and the species is an important human food source. PUCs were isolated from Wharton's jelly using an explant technique. They attached on the plastic and showed fibroblast-like morphology. Immunophenotype analysis showed they are positive for CD44, CD90 and CD105 and negative for CD31, CD45 and SLA-DR. Under specific in vitro conditions, PUCs were differentiated to adipocytes, chondrocytes and osteocytes. The growth curve of PUCs exhibited a lag phase, log phase and doubling time of 24, 60 and 13.8 hour respectively.

Engraftment potential of allogeneic PUCs administered orally and intraperitoneally (IP) was evaluated. Newborn, 1-day, 1-week, 2-week and 3-week old pigs were administered a dose of fluorescently labeled PUCs ($1.1x10^7$ cells/kg body weight) and their tissue incorporation were evaluated using confocal microscopy with confirmation by PCR to detect SRY gene, the Y-chromosome gene of male PUCs in female recipients. One week after PUCs administration, they were found mostly in the gastrointestinal tract and abdominal organs after either oral or intraperitoneal transplantation. The intestinal mucosa layer around the base of villi and intestinal crypts was the main location. PUCs were also detected in thoracic organs, muscle and bone marrow. Additionally, PKH26-labeled fibroblasts labeled were detected in recipient intestine 1 week after IP injection. Donor cells were not found in blood at one week post transplantation. When recipients were sacrificed at 6 h after IP injection PKH26-labeled PUCs were found mostly in omentum and diaphragm by PCR. It is likely these are the primary sites for donor cells in the peritoneal cavity to enter the circulation. Fluorescent in situ hybridization (FISH), using an SRY probe and PCR, demonstrated the PUCs isolated from recipient intestines by enzymatic digestion. Therefore, transplanted PUCs were recovered from the intestinal mucosa and were viable and able to proliferate in vitro.

Table of Contents

List of Figures

List of Tables

Acknowledgements

Thank you, Dr. Davis for making this possible. You have helped me to push my research in a correct direction. Thank you for your advice, continued support and friendship. I would also like to thank Dr. Deryl Troyer, Dr. Mark Weiss, Dr.Tona Melgarejo and Dr. Ernest Minton for sharing their knowledge on various areas of physiology, immunology and stem cells. I also appreciate the support of the Center of Biomedical Research Excellence (COBRE) for allowing me to use their experimental tools.

Dedication

To my family; Somporn Packthongsuk, Malee Packthongsuk and Nathapan Packthongsuk for their example of support, patience, faith and love.

Chapter 1 - Literature Review

Introduction

Mesenchymal stem cells (MSCs) are multipotent cells that have the potential to differentiate into various mesodermal lineages (Bianco et al., 2001). In addition, the ability to transplant across major histocompatibility complex (MHC) barriers without the need for immune suppression makes MSCs an attractive source for cell therapy. Multiple studies have shown that MSCs suppress the proliferation of alloreactive T cells (Bartholomew et al., 2002), inhibit the differentiation and maturation of dendritic cells (Jiang et al., 2005), and decrease the production of inflammatory cytokines by immune cells (Aggarwal and Pittenger, 2005). Immunosuppressive properties of MSCs have been used in treatments for acute refractory graft-versus host disease (GVHD) following allogeneic hematopoietic stem cells transplantation (Le Blanc et al., 2004).

Although bone marrow (BM) represents the main source of MSCs for both experimental and clinical studies, the use of BM-MSCs is not always acceptable because of the invasive harvesting procedure. Furthermore, the number of BM-MSCs has been reported to decline with increasing age (Stenderup et al., 2003). Recent studies have indicated that MSCs can be isolated from a variety of tissues, including adipose tissue (De Girolamo et al., 2008), umbilical cord (Wang et al., 2004; Lu et al., 2006), placenta (Barlow et al., 2008) and amnion (Bilic et al., 2008). Tissue from amnion, placenta, Wharton's jelly and umbilical cord represent promising sources of MSCs due to abundant and easily obtained by non-invasive procedures.

The umbilical cord (UC) is an essential part of the conceptus and contributes to fetal development by providing the blood flow between placenta and fetus. In most species, including pigs and humans, the UC contains two arteries and one vein which are surrounded by a bulk of mucous connective tissue called Wharton's jelly (Corrao et al., 2013). In addition, the UC may contain the remnants of yolk sac (omphalomesenteric duct) and allantois (urachus). The UC vessels are formed by extraembryonic mesoderm and connect the embryo to the extraembryonic blood circulation. The cord is covered by epithelium derived from the amnion sac. The UC contains a reservoir of mesenchymal stromal cell populations that are in the sub-amnion layer, Wharton's jelly and the perivascular region (Troyer and Weiss, 2008).

Fine structural, immuno-histochemical and functional analysis performed in vitro show significant differences in the number and nature of cells among subamniotic, intervascular and perivascular regions. However, they all express similar surface markers suggesting that they are all of mesenchymal stem cell (also called mesenchymal stromal cell: MSC) origin (Nanaev et al., 1997; Karahuseyinoglu et al., 2007). Wharton's jelly is a mucus connective tissue component of the umbilical cord matrix stem cells (UMCs) in vivo environment and is considered to contribute to the distinct features of UMCs including high colony forming unit-fibroblast (CFU-F) capability, high proliferative potential, short population doubling time and long life in vitro (Guillot et al., 2007). Wharton's jelly contains growth factors including insulin-like growth factor I (IGF-1), basic fibroblast growth factor (bFGF), transforming growth factor β (TGF-β) and epidermal growth factor (EGF) (Sobolewski et al., 2005). Wharton's jelly extracts contain extracellular matrix protein and growth factors that in a reconstructed microenvironment for culturing MSCs resulted in a delay of MSCs replication senescence during in vitro long term culture (Hao et al., 2013).

An important role of the Wharton's jelly is to prevent compression, torsion and bending of the umbilical vessels which provide the oxygen and nutrients and remove carbon dioxide and waste products of developing fetus. Wharton's jelly is characterized by a loose aggregation of cells surrounded by extracellular matrix. It contains laminin, abundant collagen (type I, III and VI) and glycosaminoglycans (GAGs). Hyaluronic acid and heparin sulphate proteoglycan constitute 70% of the total GAGs (Bankowski et al., 1996).

During embryogenesis, the totipotent primordial germ cells and hematopoietic stem cells migrate from yolk sac through the region that becomes the umbilical cord on their way to populate target tissues in the embryo and fetus (Mitchell et al., 2003). MSC precursors have been found in the yolk sac (Wang et al., 2008a) and these cells might be trapped in the connective tissue matrix of the developing umbilical cord as they migrate along with HSCs precursors from blood islands located in yolk sac to the aorta-gonad-mesonephros region during early embryogenesis (Ueno et al., 2010).

UMCs can be collected from Wharton's jelly pre- or perinatally. In humans, the UC are normally discarded after birth and there are no ethical concerns for UMCs harvest. Isolation of UMCs from cords postnatally is non-invasive and without pain, in contrast, to adult stem cell (ASC) isolation. Moreover, the numbers of isolated MSCs from adult tissues such as a bone

marrow significantly decreases with age and infirmity (Rao and Mattson, 2001) and there is a potential risk of viral contamination during the isolation of MSCs from bone marrow (Romanov et al., 2003).

Unlike ASCs, UMCs possess characteristics of embryonic stem cells in that they consistently express ESC markers and pluripotency markers including alkaline phosphatase, Nanog, Oct-4, Sox-2, Tra-1-60, Tra-1-81, stage specific embryonic antigen-1 (SSEA-1), SSEA-4, Hoechst 33342 dye exclusion and even form embryoid bodies in vitro (Carlin et al., 2006; Weiss et al., 2006; Fong et al., 2007; La Rocca et al., 2009; Nekanti et al., 2010a). They also do not form teratomas after in vivo transplantation, a significant drawback of ESCs (Mitjavila-Garcia et al., 2005).

The most common methods to isolate MSCs from Wharton's jelly are based on the use of explant-culture or enzymatic digestion techniques. Fresh umbilical cord is transported immediately to the lab and the umbilical cord vessels are removed. Wharton's jelly is excised and minced to small pieces before being plated directly for the explant method or digested using a cocktail of proteolytic enzymes (for example collagenase/hyaluronidase/trypsin). The advantage of enzymatic digestion is that it reduces the contamination with other cell types such as red blood cells and endothelial cells (Troyer and Weiss, 2008). Higher rates of expression of MSC markers was observed in cells isolated from Wharton's jelly by the explant-culture method and, also, these cells had a higher proliferation rate compared to cells derived by enzymatic digestion methods (collagenase/hyaluronidase/trypsin, collagenase/trypsin and trypsin) (Salehinejad et al., 2012).

The collagenase/trypsin method of cell isolation yields higher cell numbers than other enzymatic digestion methods such as collagenase/hyaluronidase/trypsin and trypsin. These isolated cells expressed a greater amount of the pluripotent markers as C-kit and Oct-4 than cells isolated from explant and collagenase/hyaluronidase/trypsin methods (Salehinejad et al., 2012). Yoon et al (2013) also reported advantages of explant culture of Wharton's jelly for acquiring both UMCs and the secreted natural cytokine bFGF (Yoon et al., 2013). A simple and rapid method for isolation UMCs from the whole UC is by injection of enzymatic solution into the tied cord. The direct delivery of enzymatic solution into Wharton jelly was reported to provide a high yield of isolated cells (1.5-2 x 10^6/cm) with MSCs properties (Montanucci et al., 2011).

Characterization of UMCs

Cells isolated from Wharton's jelly possess the MSCs properties proposed by the Mesenchymal and Tissue Stem Cell Committee of the International Society for Cellular Therapy (ISCT) (Dominici et al., 2006). The three minimal criteria to define MSCs: are adherence to plastic culture ware, specific surface antigen expression, and multipotent differentiation potential. Flow cytometric analysis of MSCs should demonstrate surface antigen expression of CD90, CD105 and CD73. Furthermore, these cells should show low expression of CD34, CD45, CD14 or CD11b, CD79a or CD19 and HLA class II proteins. Other markers such as CD140b, SSEA-4 and a neural ganglioside GD2 may also be prospective markers for MSCs to distinguish MSCs from all other cells within marrow (Gang et al., 2007; Martinez et al., 2007; Roobrouck et al., 2011). Finally, these cells must demonstrate the ability to differentiate along osteogenic, adipogenic and chondrogenic lineages under standard in vitro differentiating conditions. These criteria were developed for human MSCs and human UMCs possess plastic adherence, can be differentiated into chondrogenic, adipogenic and osteogenic lineages and possess expression of the follow cell markers: CD105+ (endoglin, SH2), CD73+ (SH3), CD90+ (Thy-1), HLA-A,B,C+ (MHC class I). They are CD34-, CD45-, HLA-DR- (MHC class II) (Christodoulou et al., 2013). UMCs express the mesodermal markers vimentin, alpha smooth muscle actin (α-SMA) and CD117 (the receptor for stem cell factor (SCF)); moreover, a subset of UMCs express nestin, the intermediate filament of neuroectodermal cellular lineage (Fu et al., 2006; La Rocca et al., 2009). Recently UMCs have been reported to express the mRNA and proteins for the transcription factors GATA-4, GATA-5 and GATA-6 (La Rocca et al., 2009) that are involved in development pathways of mesoderm and endoderm-derived organs. Moreover, UMCs isolated by non-enzymatic methods express a subset of epithelial cytokeratins (CK); CK8, CK18 and CK19 (Moll et al., 2008; La Rocca et al., 2009).

Although human UMCs present a phenotypic profile mostly resembling human BM-MSCs, some differences exist in the two cell populations. UMCs expressed CD49b (integrin-α2) but BM-MSCs lacked this surface marker. The expression level of CD73 and HLA-I were lower in UMCs than BM-MSCs (Friedman et al., 2007). Moreover, CD106 (VCAM-1) was expressed weakly in BM-MSCs but UMCs do not have this surface marker (Martin-Rendon et al., 2008).

Wharton's jelly of UC is a rich source of MSCs, with 6-8x10^5 isolated cells/cm of human umbilical cord length reported (Tsagias et al., 2011). CFU-F analysis showed higher frequency

of CFU-F of MSCs derived from Wharton's jelly compared to bone marrow and umbilical cord blood (UCB) MSCs (Karahuseyinoglu et al., 2007; Lu et al., 2008). Oxygen concentration and plating density affect the proliferation of UMCs with relative hypoxia and low cell plating density enhancing CFU-F frequency and cumulative population doubling without an impact on cell surface marker expression and differentiation potential (Nekanti et al., 2010b; Lopez et al., 2011).

Compared to BM-MSCs, UMCs are reported to have a relatively higher proliferation potential, higher telomerase activity, shorter population doubling time and longer time to senescence without loss of stem cell potency. UMCs also did not show contact-inhibited cell growth like BM-MSCs (Baksh et al., 2007). UMCs have a steeper log phase and short doubling time. The mean doubling time of early passage UMCs has been reported to be 24 hours and remained almost constant up to passage 10 (Lu et al., 2006). In contrast, early BM-MSCs and adipose tissue-derived MSCs (ADCs) had a longer mean doubling time of 40 and 45 hours respectively (Peng et al., 2008).

Besides the higher proliferative activity of UMCs, they showed no sign of senescence over several passages. Conconi et al (2006) cultured UMCs over 30 doublings in 16 serial passages and found no variation in cell morphology or senescence (Conconi et al., 2006). Also, porcine UMSCs were cultured in vitro for more than 80 doublings with no decrease of proliferative capacity (Mitchell et al., 2003). Mean population doubling (PD) per passage of UMCs and ADCs has been reported as 2.8 and 0.8 respectively (Christodoulou et al., 2013). Karahuseyinoglu et al (2007) were able to expand UMCs more than 300 fold over 7 passages (Karahuseyinoglu et al., 2007) and Lund et al (2007) reported that UMCs could be expanded to more than 10^{15} cells (Lund et al., 2007). UMCs had a normal karyotype after in vitro culture (P1-P60), indicating that cell culture may not alter chromosomal organization (Cardoso et al., 2012).

Telomeres are the repetitive DNA sequence localized at the end of all chromosomes to protect the end of the chromosome from deterioration or from fusion with neighboring chromosomes. Cell division results in shortening of telomeres and when they get too short, the cell no longer can divide and becomes "senescent" or dies (Blackburn, 2001). Telomerase is a complex of telomeric RNA and telomerase reverse transcriptase (TERT) that functions by adding telomeric repeats onto chromosome ends to extend the possible cell divisions. This enzyme prevents the replication-dependent loss of telomeres and cellular senescence in highly

proliferative cells (Blasco, 2005). MSCs with high proliferation potential contain telomere lengths around 10-15 kb longer than somatic cell with telomere lengths 5-8 kb (Cheng et al., 2008a). UMCs have telomeres around 9 kb similar to dental papilla-derived MSCs and ADCs but longer than cancer cell lines and somatic cells. Relative telomerase activity (RTA) of UMCs was higher than ADCs but lower than cancer cell lines (Jeon et al., 2011). UMCs with long telomeres and high levels of telomerase activity are consistent with high proliferation in long-term culture.

Differentiation potential of UMCs

Adipogenic, Osteogenic, and Chondrogenic differentiation

UMCs can be induced to differentiate into mesodermal and non-mesodermal lineages. Human UMCs could differentiate to osteoblasts, adipocytes and chondrocytes under specific in vitro conditions (Wang et al., 2004; Karahuseyinoglu et al., 2007; Chen et al., 2009; Huang et al., 2012), therefore fulfilling one of the minimal criteria proposed by ISCT for MSCs. Under adipogenic differentiation conditions with supplements of 1-methyl-3- isobutylxanthine (IBMX), dexamethasone, insulin and indomethacin, UMCs differentiate into adipocytes. However, lipid accumulation staining with Oil Red O takes longer to develop in UMCs and the adipocytes are less mature than those derived from BM-MSCs (Karahuseyinoglu et al., 2007; Troyer and Weiss, 2008; Shetty et al., 2010). UMCs displayed chondrogenic potential in vitro in micromass culture with induction by dexamethasone, ascorbic acid, ITS (insulin, transferrin and selenium), TGF-β, IGF-1 and FGF. The histological analysis revealed production of cartilage-specific highly sulphated proteoglycans and type II collagen stained specifically with Alcian blue dye (Augello et al., 2010). Up-regulated expression of Sox9, a key transcription factor for chondrogenesis, has been reported after inducing with TGF-β (Kawakami et al., 2006; Lorda-Diez et al., 2009).

UMCs embedded in a scaffold of a collagen (type I) hydrogel underwent chondrogenesis after culturing with chondrogenic differentiation medium (Chen et al., 2013). UMCs seeded on a polyglycolic acid (PGA) scaffold and cultured with chodrogenic medium differentiated into chondrocytes. They outperformed temporomandibular joint (TMJ) condylar cartilage cells for proliferation and synthesis of collagen type I, and type II, and glucoaminoglycans. UMCs may therefore be an attractive alternative to condylar cartilage cells for TMJ tissue engineering applications (Bailey et al., 2007). Incubation monolayers of UMCs with dexamethasone,

ascorbic acid and β-glycerol phosphate showed osteogenic differentiation based on alkaline phosphatase activity, increase of collagen (type I) production, calcium incorporation into the extracellular matrix and up-regulation of the osteogenic related genes osteopontin and osteocalcin (Lovati et al., 2011).

UMCs seeded in high density in 3D scaffolds of polyglycolic acid (PGA) differentiated into osteocytes after culturing in osteogenic differentiation medium. This provides the foundation for future applications of stem cells-based bone tissue engineering (Wang et al., 2010). In addition, UMCs have been shown to possess weaker osteogenic (Hsieh et al., 2010) and chondrogenic (Wang et al., 2009a; Melania et al., 2011) potential as compared to BM-MSCs. UMCs genetically engineered to overexpress Osx a transcription factor essential for osteoblast differentiation showed more osteogenic differentiation in both in vivo and in vitro (Wang et al., 2012). Gene expression profiles of UMCs exposed to hypoxia reveal up-regulation of early mesodermal and endothelial genes including DESMIN, CD34 and ACTC, suggesting that in vitro culturing of WJ-MSCs under hypoxic conditions leads to adoption of a mesodermal/endothelial fate (Nekanti et al., 2010b).

Neural differentiation

UMCs have been shown to express the morphological and biochemical properties of neural cells when exposed to appropriate differentiation media. Basic FGF, EGF, retinoic acid, valproic acid, insulin, hydrocortisone, β-mercaptoethanol (BME), butyrated hydroxyanisole (BHA) and dimethyl sulfoxide (DMSO) were added for inducing neurogenesis (Fu et al., 2006). Neural-like cells derived from UMCs cultured in neurogenic differentiation medium expressed neuronal precursors and the mature neuron specific proteins nestin, β-III tubulin, microtubule-associated protein 2 (MAP-2), neurofilament-M, Neu-N and neuron specific enolase (NSE) (Ma et al., 2005; Karahuseyinoglu et al., 2007). Glial fibrillary acidic protein (GFAP) and 2',3'-Cyclic-nucleotide 3'-phosphodiesterase (CNPase), markers for glial cells, astrocytes and oligodendrocytes were expressed in UMCs induced by neurogenic differentiation medium (Mitchell et al., 2003). Neuronal conditioned medium containing sonic hedgehog and FGF8 induced in vitro differentiation of UMCs into dopaminergic neurons containing tyrosine hydroxylase (TH), indicating UMCs may be therapeutic for Parkinson's disease (Fu et al., 2006).

Undifferentiated UMCs derived from preterm birth displayed the neural progenitor cell markers Nestin and Musashi-1 and the mature neural markers MAP-2, GFAP and myelin basic protein. They could be successful induced into neural progenitors similar to UMCs derived from term birth controls (Messerli et al., 2013). It has been suggested that UMCs may be more primed for neuronal differentiation than BM-MSCs because they expressed higher levels of the neuronal associated genes NESTIN, GFAP and SEM3A in a non-differentiated state (Nekanti et al., 2010a). Under identical in vitro induction conditions, earlier generation of neurospheres was noted from UMCs compared to BM-MSCs. UMC derived neurospheres were able to differentiate to neuronal cells when culturing with brain-derived neurotrophic factor (BDNF). They also promoted functional recovery after spinal cord transection (Hermann et al., 2004; Zhang et al., 2009a). UMC-derived neurospheres express nestin, Sox2 and Pax6 transcription factors and self-renew and differentiate to neuron/glial-like cells. Evaluation of the secretome profile suggests that UMCs secrete more neurotrophic factors, consistent with UMCs ability to make neural progenitors with higher efficiency than BM-MSCs and ADCs (Balasubramanian et al., 2013).

UMCs migrate and survive in brain injury sites and differentiate in vivo into neurons and glia (Weiss et al., 2003; Jomura et al., 2007). Matsuse et al (2010) reported high efficiency differentiation of human UMCs to Schwann cells after incubation in neurogenic differentiation medium comprised of beta-mercaptoethanol, retinoic acid, bFGF, PDGF and the heregulin-A1-EGF domain and forskolin. The function of Schawann cells derived from UMCs is comparable to that of native human Schwann cells in vivo (Matsuse et al., 2010). Growth factor-based methods enable the differentiation of UMCs toward immature neuronal-like cells that retain their immunomodulatory and anti-oxitative activities (Li et al., 2012).

Endodermal-lineage differentiation

Beta cells

Recent studies suggest that UMCs can also differentiate into endodermal lineages. After culturing in low-glucose medium supplemented with nicotinamide, UMCs were differentiated into mature islet-like cell clusters possessing insulin-producing ability in vitro and in vivo. Differentiated UMCs expressed insulin and other pancreatic beta-cell-related genes including Pdx1, Hlxb9, Nkx2.2, Nkx6.1, and Glut-2. The hyperglycemia and glucose intolerance in

streptozotocin-induced diabetic recipients was significantly alleviated after transplantation of these islet-like cell clusters (Chao et al., 2008). UMCs had higher pancreatic differentiation potential than BM-MSCs and may therefore be more suitable for pancreatic tissue engineering in the treatment of type I diabetes than BM-MSCs (Wu et al., 2009b). Genetic reprogramming by transfection of neurogenic differentiation 1 gene (NeuroD1) into UMCs together with in vitro culture in beta-mercaptoethanol (BME) and nicotinamide differentiated UMCs to insulin producing cells that expressed the pancreatic β-cell marker, PDX-1 (Wang et al., 2011).

Hepatic cells

Non-differentiated UMCs constitutively expressed markers of the hepatic lineage including albumin, alpha-fetoprotein, cytokeratin-19, conexin-32 and dipeptidyl peptidase IV as well as weaker hepatocyte-specific functions were observed when compared to adult hepatocytes (Zhang et al., 2012b). UMCs cultured in hepatic differentiation medium showed up-regulation of hepatic markers, stored glycogen, produced urea and exhibited an inducible CYP 3A4 activity. (Campard et al., 2008; Anzalone et al., 2010). One step hepatic induction of human UMCs using hepatocyte growth factor (HGF) and fibroblast growth factor-4 (FGF-4) has been reported. The hepatocyte-like cells expressed the hepatocyte-specific markers albumin (ALB), human alpha-fetoprotein (AFP) and cytokeratin 18 (CK-18), stored glycogen and took up low-density lipoprotein (LDL) (Zhang et al., 2009b). Functional hepatocyte-like cells derived from induced UMCs retained low immunogenicity in vitro and they incorporated into the liver parenchyma after transplantation into damaged liver (Zhao et al., 2009).

Cardiac muscle

UMCs also have cardiac muscle differentiation potential. They exhibit myocardial morphology and express the myocardial markers cardiac troponin I, connexin-43 and desmin after being treated with 5-azacytidine (Wang et al., 2004). 5-Azacytidine induces cardiac differentiation of human UMCs by activating extracellular regulated kinase (ERK) (Qian et al., 2012). UCMs induced by 5-azacytidine and bFGF and platelet-derived growth factor (PDGF) expressed in vitro cardiac myosin and cardiac troponin T (cTnT). UMCs transplanted into infarcted areas incorporated into foci of neovascularization, differentiated into cardiomyocyte-like cells and improved the cardiac function (Wu et al., 2009a). Cardiomyocyte conditioned medium supplemented with a bioactive lipid metabolite, sphingosine 1-phosohate (S1P) induce

differentiation of UMCs to functional cardiomyocyte-like cells with cardiomyocyte-like action potential and voltage gated currents (Zhao et al., 2011b).

UMCs are induced toward skeletal muscle cells when they are cultured in myogenic differentiation medium. The differentiated cells expressed myogenic factor-5 (Myf-5) and the myogenic regulatory factor MyoD. UMCs not only differentiate in vivo towards the myogenic lineage, but also to contribute to the muscle regenerative process (Conconi et al., 2006). Cell reprogramming by transfection of the transcription factor MyoD, the master regulator of skeletal muscle differentiation, into UMCs induced myogenic differentiation. Transfected UMCs formed multinucleated myofibers in vitro, and they exhibited the functional markers of fusion machinery including M-cadherin, β-catenin, and muscle cell-specific structural proteins including desmin, α-actinin, dystrophin, myosin heavy chain, and myoglobin (Kocaefe et al., 2010).

Endothelial cells

Mature endothelial cells are highly effective for promoting vascularization to improve blood transfusion, cell viability and survival of engrafted tissues after transplantation. However, they have limited proliferation potential (Levenberg et al., 2005). UMCs may be an alternative cell source for neovascularization because they differentiate into endothelial cells after culturing in vitro with vascular endothelial growth factor (VEGF) and bFGF. The UMC-derived endothelial-like cells incorporated acetylated low-density lipoprotein and expressed the endothelial-specific proteins PECAM and CD34.

After transplantation into an ischemic mouse model, UMCs grew from the injection point and differentiated into endothelial cells in a lesioned hind limb (Wu et al., 2007a). UMCs had higher proliferative potential, higher expression of endothelial-specific markers after induction and significantly greater total tubule length, diameter, and area in angiogenesis assays than those of differentiated BM-MSCs (Chen et al., 2009). UMCs transplanted into wire-injured femoral arteries in mice play an important role in re-establishing endothelial integrity by inhibiting neointimal hyperplasia (Wang et al., 2009b).

Under hypoxic conditions, UMCs support angiogenesis both in vitro and in vivo. They secrete membrane microvesicles (MVs) promoting proliferation of endothelial cells and the formation of capillary networks. This significantly improved blood flow recovery in ischemia (Zhang et al., 2012a).

UMCs in co-culture

Hematopoietic stem cells (HSCs)

MSCs facilitate hematopoietic stem cell growth in vitro and in vivo by constitutive secretion of hematopoietic cytokines including IL-6, IL-7, IL-8, IL-11, IL-14, IL-15, macrophage colony-stimulating factor (M-CSF) and stem cell factor (SCF) (Kim et al., 2004; Li et al., 2007). UMCs express stromal supporting properties that are similar to BM-MSCs and they express mRNA for SCF, leukemia inhibitor factor (LIF), M-CSF, Flt3-ligand, IL-6, VEGF, stromal-derived factor-1 (SDF-1) granulocyte macrophage colony-stimulating factor (GM-CSF) and granulocyte colony-stimulating factors (G-CSF) (Lu et al., 2006).

Umbilical cord blood (UCB) transplantation has several advantages over bone marrow (BM) transplantation. Collection of UCB is a non-invasiveness procedure and is technically easier than BM collection. There is reduced risk of infections, and a greater HLA disparity is tolerated for UCB grafts with a decreased frequency of acute or chronic graft versus host disease (GVHD) as compared to BM grafts (Mayani and Lansdorp, 1998; Gluckman, 2000). Bakhshi et al (2008) reported that human UMCs are similar to BM-MSCs for supporting the growth of CD34+ cord blood cells in long term ex vivo culture (Bakhshi et al., 2008). UMCs produce more G-CSF, GM-CSF, hepatocyte growth factor (HGF), LIF, IL-1a, IL-6, IL-8 and IL-11 than BM-MSCs in culture. UMCs augmented hematopoietic colony formation when co-cultured with UCB mononuclear cells in vitro and promoted engraftment of human UCB cells or CD34+ selected cells in mice when co-transplanted (Friedman et al., 2007). UMCs also increased homing and improved migration efficiency of UCB CD34+ cells to bone marrow and spleen in vivo by expressing the homing molecules CD49e, CD 31, CD62L and CD11a (Hao et al., 2009).

Embryonic stem cells (ESCs)

Hiroyama et al (2008) reported that human UMC feeder cells could maintain the lineage and hematopoietic differentiations of ESCs more than 3 months. ESCs express the pluripotent markers alkaline phosphatase, SSEA-4 and Oct-3/4 after they are co-cultured with irradiated human UMCs (Hiroyama et al., 2008).

Immuno-modulation

UMCs possess various immunoregulatory properties that make them appealing candidates for cell based therapies. UMCs inhibit the splenocyte proliferation response to concanavalin A stimulation and proliferation of stimulated T cells in a two way mixed lymphocyte reaction (MLR). UMCs block non-stimulated splenocyte proliferation and stimulate T-cell proliferation in a one-way MLR. Mitogen-induced splenocyte proliferation is inhibited by UMCs in co-culture assay but there was no effect in non-stimulated splenocytes (Zhou et al., 2011).

UMCs have been observed to produce VEGF and IL-6 and these could be involved in modulation but expression of co-stimulatory surface antigens like CD40, CD80 and CD86 was not detected (Weiss et al., 2008; Manochantr et al., 2013). Comparative analysis of immunomodulatory properties and immunesuppressive effect of MSCs derived from bone marrow, adipose tissue, UCB and Wharton's jelly showed that there were no significant differences in the level of secreted factors in non-stimulated MSCs from the different sources and they have similar effects on phytohemagglutinin-induced T-cell proliferation (Yoo et al., 2009).

UMCs suppressed mitogen-induced T-cell proliferation and the suppressive effect of IFN-ɣ and/or TNF-α produced by activated T-cells was correlated to the ability of the factor to stimulate production of indoleamine 2,3 dioxgenase (IDO) by UMCs, which, in turn, inhibited T-cell proliferation (Yoo et al., 2009). Human leukocyte antigen (HLA) class I molecule, HLA-G, and IDO have been shown to play crucial immunosuppressive roles in fetal-maternal tolerance. HLA-G inhibits natural killer and T cell function by high-affinity interaction with inhibitory receptors, and IDO acts by depleting the surrounding microenvironment of the essential amino acid tryptophan, thus inhibiting T cell proliferation (Mellor et al., 2002). B7-H1 (programmed death ligand-1) one of the members of B7 family molecules is able to bind to programmed cell death receptor expressed on T-cells. Activation of B7-H1 expressed on murine BM-MSCs inhibited lymphocyte proliferation (Sheng et al., 2008). The study of Tipnis et al. (2010) has shown that human UMCs induced by IFN-ɣ up-regulated IDO and B7-H1 and these molecules were actively involved in suppressing T-cell proliferation.

UMCs express low amounts of HLA-ABC (MHC class I) and do not express HLA-DR (MHC class II) enabling them to escape immune recognition. In comparison to BM-MSCs

derived from aged donors, UMCs expressed significantly lower levels of HLA class I and exhibit significantly higher intracellular concentrations of the immunosuppressive molecule HLA-G (Deuse et al., 2011). Cho et al (2008) found that porcine UMCs could be activated to express MHC class II and increase MHC class I with IFN-ɣ stimulation in vitro. UMCs could induce an immune response when they were injected in an inflamed region or injected repeatedly in the same region or stimulated with IFN-ɣ prior to injection. However a single injection of MHC-mismatched unactivated UMCs did not induce a detected immune response (Cho et al., 2008). Deuse et al (2011) reported that IFN-ɣ at doses below 50 ng/ml up-regulated HLA-DR and HLA class I expression, therefore increasing UMCs immunogeneticity. However, higher doses of IFN-ɣ enhanced the UMCs immunosuppressive phenotype by down-regulating HLA-DR expression and further increasing IDO. Also, IFN-ɣ treatment induced tolerogenicity by increasing intracellular HLA-G expression, TGF-β and IL-10 release as well as stimulation of IDO production (Deuse et al., 2011).

UMCs and their culture supernatant inhibit the proliferation of phytohemagglutinin-stimulated human peripheral blood lymphocytes and mouse splenocytes. They also suppressed secretion of transforming growth factor-β1 and interferon-γ by human peripheral blood lymphocytes. Zhou et al (2011) suggested that the immunomodulatory effect of UMCs may be related to direct cell contact and the secreted soluble factors HGF, prostaglandin E2 (PGE2), TGF-β and IDO (Zhou et al., 2011). Immune suppression exerted by UCMs is mediated by cycloxygenase (COX) 1 and COX2 enzymes that regulate PGE2 synthesis whereas HGF did not seem to be implicated (Chen et al., 2010).

UMCs stimulated by inflammatory cytokines displayed potent immunosuppressive effects on lymphocyte responses in a dose-dependent manner that prevented lymphocyte activation and suppressed T-cell proliferation. CD4+ and CD8+ T subpopulations were equally targeted for proliferation inhibition regardless of the stimulus used to activate T-cells. Furthermore, UMC-mediated inhibitory effects were higher than with BM-MSCs (Najar et al., 2010).

UMCs were found to inhibit B cell proliferation, differentiation and antibody production in vitro. Soluble factors secreted from UMCs, at least in part, might down-regulate Blimp-1 and up-regulate PAX-5, two master regulators of B-cell differentiation. UMCs inhibited Akt and p38 MAPK phosphorylation that signal transduction pathways are involved in regulation of B-cell

proliferation and differentiation (Che et al., 2012). UMCs have immunomodulatory effects on antigen presenting cells (APCs) by inhibiting differentiation, maturation and endocytosis of monocyte-derived dendritic cells through secreted factors without direct cell contacts. CD 14+ monocytes were down-regulated for CD80, CD86, CD83 and HLA-DR the key markers in mature dendritic cells, when they were co-cultured in induction medium containing IL-4 and GM-CSF. UMCs caused decreased endocytic activity as measured by uptake of fluorescent dextran by immature dendritic cells (Saeidi et al., 2013).

GVHD

A recent study reported a clinical test for the immunosuppressive potential of UMCs in GVHD (Hu et al., 2013). The third party culture of expanded UMCs was transplanted into patients with severe, steroid-resistant acute GVHD (aGVDH). The aGVHD improved dramatically after each of four infusions of UMCs into the two patients. No adverse effects were noted (Wu et al., 2011). Nineteen patients with steroid-resistant severe aGVHD received in vitro expanded UMCs infusion treatment (Chen et al., 2012). Eleven patients had a complete response and survived. The other treated patients had partial and no response before they died because of aGVHD and infection. No patients had side-effects during or immediately after infusions and no UMC-related tumorigenesis was detected.

Lupus

Systemic lupus erythematosus (SLE) is a multisystem autoimmune disease (Batsali et al., 2013). It has recently been reported that transplantation of UMCs in patients with severe and refractory SLE resulted in clinical and serologic improvement. Disease remission may be associated with an increase of T-regulatory cells in peripheral blood along with a decrease in serum IL-4 resulting in inhibiton of humoral activity (Sun et al., 2010). Another recent study demonstrated that allogeneic UMCs provided clinical benefit in diffuse alveolar hemorrhage, a rare complication of SLE with high clinical mortality (Shi et al., 2012).

Other therapeutic potentials of UMCs

Properties of UMCs make them as the highly effective candidate for stem cell based therapies. UMCs can overcome three major hurdles of stem cell based clinical treatment. They

have high proliferative potential and are able to reach high cell numbers in a short time. They have low immunogenicity and do not produce tumors after transplantation (Bongso et al., 2008).

Porcine umbilical cord matrix stem cells (PUCs) modify their morphology and neurochemical phenotype to resemble neural cells and survive 6 weeks in brain of rats after local xenotransplantation without immune suppression therapy (Weiss et al., 2006). Undifferentiated human UMCs were transplanted into the brain of hemi-parkinsonian immune-competent rats. There was a significant decrease in apomorphine-induced rotations at 4-12 weeks post transplantation in Parkinson's disease (PD) rats compared to PD rats that received a sham transplantation (Weiss et al., 2006). Fu et al (2006) induced UMCs in vitro toward dopaminergic neurons and then transplanted them into hemi-parkinsonian rats (without immunosuppression). They detected the transplanted cells 5 month later. UMCs transplantation prevented the progression of behavioral deterioration seen in untreated control rats (Fu et al., 2006). Xiong et al. (2011) showed that intrastrial infusion of either human UMCs or VEGF-expressing human UMCs to rotenone-induced parkinsonian rats resulted in a reduction of apomorphine-induced rotations and a revival of tyrosine hydroxylase (TH) immunoreactivity in the lesioned striatum and substantia nigra. Transplanted human UMCs could differentiate into dopaminergic neuron-like cells in the lesions and VEGF expression significantly enhanced the neuroprotective effects by promoting dopaminergic neuron-orientated differentiation of human UMCs (Xiong et al., 2011).

Oct-4 (+) rat UMCs was transplanted into the brains of rats experiencing the global cerebral ischemia caused by cardiac arrest and resuscitation. The transplanted rats had reduced neuronal loss due to a rescue phenomenon (Jomura et al., 2007) compared to controls. Intracerebral transplantation of xenogeneic UMCs accelerated neurologic function recovery in rat with intracerebral hemorrhage. The underlying mechanism may be due to their ability to inhibit inflammation and promote angiogenesis (Liao et al., 2009a). Donor UMCs transplanted into a rat model of stroke rarely adopted a neural cell identity after brain transplantation. However UMCs treatment substantially increased vascular density and vascular endothelial growth factor and basic fibroblast growth factor expression in the hemisphere of the stroke. UMC transplantation accelerated neurologic functional recovery of the rats after stroke and this may be due to their promoting angiogenesis (Liao et al., 2009b).

Intramyocardial transplantation of UMCs has been shown to improve cardiac function in a rat myocardial infarction model (Wu et al., 2007b,c). Locally transplanted UMCs differentiated into cardiomyogenic cells in ischemic myocardium and they incorporated into the neovascularized foci. UMCs contributed to neovascularization as a result of a direct incorporation of the cells into the ischemic myocardium, although other mechanism couldn't be ruled out. Potentially stimulation of proangiogenic factors, local stimulation of angiogenesis, or chemoattraction of endogenous stem/progenitor cells could be involved. In vivo experiments showed a marked improvement of left ventricular ejection fraction (LVEF) assessed by echocardiography (ECG) (Wu et al., 2009a).

Local administration of UMCs in the eyes of a rodent model of retinal disease exhibited histological evidence of photoreceptor rescue. Transplanted UMCs may enhance survival of photoreceptor cells by secreting growth factors. UMCs have been reported to increase production of brain derived neurotrophic factor (BDNF) as well as FGF2 compared to placenta-derived MSCs (Lund et al., 2007).

Human UMCs transplanted into the ischemic cortex of rats, after treating with neuronal conditioned medium or control medium, caused a trend toward less infarct volume and significantly less atrophy compared with the control group. Rats receiving UMCs showed improvement in motor function, greater metabolic activity of cortical neurons and better revascularization in the infarct (Lin et al., 2011).

UMCs have been applied as cellular therapy to combat cancer. Rachakatla et al. (2008) engineered human UMCs to secrete interferon-β. The cells migrated and engrafted near or within lung tumors and not in other tissues after intravenous transplantation. The administration of genetically modified UMCs combined with a low dose of 5-fluorouracil in immunodeficient mice resulted in more reduction of the tumor burden and metastasis than compared to either treatment alone (Rachakatla et al., 2008).

A more recent study has reported the ability of UMCs transplanted systemically to reduce the growth of human breast carcinoma cells in vivo in a mouse xenograft model. The human UMCs attenuated DNA synthesis, increased G2 populations, and inhibited colony growth of co-cultured breast carcinoma cells. Reduced growth of cancer cells is mainly by attenuation of Erk-1/2 and PI3 K/Akt signaling and potentially an activation of intrinsic apoptosis (Ayuzawa et al., 2009). Antitumor properties of UMCs do not seem to be specific only to breast cancer cells, but

was also demonstrated for osteosarcoma and ovarian carcinoma cell lines in vitro. UMC conditioned medium and cell lysate inhibit the growth of those cancer cell lines by inducing cancer cells to undergo metaphase arrest, apoptosis and autophagy (Gauthaman et al., 2013). Co-culture of rat UMCs with pancreatic carcinoma cells caused G0/G1 arrest and significantly attenuated the proliferation of carcinoma cells. In vivo mouse studies showed engrafted rat UMCs decreased the peritoneal tumor burden after intraperitoneal transplantation and increased mouse survival (Doi et al., 2010). Naïve rat UMCs attenuated mammary tumor growth at least in part by enhancing host anti-tumor immune responses. They significantly increased lymphocyte infiltration in the tumor tissues and that the penetrated lymphocytes, primarily CD8+ T-cells and NK cells, and induced tumor cell death causing regression of tumors. The UMCs caused lymphocyte infiltration in the tumor tissues by increasing monocyte chemotactic protein-1 (MCP-1) secretion from rat UMCs (Kawabata et al., 2013).

Human UMCs transplanted in CCl4-induced acute hepatic failure engrafted and differentiated to functional hepatocytes. However, rescue from acute liver failure (ALF) seems to be through paracrine effects to stimulate endogenous liver regeneration rather than hepatic differentiation. Engrafted UMCs were more effective in down-regulating the expression of systemic inflammatory cytokines such as interleukin (IL)-1β, tumor necrosis factor (TNF)-α, IL-6 and IL-10 compared to transplanted adult hepatocytes. Direct transplantation of native human UCMs can rescue ALF and repopulate livers of NOD-SCID mice through paracrine effects to stimulate endogenous liver regeneration rather than hepatic differentiation for compensated liver function, which is the primary effect of adult hepatocytes (Zhang et al., 2012b).

UMCs exhibit a promising potential to ameliorate endometrium damage. Human endometrial stromal cells that were damaged by exposure to mifepristone showed increased proliferation and decreased apoptosis when they were co-cultured in vitro with UMCs (Yang et al., 2011).

Migration of MSCs

The migration or homing ability of MSCs to inflamed and ischemic tissues is thought to be due to the expression of chemokines or surface receptors. BM-MSCs were shown to express C-X-C chemokine receptor type 4 (CXCR4), the receptor for the chemokine stromal-derived factor-1 (SDF-1) and C-X-C chemokine receptor type 3 (CXCR3), the receptor for fractaline.

SDF-1 is predominantly localized in ischemic regions. BM-MSC migration and localization is mediated by the CXCR4/SDF-1 reaction (Wang et al., 2008b; Yu et al., 2010). Also, carcinoma fibroblasts derived from breast cancer secrete SDF-1 in vitro and MSC homing is mediated by SDF-1/CXCR4 signaling (Huang et al., 2010). A cocktail of the cytokines SCF, IL-6 and HGF up-regulate expression of CXCR-4 and this induction might be a potential strategy to improve engraftment of MSC (Shi et al., 2007). Expression of CXCR4 has been reported in human UMCs (Weiss et al., 2006) and it most likely plays an important role in homing of the cells to infarcted myocardium following acute myocardial infarction (Ghadge et al., 2011).

The passage number of MSCs used is important for homing ability as MSCs have been shown to gain or lose certain surface receptors during culture and this might influence their migration capability. Freshly isolated MSCs have enhanced homing ability compared to their culture-expanded counterparts (Rombouts and Ploemacher, 2003). CXCR4 is usually expressed in lower levels on the surface of culture-expanded MSCs (Wynn et al., 2004). However, treating MSCs with a cocktail of cytokines in culture has been shown to induce higher surface expression of CXCR4 and enhanced homing ability (Shi et al., 2007). Simulating ischemic environments in culture is representative of MSCs niche and may increase MSCs motility. Hypoxic preconditioning increased MSCs migration through Matrigel and on tissue culture plastic by up-regulating of matrix metalloprotease (MMPs) compared to MSCs maintained in normoxic environment (Annabi et al., 2003; Rosova et al., 2008)

For MSC migration experiments, the timing of delivery, number of cells delivered and site of infusion may affect the engraftment efficiency and the destination of exogenously delivered cells. MSCs were found to engraft in the myocardium at higher rates 1 day after myocardial infarction (MI) as compared to 14 days after MI, indicating that MSCs engraft in response to acute MI (Schenk et al., 2007). Omori et al (2008) reported that transplanting higher numbers of MSCs and MSCs delivered sooner after starting of ischemia resulted in higher engraftment rates (Omori et al., 2008). In a rat model of brain injury, Wu et al (2008) demonstrated systemic infusion of $1x10^6$ BM-MSCs improved neurological function however no additional enhancement was observed when $3x10^6$ MSCs were infused (Wu et al., 2008).

The confluency of cultured MSCs prior to therapeutic infusion also affects migration potential. Lee et al. (2009) investigated the differences between low-passage and low-density cultures of MSCs. Six surface markers were found preferentially expressed on early passage

MSCs in low confluency cultures: podocalyxin-like protein PODXL, CD49f, CD49d, cMet, CXCR4, and CX3C chemokine receptor 1 (CX3CR1) (Lee et al., 2009). De Becker et al. (2007) demonstrated that high culture confluence inhibited transendothelial migration in MSCs by increasing the production of a natural matrix MMP inhibitor, TIMP-3. Exposure of MSCs to hypoxic conditions increased CXCR4 and CX3CR1 expression, which leads to increased migration in response to SDF-1α (Hung et al., 2007).

The site of MSCs delivery may impact the route that MSCs travel to reach the target organ. Systemic administration can be achieved by intravenous (IV) injection, intraperitoneal (IP) injection, intra-arterial (IA) injection or intracardiac (IC) injection. IC and IA delivery resulted in higher engraftment rates than IV delivery in models of MI (Barbash et al., 2003; Freyman et al., 2006). Also, IA injection close to the site of brain injury significantly enhanced homing to the brain compared to IV injection (femoral vein) (Walczak et al., 2008). The advantage of IA injection may be involved in reducing of aggregation of MSCs within filtering organs such as the lung, liver or spleen often observed in IV delivery (Barbash et al., 2003; Kraitchman et al., 2005; Sackstein et al., 2008). However, IA may increase the possibility of microvascular occlusions (Walczak et al., 2008). IP injection has rarely been used for MSCs transplantation but IP administration has been employed to deliver MSCs to murine fetuses in a mouse model of muscular dystrophy (Chan et al., 2007). The distribution and migratory properties of systemically injected MSCs is helpful in studying homing efficiency. MSCs, after intravenous delivery, are found at low or very low frequencies in most target organs shown by various tracking techniques as fluorescent protein labeling (Devine et al., 2003; Kawada et al., 2004; Nagaya et al., 2004), transduction with reporter genes (Horita et al., 2006), detection of human genes in animal recipients (Barbash et al., 2003; Mahmood et al., 2005; Francois et al., 2006), sex-linked chromosome gene for sex mismatch transplants (Ortiz et al., 2003; Jiang et al., 2006), histology (Morigi et al., 2008), immunohistochemistry (Mahmood et al., 2005; Horita et al., 2006, Fatar et al., 2008; Omori et al., 2008), real-time PCR (Devine et al., 2003; Ortiz et al., 2003) and fluorescent in situ hybridization (Ortiz et al., 2003; Jiang et al., 2006). Devine et al (2003) demonstrated a high number of transplanted cells observed in gastrointestinal tissues and a relatively high number of cells also observed in the kidney, lung, liver, thymus, and skin. The levels of engraftment in these tissues were estimated, ranging from 0.1% to 2.7% of the administered cells.

In non-injury models, by detecting enhanced green fluorescent protein (GFP)-transfected murine MSC, the highest frequency of GFP-positive organs were found in the lungs, liver, kidney, skin, and gut among investigated tissues 24 h after MSC intravenous transplantation (Deak et al., 2010). Non- or minimally-invasive procedures to track MSC migration in real time was performed using various techniques including magnetic resonance imaging (MRI) on superparamagnetic iron oxide (SPIO) nanoparticle-labeled MSCs (Hsiao et al., 2007; Song and Ku, 2007; Reagan and Kaplan, 2011), combined single-photon emission CT (SPECT)/CT scanning (Kraitchman et al., 2005) and quantum dot tracking (Yukawa et al., 2012). These techniques have enhanced the ability to investigate MSC homing as well as the behavior and organ-specific accumulation of transplanted MSCs. MRI cell tracking using SPIO is thought to be the lowest risk alternative for monitoring stem cell activity in humans due to the widely available data regarding the risk of MRI and the fact that SPIOs are Food and Drug Administration approved.

Using SPECT/CT imaging in an acute myocardial infarction model, the initial localization of BMMSCs was observed in the lung and the cells moved to nontarget organs such as the liver, kidney, and spleen within 24 to 48 h after infusion. An increase in MSCs was found in the infarcted heart tissue with a simultaneous decrease in the initial concentration of MSCs in the lung 24 h after infusion, and MSCs persisted until 7 days after injection (Kraitchman et al., 2005).

The labeling of BMMSCs with bioconjugated quantum dots (QDs) does not alter the self-replication and differentiation potential of MSCs into chondrogenic, osteogenic, and adipogenic cells (Shah et al., 2007). MSCs labeled with QDs are very useful not only for tracking MSCs but also in investigating the behavioral changes of cells when MSCs are injected in combination with chemical compounds such as drugs like heparin. Mice induced to acute liver failure and then transplanted intravenously with ADCs without heparin treatment showed accumulation of almost all injected ADCs in the lungs within 10 minutes. However, when heparin was used in combination with ADCs, the accumulation of the transplanted stem cells was found not only in the lungs but also in the liver, and the accumulation increased by about 30% in the injured liver (Yugawa et al., 2012). Collectively, studies using different methods for tracking MSCs have shown most of MSCs located in the lung after transfusion and then they moved gradually to injured sites or to the liver, spleen, kidney, and bone marrow.

Intraperitoneal administration of BM-MSCs and osteogenic-induced BM-MSCs has been studied in rats. Distribution of BM-MSCs injected peritoneally was tracked by detecting Y-chromosome specific sequences by amplifying with PCR. Regardless of cell culturing protocols prior to transplantation, they were found to migrate and engraft into lung, bone marrow, thymus, liver and spleen of recipients after 1 week of intraperitoneal injection (Wilson et al., 2010).

It is unclear if MSCs actively home to tissues using leukocyte-like cell-adhesion and transmigration mechanisms (Springer, 1994) or become passively entrapped in small diameter blood vessels. It is possible that MSCs become passively arrested in capillaries or microvessels including arterioles and postcapillary venules. Active arrest of MSCs within inflamed tissues is supported by studies of integrin blocking and P-selectin knockouts. Blocking of MSCs β1-integrin, the adhesion molecule that governs the arrest of leukocytes on activated endothelium, reduces the engraftment in ischemic myocardium (Ip et al., 2007). Using P-selectin knockout mice, Ruster et al. (2006) reported that fewer MSCs slowed down in postcapillary venules compared to wild type mice. These results suggest that the engraftment of MSCs within target tissues depends on specific molecular interactions for extravasation prior to the migration step. It has been reported that MSCs transmigrate through non-activated endothelial monolayers via VCAM/VLA-4 and β1-integrin interaction including MMP-2 secretion and that they tend to integrate within the endothelial layer instead of completing diapedesis as observed for leukocytes (Steingen et al., 2008). The time course for transmigration was 240 min, which is longer than leukocytes which take 5-20 minutes (Ley et al., 2007).

It is generally assumed that factors released upon tissue damage or apoptosis mobilize and recruit stem and progenitor cells to the damaged site, where they proliferate and differentiate and eventually replace the damaged tissues (Gurtner et al., 2008). Chemokines released from tissues or endothelial cells likely promote activation of adhesion ligands, transendothelial migration, chemotaxis and subsequent retention in surrounding tissue. Numerous studies have confirmed that systemically infused MSCs can migrate to injured, inflamed tissues and exert therapeutic effects (Chapel et al., 2003; Chavakis et al., 2008).

BM-MSCs, delivered intravenously to rats following myocardial infarction localize in the infarct region and improve ventricular function, while MSCs delivered intravenously to noninfarcted rats localized to the bone marrow (Saito et al., 2002). In addition, localized abdomen irradiation has been shown to significantly enhance MSC homing specifically to

radiation-injured tissues in mice (Mouiseddine et al., 2007). Human ADCs infused into the tail vein mobilized to cell-damaged areas in an allergic rhinitis animal model (Cho et al., 2009).

Monocyte chemotactic protein-1 (MCP-1) is typically expressed at site of inflammation and is known to up-regulate adhesion molecules on the endothelial surface and increase endothelial permeability (Stamatovic et al., 2003). Using transgenic mice genetically modified to express MCP-1 in the myocardium, Belema-Bedada et al (2008) reported that MSCs expressed surface C-C chemokine receptor type 2 (CCR2), a specific receptor of MCP-1, and migrated and then were engrafted with high frequency to myocardium of transgenic mice compared to normal mice.

The direct interaction of CCR2 with MCP-1 is crucial (Belema-Bedada et al., 2008). MSCs secrete proteases that regulate transmigration and invasion of the basement membrane of endothelium and degrade extracellular matrix (ECM) during chemotaxis. De Becker et al (2007) demonstrated that blocking antibodies toward MMP2 and SiRNA knockdown of MMP2 reduced trans-endothelial migration in vitro (De Becker et al., 2007). Induction of expression of specific MMPs and their inhibitors MMP-2, membrane type 1 MMP (MT1-MMP), tissue inhibitor of metalloproteinase 1 (TIMP-1), and tissue inhibitor of metalloproteinase 2 (TIMP-2) in human MSCs by inflammatory cytokines promotes directed cell migration across reconstituted basement membranes in vitro. Detailed studies by RNA interference revealed that gene knock-down of MMP-2, MT1-MMP, or TIMP-2 substantially impaired MSCs invasion, whereas silencing of TIMP-1 enhanced cell migration, indicating opposing roles of these TIMPs in this process (Ries et al., 2007). The interactions of SDF-1α and CXCR4 were found to mediate the trafficking of transplanted BM-MSCs in a rat model of left hypoglossal nerve injury.

Inflammatory cytokines TGF-β1, IL-1β, and TNF-α up-regulate the production of MMPs in MSCs, resulting in a strong stimulation of chemotactic migration through the extracellular matrix, while the chemokine SDF-1α exhibited minor effects on MMP/tissue inhibitor of metalloproteinase (TIMP) expression and cell invasion (Ries et al., 2007). BM-MSCs are mobilized by chemokines that are present in the supernatants of primary cultures of human pancreatic islets cultured in vitro and in vivo. CXCR-4/CXCL-12 and CX3CR1/CX3CL-1 axes played the major role for homing of BM-MSCs to the inflamed region (Sordi et al., 2005). Human ADCs migrate in response to a variety of growth factors and cytokines including platelet-derived growth factor (PDGF), TGF-β1, TNF-α, and SDF-1α. Pre-treatment of ADCs with TNF-

α caused enhanced migratory activity compared to the non-pretreated control group (Baek et al., 2011). These results indicate that enhancement of the homing capacity of MSCs can be achieved by modulating the response of MSCs to a variety of growth factors and cytokines, thereby improving their therapeutic potential.

A key player in MSC migration is the CXCR4-SDF-1α axis. Many studies have focused on ways to enhance the functional expression of CXCR4 in MSCs to migrate toward chemotactic SDF-1α secreted at injury sites. Modification of CXCR4 expression with retroviral overexpression (Cheng et al., 2008b), mRNA transfection of CXCR4-GFP (Ryser et al., 2008) and cytokine pretreatment especially TNF-α have resulted in increased migration toward SDF-1α in vitro (Xiao et al., 2012). Maijenburg et al. (2012) investigated gene expression profiles involved in the process of MSC migration and found 12 differentially expressed genes in migratory MSCs compared to nonmigrating MSCs. Among them, the nuclear receptors Nur77 and Nurr1 showed the highest expression in migratory MSCs. The expression of these receptors rapidly increased under stimulation with SDF-1α and PDGF-BB. Genetically engineered MSCs overexpressing Nur77 or Nurr1 showed enhanced migration toward SDF-1α and decreased the proportion of cells in the S-phase of the cell cycle (Maijenburg et al., 2012).

The up-regulation of the α4 subunit of the VLA-4-integrin on MSCs using an adenovirus vector resulted in successful dimerization with β1-integrin and increased the homing ability of MSCs to the bone marrow by more than 10 fold as compared to non-transduced MSCs (Kumar and Ponnazhagan, 2007). Human MSCs do not express the surface adhesion molecules P-selectin glycoprotein ligand-1 (PSGL-1) and sialofucosylated glycoform of the CD44 protein (HCELL) specific to E-selectin expressed on bone marrow vasculature cells. Sackstein et al. (2008) enzymatically modified the native CD44 glycoform on MSCs into hematopoietic cell ligands that bind specifically to E-selectin of bone marrow endothelial cells and observed increased MSC migration to the bone marrow (Sackstein et al., 2008).

In a variety of clinical indications, MSCs are administered to damaged tissues at the subchronic or chronic phases of injury at which time the migratory signals for MSCs may be minimal or absent. Electrical current applied to wounded tissue activates and stimulates migration of fibroblasts which play a critical role in wound healing (Choi et al., 2011). Zhao et al. (2011a) demonstrated that physiological electric field (EF) of ~25 mV/mm in vitro directed the migration of cultured BMMSCs mainly to the anode. Increasing the EFs enhanced the

migration of the MSC and the response peaked at 300 mV/mm at a rate of 42±1 μm/h. This is around double the migration rate of the control (no EF). Of importance, EF did not influence cell senescence, phenotype, or the osteogenic potential of MSCs, regardless of passage number within the range tested (P3–P10) (Zhao et al., 2011). Moreover, electrical stimulation (ES) could ameliorate survival of MSCs after local transplantation. Wu et al. (2011) demonstrated that implanted spike wave electrical stimulation (ES) improved the survival of BMMSCs after transplantation compared to BM-MSCs transplantation or ES treatment alone using an in vivo rat model of spinal cord injury. Furthermore, analysis of functional parameters demonstrated improved functional recovery in the BM-MSCs + ES groups (Wu et al., 2011).

Therapeutic and clinical application of MSCs

Mesenchymal stem cells (MSCs) have generated a great amount of interest over the past decade as novel therapeutics for a variety of diseases. Currently, MSC based clinical trials have been conducted for numerous kinds of pathological conditions, with some completed trials demonstrating MSCs safety and efficacy. In vitro and in vivo animal and human clinical data indicate broad fields of application for MSCs. Overwhelming evidence of usefulness of MSCs in regenerative medicine, tissue engineering and immune therapy have been reported. The first clinical trial using culture-expanded BM-MSCs was carried out in 1995 and the patients were recipients of autologous cells (Lazarus et al., 1995). Since, a number of clinical trials have been conducted to test the feasibility and capability of MSCs-based therapy. Most of the trials are in a mixture of PhaseI/II studies. A number of these trials are in Phase III. Immune rejection, autoimmunity and bone/cartilage related diseases are the most frequent clinical trials using MSCs (Trounson et al., 2011).

GVHD

Acute GVHD occurs after allogeneic hematopoietic stem cell transplantation and is associated with high morbidity and mortality (Messina et al., 2008). Corticosteroids are used for initial treatment of acute GVHD. However, they are only effective for some patients. The immunomodulatory properties of MSCs have stimulated interest in their application for GVHD. The first report of successful use of MSCs for treatment of severe steroid-refractory acute GVHD was in 2004 (Le Blanc et al., 2004). Ex vivo expanded haplo-identical human BM-MSCs were

used. Intravenously infused MSCs had a striking immunosuppressive effect and the cells seemed to have had a rapid healing effect on the damaged gut epithelium.

In phase I and phase II clinical trials, with the median dose as $1.4x10^6$ cells per kg bodyweight, 55 steroid resistant severe acute GVHD patients were treated with single or multiple infusions of BM-MSCs derived from HLA-identical sibling donors, haploidentical donors, and third-party HLA-mismatched donors. The results showed complete response in 30 patients, partial response in 9 patients, no response in 3 patients and progressive disease in 13 patients. (Le Blanc et al., 2008). Of 31 acute GVHD patients treated in another phase II clinical trial using allogeneic MSCs (Prochymal®), 94% showed initial response to MSCs, 77% showed complete response (CR), and 17% showed a partial response (PR) with no infusion related toxicity or ectopic tissue formation. A CR was defined as the absence of symptoms referable to acute GVHD in all organs. A PR was defined as a decrease by at least 1 GVHD stage in any 1 organ system without deterioration in others (Kebriaei et al., 2009).

Crohn's disease

Therapeutic benefits of MSCs have also been observed for Crohn's disease, a type of inflammatory bowel disease. Patients with refractory Crohn's disease were infused inravenously with autologous BM-MSCs and showed clinical response by significantly decreasing of Crohn's disease activity index (CDAI) (Duijvestein et al., 2010). In vitro co-culture of ADCs and peripheral blood mononuclear cells (PBMCs) induced by superantigen Staphylococal enterotoxin showed inhibitory effects measured by cytokine secretion and T-cell proliferation. The inhibitory effect was partially reversed when PBMCs and ADCs were separated by a semi-permeable transwell membrane. IP injection of ADCs significantly ameliorated the clinical and histopathological severity of colitis. It abrogated weight loss, diarrhea and inflammation and increased the survival rate. The therapeutic effect was associated with down-regulation of the Th1-driven inflammatory responses and APCs maturation. Reduced levels of inflammatory cytokines (TNF-α, IFN-ɣ, IL-6, IL-1β and IL-12) were observed. Also, increasing levels of the anti-inflammatory/regulatory cytokine, IL-10, as well as regulatory T cells (Treg) in affected organs was detected (Gonzalez-Rey et al., 2009; Panes and Salas, 2009).

Ko et al. (2010) recently showed that MSCs coated with antibody against addressin, a mucosal vascular addressin cell adhesion molecule 1 (MAdCAM-1), and intravenously injected

into dextran sulfate sodium (DSS)-induced colitis mice increased efficacy of treatment, as indicated by survival rate, body-weight recovery, colon length and histological score. It was suggested that improved therapeutic effects are induced by increased MSC delivery to sites of inflammation due to the addressin antibody coating. Liang et al. (2012) reported that seven inflammation bowel disease (IBD) received a single IV infusion of 1×10^6 allogenic MSC from a related healthy donor. All seven patients experienced improvement in symptoms and five of seven patients had complete remission.

Multiple sclerosis (MS)

Experimental autoimmune encephalomyelitis (EAE) is an animal model of MS. MS is an autoimmune disease of the CNS and involves in T cells and macrophages. Currently, the established treatment for EAE is based on targeting T cells to induce immunosuppression or tolerance. Human and mouse MSC treatment of EAE demonstrates improved clinical progress, stimulation for tissue repair, decreased demyelination, and infiltration of the CNS by T cells and macrophages. Injected MSCs accumulate in the CNS, reduce the extent of damage and increase oligodendrocyte lineage cells in the lesion areas. Host immune responses were also influenced by transplanted MSCs. Inflammatory T-cells including interferon gamma producing Th1 cells and IL-17 producing Th17 inflammatory cells, and their associated cytokines, were reduced along with concomitant increases in IL-4 producing Th2 cells and anti-inflammatory cytokines (Bai et al., 2009). Intravenous administration of ADCs before disease onset significantly reduces the severity of EAE by immune modulation and decreases spinal cord inflammation and demyelination.

Intravenous injection of MSCs was shown to suppress EAE through induction of peripheral immunomodulation as the transplanted cells were found in spleen and cervical lymph nodes (Gerdoni et al., 2007). In chronic established EAE, administration of ADCs significantly ameliorated the disease course, reduced both demyelination and axonal loss, and induced a Th2-type cytokine shift in T cells. ADCs suppressed the autoimmune response in early phases of the disease as well as by inducing local neuroregeneration of endogenous progenitors in animals with established disease (Constantin et al., 2009).

BM-MSCs, when intraperitoneally delivered accessed the CNS in minimal numbers. They were found in barely detectable levels of CNS infiltration, and produced a pronounced

therapeutic impact of these cells on EAE severity (Gordon et al., 2008). MSCs delivered IP infiltrate lymph nodes and this may be highly relevant to their mode of action. The engrafted MSCs induced peripheral T-cell tolerance to the immunising antigen myelin oligodendrocyte glycoprotein, thereby leading to a large improvement in clinical course, reduction of demyelination, and CNS infiltration by T cells and macrophages (Parekkadan et al., 2008).

Amylotrophic lateral sclerosis

Amylotrophic lateral sclerosis (ALS) is a degenerative disease which occurs due to loss of upper and lower motor neurons in the cerebral cortex, brainstem, and spinal cord. ALS leads to death within five years after first appearance of symptoms. In a phase I/II study patients with MS and ALS were treated with intravenous MSC infusion which led to an increase in the proportion of CD4+ CD25+ Treg cells in the peripheral blood of the patients (Karussis et al., 2008).

Thus, at least two different mechanisms, namely peripheral modulation of pathogenic immune responses and neuroprotection, provide a strong rationale for the use of MSCs in therapeutic trials for neurological diseases characterized by inflammation and neural damage, such as MS (Uccelli et al., 2011).

Diabetes

Diabetes mellitus (DM) is characterized by hyperglycemia resulting from defects in insulin secretion, insulin action, or both. Type I DM is characterized by beta-cell destruction, typically by an autoimmune T cell-mediated mechanism, which usually leads to an absolute deficiency of insulin. Type 2 diabetes or adult onset diabetes is defined by the inability of insulin to properly regulate glucose concentrations in the blood. DM is implicated in pathologies such as adult blindness, kidney failure, amputation of legs and feet, pregnancy complications, and heart attack (Mishra et al., 2010).

In vitro differentiation of MSCs into insulin-producing cells (IPCs) is reported. The protocols include a combination of nicotinamide, activin A, and β-cellulin in high glucose medium (Karaoz et al., 2013). The differentiated cells show a similar morphology to that of pancreatic islet-like cells with high expression of Pdx1, insulin and glucagon genes and glucose dependent insulin production (Sun et al., 2007).

UMCs have been differentiated to IPCs. Real-time RT-PCR detected the expressions of insulin and other pancreatic beta-cell-related genes (Pdx1, Hlxb9, Nkx2.2, Nkx6.1, and Glut-2) in these islet-like cell clusters. The islet-like clusters possessed insulin-producing ability in vitro and in vivo and released insulin and C peptide in response to physiological glucose concentration. The hyperglycemia and glucose intolerance in streptozotocin-induced diabetic rats was significantly alleviated after xenotransplantation of islet-like cell clusters, without the use of immunosuppressants (Chao et al., 2008).

Combined transfection of the three transcriptional factors, PDX-1, NeuroD1, and MafA, causes differentiation of bone marrow MSCs into insulin-producing cells (Guo et al., 2012). Undifferentiated human ADCs were able to adopt a pancreatic endocrine phenotype ex vivo and they expressed the pancreatic endocrine transcription factor, Isl-1. Incubation of ADCs in differentiation medium that contained nicotinamide, activin-A, exendin-4, hepatocyte growth factor, and pentagastrin resulted up-regulation of pancreatic developmental transcription factors Isl-1, Ipf-1, and Ngn3. This protocol showed the possibility to generate IPCs from adipose derived MSCs (Timper et al., 2006).

The immunomodulatory capability of MSCs is considered equally important for diabetes treatment especially in diabetes type I. A preclinical study suggested that anti-diabetic effect of mesenchymal stem cells is unrelated to their transdifferentiation potential but to their capability to modulate immune response and to modify the pancreatic microenvironment. Syngeneic MSCs intravenously administered were found engrafted in secondary lymphoid organs and this correlated with a systemic and local reduction of auto-aggressive T cells together with an increase in regulatory T cells. In addition, the cytokine profile was shifted from proinflammatory to antinflammatory. MSC transplantation did not reduce pancreatic cell apoptosis but recovered local expression and increased the circulating levels of epidermal growth factor, a pancreatic trophic factor (Ezquer et al., 2012). However, Ho et al. (2012) suggested that the lasting therapeutic effects of MSCs were due to MSC engraftment and differentiation into insulin producing cells and also due to immunomodulation properties (Ho et al., 2012).

BM-MSCs infused intravenously contributed to amelioration of insulin resistance by peripheral insulin target tissues and increased the expression of glucose transport protein (GLUT4), phosphorylated insulin receptor substrate 1 (IRS-1) and protein kinase B (Akt). Transplanted MSCs alleviated hyperglycemia in rats with type 2 diabetes (T2D). Infusion of

MSCs during the early phase not only promoted beta-cell function but also improved insulin resistance whereas infusion in the late phase only affected the insulin resistance (Si et al., 2012).

Usage of MSCs was also implemented in several diabetes related complications like cardiomyopathy, nephropathy, polyneuropathy and diabetic wounds. Chronic hyperglycemia is responsible for diabetic cardiomyopathy (DCM) which is characterized by hypertrophy and apoptosis of cardiomyocytes as well as increased collagen deposition.

Intravenous administration of BM-MSCs improved myogenesis and angiogenesis and reduced myocardial fibrosis. In a glycerol-induced acute renal failure (ARF) of mice model, intravenous administration of BM-MSCs showed improvement of kidney function and regeneration of glomerular structure. Engrafted MSCs were able to differentiate into tubular epithelial cells and enhanced tubular proliferation resulting in reconstitute necrotic segment of diabetic kidneys (Herrera et al., 2004).

Diabetic polyneuropathy (DPN) involved in microvascular injury is the most common complication of DM which is characterized by damage to nerve fibers. Although studies suggested that MSCs have the capacity to differentiate into neural cells in vitro, this was not observed during in vivo studies using diabetic rat model. BM-MSCs transplanted into hind limb skeletal muscles of streptozotocin (STZ)-induced diabetes rats were able to engraft and secrete vascular endothelial growth factor (VEGF) and basic fibroblast growth factor (bFGF). The paracrine action of MSCs ameliorated DPN (Shibata et al., 2008).

Studies on rats and mice showed that systematic and local administration of bone marrow-derived MSCs improves healing of diabetic wounds. MSC injection resulted in increase in several growth factors important for successful wound healing. Treatment with BMSC systemically or locally at the wound site improved the wound-breaking strength (WBS) of fascial wounds. The improvement in WBS was associated with an immediate and significant increase in collagen levels (type I–V) in the wound bed. In addition, treatment with BMSCs increased the expression of growth factors critical to proper repair and regeneration of moderately to markedly damaged tissue TGF-β, KGF, EGF, VEGF, PDGF (Kwon et al., 2008).

UMCs for treating diabetes

In a phase I clinical trial, allogeneic Wharton's jelly derived MSCs show long-term beneficial effects on newly diagnosed diabetes mellitus (DM) type 1 (T1DM) patients after intravenous transplantation (Hu et al., 2013a). Both the glycosylated hemoglobin (HbA1c) and C

peptide in transplanted patients were improved compared to either pre-therapy values or control patients during the follow-up period. These data indicate that transplantation of UMCs for the treatment of onset T1DM is safe and effective. However, the precise mechanisms are unknown (Hu et al., 2013a).

Heart

The heart has limited capacity for self-renewal and undergoes remodeling with resulting depressed left ventricular function after acute myocardial infarction (MI). Investigations of MSCs as therapeutics for cardiac repair have resulted clinical trials (Williams and Hare, 2011). Autologous MSCs injected directly to infarcted regions showed engraftment into scarred myocardium and expressed the cardiomyocyte markers like α-actin, desmin, tropomyosin, and myosin heavy chain (Shake et al., 2002). In a swine model of chronic ischemic cardiomyopathy, allogeneic MSCs were transplanted by catheter-based trans-endocardial injections to engraft at the infarct and border zone. The MSCs differentiated into cardiomyocytes as indicated by expression of GATA-4, Nkx2.5, and α-sarcomeric actin. In addition, MSCs exhibited vascular smooth muscle and endothelial cell differentiation, contributing to large and small vessel formation. Infarct size was reduced with increasing regional contractility, myocardial blood flow (MBF) and left ventricular ejection fraction (LVEF) (Quevedo et al., 2009). In a double-blind, placebo-controlled, dose-range phase I trial, intravenous injection of MSCs in acute MI demonstrated a reduction in ventricular arrhythmias and improved pulmonary function whereas the patients had a 6% increase in LVEF at 3 months (Hare et al., 2009).

Despite numerous studies on the transplantation of MSCs in patient and animal models, the mechanisms issues underlying the effect of MSC transplantation remains vague. A recent study suggested the importance of IL-6 secreted from MSCs in paracrine action that activated Janus kinase/signal transducers and activators of transcription (JAK/STAT3). The trophic cascade initiated by JAK/STAT3 signaling increased growth factor levels in multiple tissues, leading to elevated circulating HGF and VEGF. Synergistic actions of these trophic factors further activated the myocardial repair mechanisms orchestrated by the Ark, ERK and JAK/STAT3 (Shabbir et al., 2010). A recent study demonstrated that paracrine signaling resulted in increased survival of ventricular myocytes by Akt induced change in calcium signaling which resulted in antiapoptotic effect by transplanted MSCs (DeSantiago et al., 2012).

Liver

Liver transplant is the preferred solution in case of liver diseases but donor organ shortage is the main reason why whole organ or hepatocyte transplants frequently cannot be done. Therefore, generation of hepatocyte-like cells from MSCs has become a real alternative to the isolation of primary hepatocytes. Stock et al. (2010) reported MSCs isolated from human bone marrow could differentiate to human hepatocyte-like cells in vitro after culturing in medium containing 5-azacytidine, insulin, dexamethasone, insulin-transferrin-sodium selenite (ITS), epidermal growth factor (EGF) and hepatic growth factor (HGF). Differentiated MSCs adopted functional features of hepatocytes with expression of proteins of the cytochrome P450 enzyme family, synthesis of glycogen and expression of hepatocyte markers on the protein level. Xenogenic transplantation of human hepatocyte-like cells into livers of immunocompromised mice undergoing hepatectomy was successful (Stock et al., 2010). In allylalcohol- (AA-) treated rat liver, xenografting of allogeneic MSCs by intrahepatic injection differentiated into hepatocytes-like cells which showed positive immunostaining for albumin, CK-19, CK-18, and asialoglycoprotein receptor (AGPR). Cell fusion between engrafted MSCs and recipient hepatocytes was not likely involved since both human and rat chromosomes were independently identified by fluorescence in situ hybridization (FISH). The differentiation appeared to follow the process of hepatic ontogeny, reprogramming of gene expression in the genome of MSCs, as evidenced by expression of the AFP gene at an early stage and the albumin gene at a later stage (Sato et al., 2005).

Liver cirrhosis was induced in rats using thioacetamide (TAA) followed by transplantation with BM-MSCs into spleen and liver. There was engraftment and hepatic differentiation in the liver parenchyma. BM-MSCs-derived hepatocyte-like cells with oval morphology expressed CK19 (cytokeratin 19) and thy1 including finally producing albumin. MSC injection resulted in apoptosis of hepatic stellate or perisinusoidal cells and resultant resolution of fibrosis, but did not cause apoptosis of hepatocytes (Hwang et al., 2012). In a swine model of acute liver failure, placenta-derived MSCs transplanted via the portal vein not only supported liver regeneration but also prolonged host survival (66.7 vs. 0%) (Cao et al., 2012).

In rat liver fibrosis model, transplantation of BM-MSCs through intravenous injection has been shown to give the best results and protect the liver against fibrosis through IL-10

expression compared to intrahepatic, and intraperitoneal transplantation. Action of IL-10 is by inhibiting IL6, TNF-α and TGF-β cytokines that stimulate tissue fibrosis (Zhao et al., 2012).

Non-induced and hepatocyte-induced MSCs have been used for the treatment of liver fibrosis. The MSC-derived hepatocyte-like cells engrafted in liver secrete growth factors that promote liver regeneration, suppress hepatic stellate cell activity, and secrete MMP, thereby removing deposited ECM (Takeda et al., 2005; Yannaki et al., 2005). Some studies have demonstrated that undifferentiated MSCs injected into rats with cirrhotic livers differentiated mainly into myofibroblasts and hepatic stellate cells and that both of these are promoters of liver fibrosis (Russo et al., 2006; Carvalho et al., 2008). However, phase I and II clinical trials for liver cirrhosis suggest that both differentiated (Kuo et al., 2008) and undifferentiated MSCs transplantation improved liver function (Kharaziha et al., 2009; El-Ansary et al., 2012a).

Patients intravenously transplanted with 10^6 MSCs/Kg of autologous BM-MSCs were followed up at 3 and 6 months after infusion. They showed partial improvement of liver function tests with elevation of prothrombin concentration and serum albumin levels, decline of elevated bilirubin and Model for End-Stage Liver Disease score (MELD) (El-Ansary et al., 2012a). Decompensated liver cirrhosis is a life-threatening complication of chronic liver disease. Thirty patients having a history of chronic HBV infection were intravenous transplanted with 5 x 10^6 allogenic UMCs /Kg. This transplantation showed a significant reduction in the volume of ascites. UMCs therapy significantly improved liver function, as indicated by the increase of serum albumin levels, decrease in total serum bilirubin levels, and decrease in the MELD scores during one-year follow-up studies (Zhang et al., 2012c).

UMCs for liver therapies

UMCs transplanted into the portal vein migrated and engrafted in fibrotic areas of chemically induced- liver fibrosis. Recovery of liver functions was observed with improved serum prothrombin time and serum albumin level. Immunohistochemical analysis showed engrafted UMCs produced albumin, HGF and MMPs. The transplanted UMCs may help to decrease liver collagen and may be useful for treating liver fibrosis (Lin et al., 2010). Liver injury induced by CCl4 administration was treated with human UMCs. Transplantation of UMCs suppressed serum transaminase activities and hepatocytes damage. Engrafted UMCs reduced hepatocyte apoptosis and promoted hepatocytes proliferation following the TUNNEL and PCNA stains (Yan et al., 2009). An investigation by Tsai et al. (2009) into the effect of human UMCs

on CCl4-induced liver fibrosis in rats have found that direct transplantation of UMCs into the liver reduced liver fibrosis significantly, as evidenced by Sirius red staining and a collagen content assay. The engrafted UMCs scattered mostly in the hepatic connective tissues and did not differentiate to hepatocytes. These undifferentiated HUMSCs appear to secrete a variety of bioactive cytokines that may restore liver function and promote regeneration (Tsai et al., 2009).

Kidney

There are multiple reports of MSCs repopulating the damaged kidney. Ischemia-reperfusion (IR) results in an inflammation response and fibrosis with immunosuppressive therapy are major causes of progressive renal failure after kidney transplantation. Intrarenal injection of bone-marrow-derived MSCs reduces kidney fibrosis after ischemia-reperfusion in cyclosporine-immunosuppressed rats. These effects were associated with a decrease in interstitial α-SMA accumulation and MMP2 activity, markers of fibrosis and renal remodeling (Alfarano et al., 2012). Initial studies reported that the exogenous administration of BM-MSCs via intravenous route to mice with acute renal injury could promote both structural and functional renal repair via the transdifferentiation of MSCs into tubular epithelium. Detection of MSCs at day 4 and day 29 after transplantation in the context of well-differentiated tubular epithelial lining indicated that MSCs repopulated the tubules, most likely by recruitment at peritubular sites where the Y-chromosome MSCs were also visualized in female kidney recipients. However, only 2–2.5% of the intravenously injected MSCs showed engraftment (Morigi et al., 2004).

The study of Herrera et al. (2007) demonstrated the role of CD44 and its major ligand, hyaluronic acid, in the trafficking of intravenously injected MSC to localize in kidney parenchyma in the glycerol-induced mouse model of acute renal failure (ARF) (Herrera et al., 2007). The direct engraftment of exogenously administered, and transdifferentiating MSCs was not the predominant mechanism in which MSCs enhance renal repair. MSCs could elicit kidney repair through paracrine and/or endocrine mechanisms, where they release trophic growth factors that modulate the immune response and consequently mediate repair. The ability of MSCs to inhibit the release of pro-inflammatory cytokines and secrete a variety of trophic growth factors that promote angiogenesis, mitogenesis, and proliferation whilst reducing apoptosis may

collectively mediate the protective and regenerative effects in the kidney of laboratory rodents (Wise and Ricardo, 2012).

In a rat model of acute kidney injury (AKI) established by unilateral renal ischemia before intravenous transplantation of UMCs, there was no evidence of UMCs engrafted at the ischemic areas. UMCs contributed to tubular EMT delay and the alleviation of renal fibrosis.

Induction of native and foreign HGF synthesis in damaged tubular epithelial cells at the initial stage of AKI leads to recovery of the disturbed balance of HGF/TGF-β1 during scar formation (Du et al., 2013). In a pilot clinical study of chronic kidney disease, two intravenous transplantations 1 week apart of ~1 million MSCs/kg body showed significant difference between each of serum creatinine and creatinine clearance levels before and after MSC injection at 1, 3, and 6 months after infusion (El-Ansary et al., 2012b).

Bone

Because of the lack of an adequate supply of autologous bone grafts and the unsuitability of allografts, there has been some motivation to use MSCs to encourage repair. Studies on murine models show promising results, especially for bone repair and metabolic bone disorders. In vitro expanded autologous BM-MSCs loaded on a 3-dimensional construct of porous hydroxyapatite scaffolds was used to cure bone nonunion and diaphyseal defects and resulted in good integration of implant (Undale et al., 2009). Complete fusion between the implant and the host bone occurred 5-7 months post operation. Follow up in patients for 6-7 years after surgery showed the good integration of implants maintained. Angiographic evaluation of implants after seven years showed vascularisation of the grafted zone, which is believed to be vital for the survival and future stability of the graft (Marcacci et al., 2007).

Autologous BM-MSCs derived from bone marrow were cultured with beta-tricalcium phosphate (β-TCP) ceramics granules before implanting into the cavity that remained after curettage of necrotic bone and ,finally, a free vascularized fibula was grafted. Osteonecrosis did not progress any further and early bone regeneration was observed (Kawate et al., 2006).

SDF-1 and its receptor CXCR4 have been shown to act as a potential homing signal for MSCs in bone healing. High expression of SDF-1 protein was observed in the periosteum of the live graft. New bone formation was inhibited by the administration of anti–SDF-1 antibody or TF14016 (Kitaori et al., 2009).

Osteogenesis imperfecta (OI) is a connective tissue disorder disease that osteoblasts produce defective type I collagen. This genetic disorder is characterized by bone fragility and other evidence of connective tissue malfunction. When MSCs from wild-type mice were infused into transgenic mice that had a phenotype of fragile bones resembling OI, the MSCs served as a source for continual renewal of cells in a number of nonhematopoietic tissues. Donor cells accounted for 4–19% of the fibroblasts or fibroblast-like cells obtained in primary cultures of the lung, calvaria, cartilage, long bone, tail, and skin (Pereira et al., 1998). Allogeneic bone marrow transplant in 3 children with OI showed osteoblast engraftment, that was nearly 2.0% donor cells. Histologic changes indicated new bone formation and increased total body bone mineral content (Horwitz et al., 1999). Horwitz et al. treated six children suffering from OI by systemic infusion of MSCs for bone regeneration. Five children showed acceleration of bone growth compared with matched unaffected children (Horwitz et al., 2002).

UMCs for lung injury

UMCs transplanted systemically into mouse model of bleomycin-induced lung injury showed engraftment at the fibrosis and inflammation areas of lung. Transplantation of UMCs reduced inflammation and secreted inflammatory cytokines. Anti-fibrotic effects of engrafted UMCs likely relate to reduction of secreted TGF-β, an activator of fibrosis through a Smad pathway (Wang et al., 2005). Moreover, UMCs increased matrix metalloproteinase-2 levels and reduced their endogenous inhibitors favoring a pro-degradative milieu following collagen deposition whereas transplanted fibroblasts did not have these properties (Moodley et al., 2009).

Antibacterial effects

MSCs possess intrinsic antimicrobial properties on the bacterial growth of Gram-negative and positive bacteria. Krasnodembskaya et al. (2010) reported MSCs derived from human bone marrow and their conditioned medium inhibited the growth of Escherichia coli, Pseudomonas aeruginosa and Staphylococcus aureus bacteria. Major antimicrobial peptide secreted from MSCs after induction by bacteria was the human cathelicidin antimicrobial peptide, hCAP-18/LL-37. In a mouse model of E. coli pneumonia, intratracheal administration of MSCs reduced bacterial growth in the lung homogenates and in the bronchoalveolar lavage (BAL) fluid indicating rapid bacterial clearance (Krasnodembskaya et al., 2010). LL-37 peptide secreted from MSCs not only had antimicrobial potential but could recruit migration of MSCs into the

damaged tissues via the formyl peptide receptor, FPLR-1 (Coffelt et al., 2009). Toll-like receptor (TLR4) expressed on the MSC surface has been reported to bind with LL-37 through a concentration gradient for activation of MSCs migration toward the source of infection and immunomodulatory properties (Tomchuck et al., 2008). A study of Meisel et al. (2011) showed that, on stimulation with inflammatory cytokines, IDO-positive human MSCs exhibited a cell autonomous, broad-spectrum antimicrobial effector function directed against clinically relevant bacteria, protozoa, parasite and virus. IDO expressed by induced MSCs played a role by depleting tryptophan, amino acid, required for microbial growth (Meisel et al., 2011)

References

Aggarwal, S., and M. F. Pittenger. 2005. Human mesenchymal stem cells modulate allogeneic immune cell responses. Blood. 105(4): 1815-1822.

Alfarano, C., C. Roubeix, R. Chaaya, C. Ceccaldi, D. Calise, C. Mias et al. 2012. Intraparenchymal injection of bone marrow mesenchymal stem cells reduces kidney fibrosis after ischemia-reperfusion in cyclosporine-immunosuppressed rats. Cell Transplant. 21(9): 2009-2019.

Annabi, B., Y. T. Lee, S. Turcotte, E. Naud, R. R. Desrosiers, M. Champagne et al. 2003. Hypoxia promotes murine bone-marrow-derived stromal cell migration and tube formation. Stem Cells. 21(3): 337-347.

Anzalone, R., M. Lo Iacono, S. Corrao, F. Magno, T. Loria, F. Cappello et al. 2010. New emerging potentials for human wharton's jelly mesenchymal stem cells: Immunological features and hepatocyte-like differentiative capacity. Stem Cells Dev. 19(4): 423-438.

Augello, A., T. B. Kurth, and C. De Bari. 2010. Mesenchymal stem cells: A perspective from in vitro cultures to in vivo migration and niches. Eur. Cell. Mater. 20: 121-133.

Ayuzawa, R., C. Doi, R. S. Rachakatla, M. M. Pyle, D. K. Maurya, D. Troyer et al. 2009. Naive human umbilical cord matrix derived stem cells significantly attenuate growth of human breast cancer cells in vitro and in vivo. Cancer Lett. 280(1): 31-37.

Baek, S. J., S. K. Kang, and J. C. Ra. 2011. In vitro migration capacity of human adipose-derived mesenchymal stem cells and their expression of a distinct set of chemokine and growth factor receptors. Exp Mol Med. 43(10): 569-603.

Bai, L., D. P. Lennon, V. Eaton, K. Maier, A. I. Caplan, S. D. Miller et al. 2009. Human bone marrow-derived mesenchymal stem cells induce Th2-polarized immune response and promote endogenous repair in animal models of multiple sclerosis. Glia. 57(11): 1192-1203.

Bailey, M. M., L. Wang, C. J. Bode, K. E. Mitchell, and M. S. Detamore. 2007. A comparison of human umbilical cord matrix stem cells and temporomandibular joint condylar chondrocytes for tissue engineering temporomandibular joint condylar cartilage. Tissue Eng. 13(8): 2003-2010.

Bakhshi, T., R. C. Zabriskie, S. Bodie, S. Kidd, S. Ramin, L. A. Paganessi et al. 2008. Mesenchymal stem cells from the wharton's jelly of umbilical cord segments provide stromal support for the maintenance of cord blood hematopoietic stem cells during long-term ex vivo culture. Transfusion. 48(12): 2638-2644.

Baksh, D., R. Yao, and R. S. Tuan. 2007. Comparison of proliferative and multilineage differentiation potential of human mesenchymal stem cells derived from umbilical cord and bone marrow. Stem Cells. 25(6): 1384-1392.

Balasubramanian, S., C. Thej, P. Venugopal, N. Priya, Z. Zakaria, S. Sundarraj et al. 2013. Higher propensity of wharton's jelly derived mesenchymal stromal cells towards neuronal lineage in comparison to those derived from adipose and bone marrow. Cell Biol. Int. 37(5): 507-515.

Bankowski, E., K. Sobolewski, L. Romanowicz, L. Chyczewski, and S. Jaworski. 1996. Collagen and glycosaminoglycans of wharton's jelly and their alterations in EPH-gestosis. Eur. J. Obstet. Gynecol. Reprod. Biol. 66(2): 109-117.

Barbash, I. M., P. Chouraqui, J. Baron, M. S. Feinberg, S. Etzion, A. Tessone et al. 2003. Systemic delivery of bone marrow-derived mesenchymal stem cells to the infarcted myocardium: Feasibility, cell migration, and body distribution. Circulation. 108(7): 863-868.

Barlow, S., G. Brooke, K. Chatterjee, G. Price, R. Pelekanos, T. Rossetti et al. 2008. Comparison of human placenta- and bone marrow-derived multipotent mesenchymal stem cells. Stem Cells Dev. 17(6): 1095-1107.

Bartholomew, A., C. Sturgeon, M. Siatskas, K. Ferrer, K. McIntosh, S. Patil et al. 2002. Mesenchymal stem cells suppress lymphocyte proliferation in vitro and prolong skin graft survival in vivo. Exp. Hematol. 30(1): 42-48.

Batsali, A. K., M. C. Kastrinaki, H. A. Papadaki, and C. Pontikoglou. 2013. Mesenchymal stem cells derived from wharton's jelly of the umbilical cord: Biological properties and emerging clinical applications. Curr. Stem Cell. Res. Ther. 8(2): 144-155.

Belema-Bedada, F., S. Uchida, A. Martire, S. Kostin, and T. Braun. 2008. Efficient homing of multipotent adult mesenchymal stem cells depends on FROUNT-mediated clustering of CCR2. Cell. Stem Cell. 2(6): 566-575.

Bianco, P., M. Riminucci, S. Gronthos, and P. G. Robey. 2001. Bone marrow stromal stem cells: Nature, biology, and potential applications. Stem Cells. 19(3): 180-192.

Bilic, G., S. M. Zeisberger, A. S. Mallik, R. Zimmermann, and A. H. Zisch. 2008. Comparative characterization of cultured human term amnion epithelial and mesenchymal stromal cells for application in cell therapy. Cell Transplant. 17(8): 955-968.

Blackburn, E. H. 2001. Switching and signaling at the telomere. Cell. 106(6): 661-673.

Blasco, M. A. 2005. Telomeres and human disease: Ageing, cancer and beyond. Nat. Rev. Genet. 6(8): 611-622.

Bongso, A., C. Y. Fong, and K. Gauthaman. 2008. Taking stem cells to the clinic: Major challenges. J. Cell. Biochem. 105(6): 1352-1360.

Campard, D., P. A. Lysy, M. Najimi, and E. M. Sokal. 2008. Native umbilical cord matrix stem cells express hepatic markers and differentiate into hepatocyte-like cells. Gastroenterology. 134(3): 833-848.

Cao, H., J. Yang, J. Yu, Q. Pan, J. Li, P. Zhou et al. 2012. Therapeutic potential of transplanted placental mesenchymal stem cells in treating chinese miniature pigs with acute liver failure. BMC Med. 10: 56-7015-10-56.

Cardoso, T. C., H. F. Ferrari, A. F. Garcia, J. B. Novais, C. Silva-Frade, M. C. Ferrarezi et al. 2012. Isolation and characterization of wharton's jelly-derived multipotent mesenchymal stromal cells obtained from bovine umbilical cord and maintained in a defined serum-free three-dimensional system. BMC Biotechnol. 12: 18-6750-12-18.

Carlin, R., D. Davis, M. Weiss, B. Schultz, and D. Troyer. 2006. Expression of early transcription factors oct-4, sox-2 and nanog by porcine umbilical cord (PUC) matrix cells. Reprod. Biol. Endocrinol. 4: 8.

Carvalho, A. B., L. F. Quintanilha, J. V. Dias, B. D. Paredes, E. G. Mannheimer, F. G. Carvalho et al. 2008. Bone marrow multipotent mesenchymal stromal cells do not reduce fibrosis or improve function in a rat model of severe chronic liver injury. Stem Cells. 26(5): 1307-1314.

Chan, J., S. N. Waddington, K. O'Donoghue, H. Kurata, P. V. Guillot, C. Gotherstrom et al. 2007. Widespread distribution and muscle differentiation of human fetal mesenchymal stem cells after intrauterine transplantation in dystrophic mdx mouse. Stem Cells. 25(4): 875-884.

Chao, K. C., K. F. Chao, Y. S. Fu, and S. H. Liu. 2008. Islet-like clusters derived from mesenchymal stem cells in wharton's jelly of the human umbilical cord for transplantation to control type 1 diabetes. PLoS One. 3(1): e1451.

Chapel, A., J. M. Bertho, M. Bensidhoum, L. Fouillard, R. G. Young, J. Frick et al. 2003. Mesenchymal stem cells home to injured tissues when co-infused with hematopoietic cells to treat a radiation-induced multi-organ failure syndrome. J. Gene Med. 5(12): 1028-1038.

Chavakis, E., C. Urbich, and S. Dimmeler. 2008. Homing and engraftment of progenitor cells: A prerequisite for cell therapy. J. Mol. Cell. Cardiol. 45(4): 514-522.

Che, N., X. Li, S. Zhou, R. Liu, D. Shi, L. Lu et al. 2012. Umbilical cord mesenchymal stem cells suppress B-cell proliferation and differentiation. Cell. Immunol. 274(1-2): 46-53.

Chen, G. H., T. Yang, H. Tian, M. Qiao, H. W. Liu, C. C. Fu et al. 2012. Clinical study of umbilical cord-derived mesenchymal stem cells for treatment of nineteen patients with steroid-resistant severe acute graft-versus-host disease. Zhonghua Xue Ye Xue Za Zhi. 33(4): 303-306.

Chen, K., D. Wang, W. T. Du, Z. B. Han, H. Ren, Y. Chi et al. 2010. Human umbilical cord mesenchymal stem cells hUC-MSCs exert immunosuppressive activities through a PGE2-dependent mechanism. Clin. Immunol. 135(3): 448-458.

Chen, M. Y., P. C. Lie, Z. L. Li, and X. Wei. 2009. Endothelial differentiation of wharton's jelly-derived mesenchymal stem cells in comparison with bone marrow-derived mesenchymal stem cells. Exp. Hematol. 37(5): 629-640.

Chen, X., F. Zhang, X. He, Y. Xu, Z. Yang, L. Chen et al. 2013. Chondrogenic differentiation of umbilical cord-derived mesenchymal stem cells in type I collagen-hydrogel for cartilage engineering. Injury. 44(4): 540-549.

Cheng, P. H., B. Snyder, D. Fillos, C. C. Ibegbu, A. H. Huang, and A. W. Chan. 2008a. Postnatal stem/progenitor cells derived from the dental pulp of adult chimpanzee. BMC Cell Biol. 9: 20-2121-9-20.

Cheng, Z., L. Ou, X. Zhou, F. Li, X. Jia, Y. Zhang et al. 2008b. Targeted migration of mesenchymal stem cells modified with CXCR4 gene to infarcted myocardium improves cardiac performance. Mol. Ther. 16(3): 571-579.

Cho, K. S., H. K. Park, H. Y. Park, J. S. Jung, S. G. Jeon, Y. K. Kim et al. 2009. IFATS collection: Immunomodulatory effects of adipose tissue-derived stem cells in an allergic rhinitis mouse model. Stem Cells. 27(1): 259-265.

Cho, P. S., D. J. Messina, E. L. Hirsh, N. Chi, S. N. Goldman, D. P. Lo et al. 2008. Immunogenicity of umbilical cord tissue derived cells. Blood. 111(1): 430-438.

Choi, H., J. S. Cho, I. H. Park, H. G. Yoon, and H. M. Lee. 2011. Effects of microelectrical current on migration of nasal fibroblasts. Am. J. Rhinol. Allergy. 25(3): 157-162.

Christodoulou, I., F. N. Kolisis, D. Papaevangeliou, and V. Zoumpourlis. 2013. Comparative evaluation of human mesenchymal stem cells of fetal (wharton's jelly) and adult (adipose tissue) origin during prolonged in vitro expansion: Considerations for cytotherapy. Stem Cells Int. 2013: 246134.

Coffelt, S. B., F. C. Marini, K. Watson, K. J. Zwezdaryk, J. L. Dembinski, H. L. LaMarca et al. 2009. The pro-inflammatory peptide LL-37 promotes ovarian tumor progression through recruitment of multipotent mesenchymal stromal cells. Proc. Natl. Acad. Sci. U. S. A. 106(10): 3806-3811.

Conconi, M. T., P. Burra, R. Di Liddo, C. Calore, M. Turetta, S. Bellini et al. 2006. CD105(+) cells from wharton's jelly show in vitro and in vivo myogenic differentiative potential. Int. J. Mol. Med. 18(6): 1089-1096.

Constantin, G., S. Marconi, B. Rossi, S. Angiari, L. Calderan, E. Anghileri et al. 2009. Adipose-derived mesenchymal stem cells ameliorate chronic experimental autoimmune encephalomyelitis. Stem Cells. 27(10): 2624-2635.

Corrao, S., G. La Rocca, M. Lo Iacono, T. Corsello, F. Farina, and R. Anzalone. 2013. Umbilical cord revisited: From wharton's jelly myofibroblasts to mesenchymal stem cells. Histol. Histopathol.

De Becker, A., P. Van Hummelen, M. Bakkus, I. Vande Broek, J. De Wever, M. De Waele et al. 2007. Migration of culture-expanded human mesenchymal stem cells through bone marrow endothelium is regulated by matrix metalloproteinase-2 and tissue inhibitor of metalloproteinase-3. Haematologica. 92(4): 440-449.

De Girolamo, L., M. F. Sartori, E. Arrigoni, L. Rimondini, W. Albisetti, R. L. Weinstein et al. 2008. Human adipose-derived stem cells as future tools in tissue regeneration:

Osteogenic differentiation and cell-scaffold interaction. Int. J. Artif. Organs. 31(6): 467-479.

Deak, E., E. Seifried, and R. Henschler. 2010. Homing pathways of mesenchymal stromal cells (MSCs) and their role in clinical applications. Int. Rev. Immunol. 29(5): 514-529.

DeSantiago, J., D. J. Bare, I. Semenov, R. D. Minshall, D. L. Geenen, B. M. Wolska et al. 2012. Excitation-contraction coupling in ventricular myocytes is enhanced by paracrine signaling from mesenchymal stem cells. J. Mol. Cell. Cardiol. 52(6): 1249-1256.

Deuse, T., M. Stubbendorff, K. Tang-Quan, N. Phillips, M. A. Kay, T. Eiermann et al. 2011. Immunogenicity and immunomodulatory properties of umbilical cord lining mesenchymal stem cells. Cell Transplant. 20(5): 655-667.

Devine, S. M., C. Cobbs, M. Jennings, A. Bartholomew, and R. Hoffman. 2003. Mesenchymal stem cells distribute to a wide range of tissues following systemic infusion into nonhuman primates. Blood. 101(8): 2999-3001.

Doi, C., D. K. Maurya, M. M. Pyle, D. Troyer, and M. Tamura. 2010. Cytotherapy with naive rat umbilical cord matrix stem cells significantly attenuates growth of murine pancreatic cancer cells and increases survival in syngeneic mice. Cytotherapy. 12(3): 408-417.

Dominici, M., K. Le Blanc, I. Mueller, I. Slaper-Cortenbach, F. Marini, D. Krause et al. 2006. Minimal criteria for defining multipotent mesenchymal stromal cells. the international society for cellular therapy position statement. Cytotherapy. 8(4): 315-317.

Du, T., X. Zou, J. Cheng, S. Wu, L. Zhong, G. Ju et al. 2013. Human wharton's jelly-derived mesenchymal stromal cells reduce renal fibrosis through induction of native and foreign hepatocyte growth factor synthesis in injured tubular epithelial cells. Stem Cell. Res. Ther. 4(3): 59.

Duijvestein, M., A. C. Vos, H. Roelofs, M. E. Wildenberg, B. B. Wendrich, H. W. Verspaget et al. 2010. Autologous bone marrow-derived mesenchymal stromal cell treatment for refractory luminal crohn's disease: Results of a phase I study. Gut. 59(12): 1662-1669.

El-Ansary, M., I. Abdel-Aziz, S. Mogawer, S. Abdel-Hamid, O. Hammam, S. Teaema et al. 2012a. Phase II trial: Undifferentiated versus differentiated autologous mesenchymal stem cells transplantation in egyptian patients with HCV induced liver cirrhosis. Stem Cell. Rev. 8(3): 972-981.

El-Ansary, M., G. Saadi, and S. M. Abd El-Hamid. 2012b. Mesenchymal stem cells are a rescue approach for recovery of deteriorating kidney function. Nephrology (Carlton). 17(7): 650-657.

Ezquer, F., M. Ezquer, D. Contador, M. Ricca, V. Simon, and P. Conget. 2012. The antidiabetic effect of mesenchymal stem cells is unrelated to their transdifferentiation potential but to their capability to restore Th1/Th2 balance and to modify the pancreatic microenvironment. Stem Cells. 30(8): 1664-1674.

Fatar, M., M. Stroick, M. Griebe, I. Marwedel, S. Kern, K. Bieback et al. 2008. Lipoaspirate-derived adult mesenchymal stem cells improve functional outcome during intracerebral hemorrhage by proliferation of endogenous progenitor cells stem cells in intracerebral hemorrhages. Neurosci. Lett. 443(3): 174-178.

Fong, C. Y., M. Richards, N. Manasi, A. Biswas, and A. Bongso. 2007. Comparative growth behaviour and characterization of stem cells from human wharton's jelly. Reprod. Biomed. Online. 15(6): 708-718.

Francois, S., M. Bensidhoum, M. Mouiseddine, C. Mazurier, B. Allenet, A. Semont et al. 2006. Local irradiation not only induces homing of human mesenchymal stem cells at exposed sites but promotes their widespread engraftment to multiple organs: A study of their quantitative distribution after irradiation damage. Stem Cells. 24(4): 1020-1029.

Freyman, T., G. Polin, H. Osman, J. Crary, M. Lu, L. Cheng et al. 2006. A quantitative, randomized study evaluating three methods of mesenchymal stem cell delivery following myocardial infarction. Eur. Heart J. 27(9): 1114-1122.

Friedman, R., M. Betancur, L. Boissel, H. Tuncer, C. Cetrulo, and H. Klingemann. 2007. Umbilical cord mesenchymal stem cells: Adjuvants for human cell transplantation. Biol. Blood Marrow Transplant. 13(12): 1477-1486.

Fu, Y. S., Y. C. Cheng, M. Y. Lin, H. Cheng, P. M. Chu, S. C. Chou et al. 2006. Conversion of human umbilical cord mesenchymal stem cells in wharton's jelly to dopaminergic neurons in vitro: Potential therapeutic application for parkinsonism. Stem Cells. 24(1): 115-124.

Gang, E. J., D. Bosnakovski, C. A. Figueiredo, J. W. Visser, and R. C. Perlingeiro. 2007. SSEA-4 identifies mesenchymal stem cells from bone marrow. Blood. 109(4): 1743-1751.

Gauthaman, K., C. Y. Fong, S. Arularasu, A. Subramanian, A. Biswas, M. Choolani et al. 2013. Human wharton's jelly stem cell conditioned medium and cell-free lysate inhibit human osteosarcoma and mammary carcinoma cell growth in vitro and in xenograft mice. J. Cell. Biochem. 114(2): 366-377.

Gerdoni, E., B. Gallo, S. Casazza, S. Musio, I. Bonanni, E. Pedemonte et al. 2007. Mesenchymal stem cells effectively modulate pathogenic immune response in experimental autoimmune encephalomyelitis. Ann. Neurol. 61(3): 219-227.

Gluckman, E. 2000. Current status of umbilical cord blood hematopoietic stem cell transplantation. Exp. Hematol. 28(11): 1197-1205.

Gonzalez-Rey, E., P. Anderson, M. A. Gonzalez, L. Rico, D. Buscher, and M. Delgado. 2009. Human adult stem cells derived from adipose tissue protect against experimental colitis and sepsis. Gut. 58(7): 929-939.

Gordon, D., G. Pavlovska, C. P. Glover, J. B. Uney, D. Wraith, and N. J. Scolding. 2008. Human mesenchymal stem cells abrogate experimental allergic encephalomyelitis after intraperitoneal injection, and with sparse CNS infiltration. Neurosci. Lett. 448(1): 71-73.

Guillot, P. V., C. Gotherstrom, J. Chan, H. Kurata, and N. M. Fisk. 2007. Human first-trimester fetal MSC express pluripotency markers and grow faster and have longer telomeres than adult MSC. Stem Cells. 25(3): 646-654.

Guo, Q. S., M. Y. Zhu, L. Wang, X. J. Fan, Y. H. Lu, Z. W. Wang et al. 2012. Combined transfection of the three transcriptional factors, PDX-1, NeuroD1, and MafA, causes differentiation of bone marrow mesenchymal stem cells into insulin-producing cells. Exp. Diabetes Res. 2012: 672013.

Gurtner, G. C., S. Werner, Y. Barrandor and M. T. Longaker. 2008. Wound repair and regeneration. Nature. 453: 314-321.

Hao, H., G. Chen, J. Liu, D. Ti, Y. Zhao, S. Xu et al. 2013. Culturing on wharton's jelly extract delays mesenchymal stem cell senescence through p53 and p16INK4a/pRb pathways. PLoS One. 8(3): e58314.

Hao, M., H. X. Meng, G. Li, P. J. Qi, Y. Xu, C. H. Li et al. 2009. Study of influence of umbilical cord mesenchymal stem cells on CD34+ cells in vivo homing in NOD/SCID. Zhonghua Xue Ye Xue Za Zhi. 30(2): 103-106.

Hare, J. M., J. H. Traverse, T. D. Henry, N. Dib, R. K. Strumpf, S. P. Schulman et al. 2009. A randomized, double-blind, placebo-controlled, dose-escalation study of intravenous adult human mesenchymal stem cells (prochymal) after acute myocardial infarction. J. Am. Coll. Cardiol. 54(24): 2277-2286.

Hermann, A., R. Gastl, S. Liebau, M. O. Popa, J. Fiedler, B. O. Boehm et al. 2004. Efficient generation of neural stem cell-like cells from adult human bone marrow stromal cells. J. Cell. Sci. 117(Pt 19): 4411-4422.

Herrera, M. B., B. Bussolati, S. Bruno, V. Fonsato, G. M. Romanazzi, and G. Camussi. 2004. Mesenchymal stem cells contribute to the renal repair of acute tubular epithelial injury. Int. J. Mol. Med. 14(6): 1035-1041.

Herrera, M. B., B. Bussolati, S. Bruno, L. Morando, G. Mauriello-Romanazzi, F. Sanavio et al. 2007. Exogenous mesenchymal stem cells localize to the kidney by means of CD44 following acute tubular injury. Kidney Int. 72(4): 430-441.

Hiroyama, T., K. Sudo, N. Aoki, K. Miharada, I. Danjo, T. Fujioka et al. 2008. Human umbilical cord-derived cells can often serve as feeder cells to maintain primate embryonic stem cells in a state capable of producing hematopoietic cells. Cell Biol. Int. 32(1): 1-7.

Ho, J. H., T. C. Tseng, W. H. Ma, W. K. Ong, Y. F. Chen, M. H. Chen et al. 2012. Multiple intravenous transplantations of mesenchymal stem cells effectively restore long-term blood glucose homeostasis by hepatic engraftment and beta-cell differentiation in streptozocin-induced diabetic mice. Cell Transplant. 21(5): 997-1009.

Horita, Y., O. Honmou, K. Harada, K. Houkin, H. Hamada, and J. D. Kocsis. 2006. Intravenous administration of glial cell line-derived neurotrophic factor gene-modified human mesenchymal stem cells protects against injury in a cerebral ischemia model in the adult rat. J. Neurosci. Res. 84(7): 1495-1504.

Horwitz, E. M., D. J. Prockop, L. A. Fitzpatrick, W. W. Koo, P. L. Gordon, M. Neel et al. 1999. Transplantability and therapeutic effects of bone marrow-derived mesenchymal cells in children with osteogenesis imperfecta. Nat. Med. 5(3): 309-313.

Horwitz, E. M., P. L. Gordon, W. K. Koo, J. C. Marx, M. D. Neel, R. Y. McNall et al. 2002. Isolated allogeneic bone marrow-derived mesenchymal cells engraft and stimulate growth in children with osteogenesis imperfecta: Implications for cell therapy of bone. Proc. Natl. Acad. Sci. U. S. A. 99(13): 8932-8937.

Hsiao, J. K., M. F. Tai, H. H. Chu, S. T. Chen, H. Li, D. M. Lai et al. 2007. Magnetic nanoparticle labeling of mesenchymal stem cells without transfection agent: Cellular behavior and capability of detection with clinical 1.5 T magnetic resonance at the single cell level. Magn. Reson. Med. 58(4): 717-724.

Hsieh, J. Y., Y. S. Fu, S. J. Chang, Y. H. Tsuang, and H. W. Wang. 2010. Functional module analysis reveals differential osteogenic and stemness potentials in human mesenchymal stem cells from bone marrow and wharton's jelly of umbilical cord. Stem Cells Dev. 19(12): 1895-1910.

Hu, J., X. Yu, Z. Wang, F. Wang, L. Wang, H. Gao et al. 2013a. Long term effects of the implantation of wharton's jelly-derived mesenchymal stem cells from the umbilical cord for newly-onset type 1 diabetes mellitus. Endocr. J. 60(3): 347-357.

Hu, L., J. Hu, J. Zhao, J. Liu, W. Ouyang, C. Yang et al. 2013b. Side-by-side comparison of the biological characteristics of human umbilical cord and adipose tissue-derived mesenchymal stem cells. Biomed. Res. Int. 2013: 438243.

Huang, M., Y. Li, H. Zhang, and F. Nan. 2010. Breast cancer stromal fibroblasts promote the generation of CD44+CD24- cells through SDF-1/CXCR4 interaction. J. Exp. Clin. Cancer Res. 29: 80-9966-29-80.

Huang, Y. C., O. Parolini, G. La Rocca, and L. Deng. 2012. Umbilical cord versus bone marrow-derived mesenchymal stromal cells. Stem Cells Dev. 21(15): 2900-2903.

Hung, S. C., R. R. Pochampally, S. C. Hsu, C. Sanchez, S. C. Chen, J. Spees et al. 2007. Short-term exposure of multipotent stromal cells to low oxygen increases their expression of CX3CR1 and CXCR4 and their engraftment in vivo. PLoS One. 2(5): e416.

Hwang, S., H. N. Hong, H. S. Kim, S. R. Park, Y. J. Won, S. T. Choi et al. 2012. Hepatogenic differentiation of mesenchymal stem cells in a rat model of thioacetamide-induced liver cirrhosis. Cell Biol. Int. 36(3): 279-288.

Ip, J. E., Y. Wu, J. Huang, L. Zhang, R. E. Pratt, and V. J. Dzau. 2007. Mesenchymal stem cells use integrin beta1 not CXC chemokine receptor 4 for myocardial migration and engraftment. Mol. Biol. Cell. 18(8): 2873-2882.

Jeon, B. G., B. M. Kumar, E. J. Kang, S. A. Ock, S. L. Lee, D. O. Kwack et al. 2011. Characterization and comparison of telomere length, telomerase and reverse transcriptase

activity and gene expression in human mesenchymal stem cells and cancer cells of various origins. Cell Tissue Res. 345(1): 149-161.

Jiang, W., A. Ma, T. Wang, K. Han, Y. Liu, Y. Zhang et al. 2006. Homing and differentiation of mesenchymal stem cells delivered intravenously to ischemic myocardium in vivo: A time-series study. Pflugers Arch. 453(1): 43-52.

Jiang, X. X., Y. Zhang, B. Liu, S. X. Zhang, Y. Wu, X. D. Yu et al. 2005. Human mesenchymal stem cells inhibit differentiation and function of monocyte-derived dendritic cells. Blood. 105(10): 4120-4126.

Jomura, S., M. Uy, K. Mitchell, R. Dallasen, C. J. Bode, and Y. Xu. 2007. Potential treatment of cerebral global ischemia with oct-4+ umbilical cord matrix cells. Stem Cells. 25(1): 98-106.

Karahuseyinoglu, S., O. Cinar, E. Kilic, F. Kara, G. G. Akay, D. O. Demiralp et al. 2007. Biology of stem cells in human umbilical cord stroma: In situ and in vitro surveys. Stem Cells. 25(2): 319-331.

Karussis, D., I. Kassis, B. G. Kurkalli, and S. Slavin. 2008. Immunomodulation and neuroprotection with mesenchymal bone marrow stem cells (MSCs): A proposed treatment for multiple sclerosis and other neuroimmunological/neurodegenerative diseases. J. Neurol. Sci. 265(1-2): 131-135.

Kawabata, A., N. Ohta, G. Seiler, M. M. Pyle, S. Ishiguro, Y. Q. Zhang et al. 2013. Naive rat umbilical cord matrix stem cells significantly attenuate mammary tumor growth through modulation of endogenous immune responses. Cytotherapy. 15(5): 586-597.

Kawada, H., J. Fujita, K. Kinjo, Y. Matsuzaki, M. Tsuma, H. Miyatake et al. 2004. Nonhematopoietic mesenchymal stem cells can be mobilized and differentiate into cardiomyocytes after myocardial infarction. Blood. 104(12): 3581-3587.

Kawakami, Y., J. Rodriguez-Leon, and J. C. Izpisua Belmonte. 2006. The role of TGFbetas and Sox9 during limb chondrogenesis. Curr. Opin. Cell Biol. 18(6): 723-729.

Kawate, K., H. Yajima, H. Ohgushi, N. Kotobuki, K. Sugimoto, T. Ohmura et al. 2006. Tissue-engineered approach for the treatment of steroid-induced osteonecrosis of the femoral head: Transplantation of autologous mesenchymal stem cells cultured with beta-tricalcium phosphate ceramics and free vascularized fibula. Artif. Organs. 30(12): 960-962.

Karaoz, E., A. Okcu, Z. S. Unal, C. Subasi, O. Saglam, and G. Duruksu. 2013. Adipose tissue-derived mesenchymal stromal cells efficiently differentiate into insulin-producing cells in pancreatic islet microenvironment both in vitro and in vivo. Cytotherapy. 15(5): 557-570.

Kebriaei, P., L. Isola, E. Bahceci, K. Holland, S. Rowley, J. McGuirk et al. 2009. Adult human mesenchymal stem cells added to corticosteroid therapy for the treatment of acute graft-versus-host disease. Biol. Blood Marrow Transplant. 15(7): 804-811.

Kharaziha, P., P. M. Hellstrom, B. Noorinayer, F. Farzaneh, K. Aghajani, F. Jafari et al. 2009. Improvement of liver function in liver cirrhosis patients after autologous mesenchymal stem cell injection: A phase I-II clinical trial. Eur. J. Gastroenterol. Hepatol. 21(10): 1199-1205.

Kim, D. W., Y. J. Chung, T. G. Kim, Y. L. Kim, and I. H. Oh. 2004. Cotransplantation of third-party mesenchymal stromal cells can alleviate single-donor predominance and increase engraftment from double cord transplantation. Blood. 103(5): 1941-1948

Kitaori, T., H. Ito, E. M. Schwarz, R. Tsutsumi, H. Yoshitomi, S. Oishi et al. 2009. Stromal cell-derived factor 1/CXCR4 signaling is critical for the recruitment of mesenchymal stem cells to the fracture site during skeletal repair in a mouse model. Arthritis Rheum. 60(3): 813-823.

Ko, I. K., B. G. Kim, A. Awadallah, J. Mikulan, P. Lin, J. J. Letterio et al. 2010. Targeting improves MSC treatment of inflammatory bowel disease. Mol. Ther. 18(7): 1365-1372.

Kocaefe, C., D. Balci, B. B. Hayta, and A. Can. 2010. Reprogramming of human umbilical cord stromal mesenchymal stem cells for myogenic differentiation and muscle repair. Stem Cell. Rev. 6(4): 512-522.

Kraitchman, D. L., M. Tatsumi, W. D. Gilson, T. Ishimori, D. Kedziorek, P. Walczak et al. 2005. Dynamic imaging of allogeneic mesenchymal stem cells trafficking to myocardial infarction. Circulation. 112(10): 1451-1461.

Krasnodembskaya, A., Y. Song, X. Fang, N. Gupta, V. Serikov, J. W. Lee et al. 2010. Antibacterial effect of human mesenchymal stem cells is mediated in part from secretion of the antimicrobial peptide LL-37. Stem Cells. 28(12): 2229-2238.

Kumar, S., and S. Ponnazhagan. 2007. Bone homing of mesenchymal stem cells by ectopic alpha 4 integrin expression. FASEB J. 21(14): 3917-3927.

Kuo, T. K., S. P. Hung, C. H. Chuang, C. T. Chen, Y. R. Shih, S. C. Fang et al. 2008. Stem cell therapy for liver disease: Parameters governing the success of using bone marrow mesenchymal stem cells. Gastroenterology. 134(7): 2111-21, 2121.e1-3.

Kwon, D. S., X. Gao, Y. B. Liu, D. S. Dulchavsky, A. L. Danyluk, M. Bansal et al. 2008. Treatment with bone marrow-derived stromal cells accelerates wound healing in diabetic rats. Int. Wound. J. 5(3): 453-463.

La Rocca, G., R. Anzalone, S. Corrao, F. Magno, T. Loria, M. Lo Iacono et al. 2009. Isolation and characterization of oct-4+/HLA-G+ mesenchymal stem cells from human umbilical cord matrix: Differentiation potential and detection of new markers. Histochem. Cell Biol. 131(2): 267-282.

Lazarus, H. M., S. E. Haynesworth, S. L. Gerson, N. S. Rosenthal, and A. I. Caplan. 1995. Ex vivo expansion and subsequent infusion of human bone marrow-derived stromal progenitor cells (mesenchymal progenitor cells): Implications for therapeutic use. Bone Marrow Transplant. 16(4): 557-564.

Le Blanc, K., I. Rasmusson, B. Sundberg, C. Gotherstrom, M. Hassan, M. Uzunel et al. 2004. Treatment of severe acute graft-versus-host disease with third party haploidentical mesenchymal stem cells. Lancet. 363(9419): 1439-1441.

Le Blanc, K., F. Frassoni, L. Ball, F. Locatelli, H. Roelofs, I. Lewis et al. 2008. Mesenchymal stem cells for treatment of steroid-resistant, severe, acute graft-versus-host disease: A phase II study. Lancet. 371(9624): 1579-1586.

Lee, R. H., M. J. Seo, A. A. Pulin, C. A. Gregory, J. Ylostalo, and D. J. Prockop. 2009. The CD34-like protein PODXL and alpha6-integrin (CD49f) identify early progenitor MSCs with increased clonogenicity and migration to infarcted heart in mice. Blood. 113(4): 816-826.

Levenberg, S., J. Rouwkema, M. Macdonald, E. S. Garfein, D. S. Kohane, D. C. Darland et al. 2005. Engineering vascularized skeletal muscle tissue. Nat. Biotechnol. 23(7): 879-884.

Ley, K., C. Laudanna, M. I. Cybulsky, and S. Nourshargh. 2007. Getting to the site of inflammation: The leukocyte adhesion cascade updated. Nat. Rev. Immunol. 7(9): 678-689.

Li, J., D. Li, X. Ju, Q. Shi, D. Wang and F. Wei. 2012. Umbilical cord-derived mesenchymal stem cells retain immunomodulatory and anti-oxidative activities after neural induction. Neural Regen Res. 7(34): 2663-2672.

Li, N., P. Feugier, B. Serrurrier, V. Latger-Cannard, J. F. Lesesve, J. F. Stoltz et al. 2007. Human mesenchymal stem cells improve ex vivo expansion of adult human CD34+ peripheral blood progenitor cells and decrease their allostimulatory capacity. Exp. Hematol. 35(3): 507-515.

Liang, J., H. Zhang, D. Wang, X. Feng, H. Wang, B. Hua et al. 2012. Allogeneic mesenchymal stem cell transplantation in seven patients with refractory inflammatory bowel disease. Gut. 61(3): 468-469.

Liao, W., J. Zhong, J. Yu, J. Xie, Y. Liu, L. Du, S. Yang, P. Liu, J. Xu, J. Wang, Z. Han and Z. C. Han. 2009a. Therapeutic benefit of human umbilical cord derived mesenchymal stromal cells in intracerebral hemorrhage rat: Implications of anti-inflammation and angiogenesis. Cell Physiol Biochem. 24(3): 307–316.

Liao, W., J. Xie, J. Zhong, Y. Liu, L. Du, B. Zhou, J. Xu, P. Liu, S. Yang, J. Wang, Z. Han and Z. C. Han. 2009b. Therapeutic effect of human umbilical cord multipotent mesenchymal stromal cells in a rat model of stroke. Transplantation. 87(3): 350-359.

Lin, S. Z., Y. J. Chang, J. W. Liu, L. F. Chang, L. Y. Sun, Y. S. Li et al. 2010. Transplantation of human wharton's jelly-derived stem cells alleviates chemically induced liver fibrosis in rats. Cell Transplant. 19(11): 1451-1463.

Lin, Y. C., T. L. Ko, Y. H. Shih, M. Y. Lin, T. W. Fu, H. S. Hsiao et al. 2011. Human umbilical mesenchymal stem cells promote recovery after ischemic stroke. Stroke. 42(7): 2045-2053.

Lopez, Y., K. Seshareddy, E. Trevino, J. Cox and M. L. Weiss. 2011. Evaluating the impact of oxygen concentration and plating density on human Wharton’s jelly-derived mesenchymal stem cells. Open Tissue Eng Regen Med J. 4: 82-94.

Lorda-Diez, C. I., J. A. Montero, C. Martinez-Cue, J. A. Garcia-Porrero, and J. M. Hurle. 2009. Transforming growth factors beta coordinate cartilage and tendon differentiation in the developing limb mesenchyme. J. Biol. Chem. 284(43): 29988-29996.

Lovati, A. B., B. Corradetti, A. Lange Consiglio, C. Recordati, E. Bonacina, D. Bizzaro et al. 2011. Comparison of equine bone marrow-, umbilical cord matrix and amniotic fluid-derived progenitor cells. Vet. Res. Commun. 35(2): 103-121.

Lu, L. L., Y. J. Liu, S. G. Yang, Q. J. Zhao, X. Wang, W. Gong et al. 2006. Isolation and characterization of human umbilical cord mesenchymal stem cells with hematopoiesis-supportive function and other potentials. Haematologica. 91(8): 1017-1026.

Lu, L. L., Y. P. Song, X. D. Wei, B. J. Fang, Y. L. Zhang, and Y. F. Li. 2008. Comparative characterization of mesenchymal stem cells from human umbilical cord tissue and bone marrow. Zhongguo Shi Yan Xue Ye Xue Za Zhi. 16(1): 140-146.

Lund, R. D., S. Wang, B. Lu, S. Girman, T. Holmes, Y. Sauve et al. 2007. Cells isolated from umbilical cord tissue rescue photoreceptors and visual functions in a rodent model of retinal disease. Stem Cells. 25(3): 602-611.

Ma, L., X. Y. Feng, B. L. Cui, F. Law, X. W. Jiang, L. Y. Yang et al. 2005. Human umbilical cord wharton's jelly-derived mesenchymal stem cells differentiation into nerve-like cells. Chin. Med. J. (Engl). 118(23): 1987-1993.

Mahmood, A., D. Lu, C. Qu, A. Goussev, and M. Chopp. 2005. Human marrow stromal cell treatment provides long-lasting benefit after traumatic brain injury in rats. Neurosurgery. 57(5): 1026-31; discussion 1026-31.

Maijenburg, M. W., C. Gilissen, S. M. Melief, M. Kleijer, K. Weijer, A. Ten Brinke et al. 2012. Nuclear receptors Nur77 and Nurr1 modulate mesenchymal stromal cell migration. Stem Cells Dev. 21(2): 228-238.

Manochantr, S., Y. U-pratya, P. Kheolamai, S. Rojphisan, M. Chayosumrit, C. Tantrawatpan et al. 2013. Immunosuppressive properties of mesenchymal stromal cells derived from amnion, placenta, wharton's jelly and umbilical cord. Intern. Med. J. 43(4): 430-439.

Marcacci, M., E. Kon, V. Moukhachev, A. Lavroukov, S. Kutepov, R. Quarto et al. 2007. Stem cells associated with macroporous bioceramics for long bone repair: 6- to 7-year outcome of a pilot clinical study. Tissue Eng. 13(5): 947-955.

Martin-Rendon, E., D. Sweeney, F. Lu, J. Girdlestone, C. Navarrete, and S. M. Watt. 2008. 5-azacytidine-treated human mesenchymal stem/progenitor cells derived from umbilical cord, cord blood and bone marrow do not generate cardiomyocytes in vitro at high frequencies. Vox Sang. 95(2): 137-148.

Martinez, C., T. J. Hofmann, R. Marino, M. Dominici, and E. M. Horwitz. 2007. Human bone marrow mesenchymal stromal cells express the neural ganglioside GD2: A novel surface marker for the identification of MSCs. Blood. 109(10): 4245-4248.

Matsuse, D., M. Kitada, M. Kohama, K. Nishikawa, H. Makinoshima, S. Wakao et al. 2010. Human umbilical cord-derived mesenchymal stromal cells differentiate into functional schwann cells that sustain peripheral nerve regeneration. J. Neuropathol. Exp. Neurol. 69(9): 973-985.

Mayani, H., and P. M. Lansdorp. 1998. Biology of human umbilical cord blood-derived hematopoietic stem/progenitor cells. Stem Cells. 16(3): 153-165.

Meisel, R., S. Brockers, K. Heseler, O. Degistirici, H. Bulle, C. Woite et al. 2011. Human but not murine multipotent mesenchymal stromal cells exhibit broad-spectrum antimicrobial effector function mediated by indoleamine 2,3-dioxygenase. Leukemia. 25(4): 648-654.

Melania, L. I., A. Rita, C. Simona, G. Mario, D. Stefano, A. Giannuzzi, P. Cappello, F. Farina and L. R. Giampiero. 2011. Perinatal and Wharton's jelly-derived mesenchymal stem cells in cartilage regenerative medicine and tissue engineering strategies. Open Tissue Eng Regen Med J. 4:72-81

Mellor, A. L., D. B. Keskin, T. Johnson, P. Chandler, and D. H. Munn. 2002. Cells expressing indoleamine 2,3-dioxygenase inhibit T cell responses. J. Immunol. 168(8): 3771-3776.

Messerli, M., A. Wagner, R. Sager, M. Mueller, M. Baumann, D. V. Surbek et al. 2013. Stem cells from umbilical cord wharton's jelly from preterm birth have neuroglial differentiation potential. Reprod. Sci.

Messina, C., M. Faraci, V. de Fazio, G. Dini, M. P. Calo, E. Calore et al. 2008. Prevention and treatment of acute GvHD. Bone Marrow Transplant. 41 Suppl 2: S65-70.

Mishra, P. K., S. R. Singh, I. G. Joshua, and S. C. Tyagi. 2010. Stem cells as a therapeutic target for diabetes. Front. Biosci. 15: 461-477.

Mitchell, K. E., M. L. Weiss, B. M. Mitchell, P. Martin, D. Davis, L. Morales et al. 2003. Matrix cells from wharton's jelly form neurons and glia. Stem Cells. 21(1): 50-60.

Mitjavila-Garcia, M. T., C. Simonin, and M. Peschanski. 2005. Embryonic stem cells: Meeting the needs for cell therapy. Adv. Drug Deliv. Rev. 57(13): 1935-1943.

Moll, R., M. Divo, L. Langbein. (2008). The human keratins: biology and pathology. Histochem Cell Biol 129: 705-733.

Montanucci, P., G. Basta, T. Pescara, I. Pennoni, F. Di Giovanni, and R. Calafiore. 2011. New simple and rapid method for purification of mesenchymal stem cells from the human umbilical cord wharton jelly. Tissue Eng. Part A. 17(21-22): 2651-2661.

Moodley, Y., D. Atienza, U. Manuelpillai, C. S. Samuel, J. Tchongue, S. Ilancheran et al. 2009. Human umbilical cord mesenchymal stem cells reduce fibrosis of bleomycin-induced lung injury. Am. J. Pathol. 175(1): 303-313.

Mori, G., G. Brunetti, A. Oranger, C. Carbone, A. Ballini, L. Lo Muzio et al. 2011. Dental pulp stem cells: Osteogenic differentiation and gene expression. Ann. N. Y. Acad. Sci. 1237: 47-52.

Morigi, M., B. Imberti, C. Zoja, D. Corna, S. Tomasoni, M. Abbate et al. 2004. Mesenchymal stem cells are renotropic, helping to repair the kidney and improve function in acute renal failure. J. Am. Soc. Nephrol. 15(7): 1794-1804.

Morigi, M., M. Introna, B. Imberti, D. Corna, M. Abbate, C. Rota et al. 2008. Human bone marrow mesenchymal stem cells accelerate recovery of acute renal injury and prolong survival in mice. Stem Cells. 26(8): 2075-2082.

Mouiseddine, M., S. Francois, A. Semont, A. Sache, B. Allenet, N. Mathieu et al. 2007. Human mesenchymal stem cells home specifically to radiation-injured tissues in a non-obese diabetes/severe combined immunodeficiency mouse model. Br. J. Radiol. 80 Spec No 1: S49-55.

Nagaya, N., T. Fujii, T. Iwase, H. Ohgushi, T. Itoh, M. Uematsu et al. 2004. Intravenous administration of mesenchymal stem cells improves cardiac function in rats with acute myocardial infarction through angiogenesis and myogenesis. Am. J. Physiol. Heart Circ. Physiol. 287(6): H2670-6.

Najar, M., G. Raicevic, H. I. Boufker, H. Fayyad Kazan, C. De Bruyn, N. Meuleman et al. 2010. Mesenchymal stromal cells use PGE2 to modulate activation and proliferation of lymphocyte subsets: Combined comparison of adipose tissue, wharton's jelly and bone marrow sources. Cell. Immunol. 264(2): 171-179.

Nanaev, A. K., G. Kohnen, A. P. Milovanov, S. P. Domogatsky, and P. Kaufmann. 1997. Stromal differentiation and architecture of the human umbilical cord. Placenta. 18(1): 53-64.

Nekanti, U., V. B. Rao, A. G. Bahirvani, M. Jan, S. Totey, and M. Ta. 2010a. Long-term expansion and pluripotent marker array analysis of wharton's jelly-derived mesenchymal stem cells. Stem Cells Dev. 19(1): 117-130.

Nekanti, U., S. Dastidar, P. Venugopal, S. Totey and M. Ta. 2010b. Increased proliferation and analysis of differential gene expression in human Wharton's jelly-derived mesenchymal stromal cells under hypoxia. Int J Biol Sci 6(5): 499-512.

Omori, Y., O. Honmou, K. Harada, J. Suzuki, K. Houkin, and J. D. Kocsis. 2008. Optimization of a therapeutic protocol for intravenous injection of human mesenchymal stem cells after cerebral ischemia in adult rats. Brain Res. 1236: 30-38.

Ortiz, L. A., F. Gambelli, C. McBride, D. Gaupp, M. Baddoo, N. Kaminski et al. 2003. Mesenchymal stem cell engraftment in lung is enhanced in response to bleomycin exposure and ameliorates its fibrotic effects. Proc. Natl. Acad. Sci. U. S. A. 100(14): 8407-8411.

Panes, J., and A. Salas. 2009. Mechanisms underlying the beneficial effects of stem cell therapies for inflammatory bowel diseases. Gut. 58(7): 898-900.

Parekkadan, B., A. W. Tilles, and M. L. Yarmush. 2008. Bone marrow-derived mesenchymal stem cells ameliorate autoimmune enteropathy independently of regulatory T cells. Stem Cells. 26(7): 1913-1919.

Peng, L., Z. Jia, X. Yin, X. Zhang, Y. Liu, P. Chen, K. Ma and C. Zhou. 2008. Comparative analysis of mesenchymal stem cells from bone marrow, cartilage, and adipose tissue. Stem Cells Dev. 17(4): 761-773.

Pereira, R. F., M. D. O'Hara, A. V. Laptev, K. W. Halford, M. D. Pollard, R. Class et al. 1998. Marrow stromal cells as a source of progenitor cells for nonhematopoietic tissues in transgenic mice with a phenotype of osteogenesis imperfecta. Proc. Natl. Acad. Sci. U. S. A. 95(3): 1142-1147.

Qian, Q., H. Qian, X. Zhang, W. Zhu, Y. Yan, S. Ye et al. 2012. 5-azacytidine induces cardiac differentiation of human umbilical cord-derived mesenchymal stem cells by activating extracellular regulated kinase. Stem Cells Dev. 21(1): 67-75.

Quevedo, H. C., K. E. Hatzistergos, B. N. Oskouei, G. S. Feigenbaum, J. E. Rodriguez, D. Valdes et al. 2009. Allogeneic mesenchymal stem cells restore cardiac function in

chronic ischemic cardiomyopathy via trilineage differentiating capacity. Proc. Natl. Acad. Sci. U. S. A. 106(33): 14022-14027.

Rachakatla, R. S., M. M. Pyle, R. Ayuzawa, S. M. Edwards, F. C. Marini, M. L. Weiss et al. 2008. Combination treatment of human umbilical cord matrix stem cell-based interferon-beta gene therapy and 5-fluorouracil significantly reduces growth of metastatic human breast cancer in SCID mouse lungs. Cancer Invest. 26(7): 662-670.

Rao, M. S., and M. P. Mattson. 2001. Stem cells and aging: Expanding the possibilities. Mech. Ageing Dev. 122(7): 713-734.

Reagan, M. R., and D. L. Kaplan. 2011. Concise review: Mesenchymal stem cell tumor-homing: Detection methods in disease model systems. Stem Cells. 29(6): 920-927.

Ries, C., V. Egea, M. Karow, H. Kolb, M. Jochum, and P. Neth. 2007. MMP-2, MT1-MMP, and TIMP-2 are essential for the invasive capacity of human mesenchymal stem cells: Differential regulation by inflammatory cytokines. Blood. 109(9): 4055-4063.

Romanov, Y. A., V. A. Svintsitskaya, and V. N. Smirnov. 2003. Searching for alternative sources of postnatal human mesenchymal stem cells: Candidate MSC-like cells from umbilical cord. Stem Cells. 21(1): 105-110.

Rombouts, W. J., and R. E. Ploemacher. 2003. Primary murine MSC show highly efficient homing to the bone marrow but lose homing ability following culture. Leukemia. 17(1): 160-170.

Roobrouck, V. D., C. Clavel, S. A. Jacobs, F. Ulloa-Montoya, S. Crippa, A. Sohni et al. 2011. Differentiation potential of human postnatal mesenchymal stem cells, mesoangioblasts, and multipotent adult progenitor cells reflected in their transcriptome and partially influenced by the culture conditions. Stem Cells. 29(5): 871-882.

Rosova, I., M. Dao, B. Capoccia, D. Link, and J. A. Nolta. 2008. Hypoxic preconditioning results in increased motility and improved therapeutic potential of human mesenchymal stem cells. Stem Cells. 26(8): 2173-2182.

Russo, F. P., M. R. Alison, B. W. Bigger, E. Amofah, A. Florou, F. Amin et al. 2006. The bone marrow functionally contributes to liver fibrosis. Gastroenterology. 130(6): 1807-1821.

Ruster, B., S. Gottig, R. J. Ludwig, R. Bistrian, S. Muller, E. Seifried et al. 2006. Mesenchymal stem cells display coordinated rolling and adhesion behavior on endothelial cells. Blood. 108(12): 3938-3944.

Ryser, M. F., F. Ugarte, S. Thieme, M. Bornhauser, A. Roesen-Wolff, and S. Brenner. 2008. mRNA transfection of CXCR4-GFP fusion--simply generated by PCR-results in efficient migration of primary human mesenchymal stem cells. Tissue Eng. Part C. Methods. 14(3): 179-184.

Sackstein, R., J. S. Merzaban, D. W. Cain, N. M. Dagia, J. A. Spencer, C. P. Lin et al. 2008. Ex vivo glycan engineering of CD44 programs human multipotent mesenchymal stromal cell trafficking to bone. Nat. Med. 14(2): 181-187.

Saeidi, M., A. Masoud, Y. Shakiba, J. Hadjati, M. Mohyeddin Bonab, M. H. Nicknam et al. 2013. Immunomodulatory effects of human umbilical cord wharton's jelly-derived mesenchymal stem cells on differentiation, maturation and endocytosis of monocyte-derived dendritic cells. Iran. J. Allergy Asthma Immunol. 12(1): 37-49.

Saito, T., J. Q. Kuang, B. Bittira, A. Al-Khaldi, and R. C. Chiu. 2002. Xenotransplant cardiac chimera: Immune tolerance of adult stem cells. Ann. Thorac. Surg. 74(1): 19-24; discussion 24.

Salehinejad, P., N. B. Alitheen, A. M. Ali, A. R. Omar, M. Mohit, E. Janzamin et al. 2012. Comparison of different methods for the isolation of mesenchymal stem cells from human umbilical cord wharton's jelly. In Vitro Cell. Dev. Biol. Anim. 48(2): 75-83.

Sato, Y., H. Araki, J. Kato, K. Nakamura, Y. Kawano, M. Kobune et al. 2005. Human mesenchymal stem cells xenografted directly to rat liver are differentiated into human hepatocytes without fusion. Blood. 106(2): 756-763.

Schenk, S., N. Mal, A. Finan, M. Zhang, M. Kiedrowski, Z. Popovic et al. 2007. Monocyte chemotactic protein-3 is a myocardial mesenchymal stem cell homing factor. Stem Cells. 25(1): 245-251.

Shabbir, A., D. Zisa, H. Lin, M. Mastri, G. Roloff, G. Suzuki et al. 2010. Activation of host tissue trophic factors through JAK-STAT3 signaling: A mechanism of mesenchymal stem cell-mediated cardiac repair. Am. J. Physiol. Heart Circ. Physiol. 299(5): H1428-38.

Shah, B. S., P. A. Clark, E. K. Moioli, M. A. Stroscio, and J. J. Mao. 2007. Labeling of mesenchymal stem cells by bioconjugated quantum dots. Nano Lett. 7(10): 3071-3079.

Shake, J. G., P. J. Gruber, W. A. Baumgartner, G. Senechal, J. Meyers, J. M. Redmond et al. 2002. Mesenchymal stem cell implantation in a swine myocardial infarct model: Engraftment and functional effects. Ann. Thorac. Surg. 73(6): 1919-25; discussion 1926.

Shetty, P., K. Cooper, and C. Viswanathan. 2010. Comparison of proliferative and multilineage differentiation potentials of cord matrix, cord blood, and bone marrow mesenchymal stem cells. Asian J. Transfus. Sci. 4(1): 14-24.

Shi, D., D. Wang, X. Li, H. Zhang, N. Che, Z. Lu et al. 2012. Allogeneic transplantation of umbilical cord-derived mesenchymal stem cells for diffuse alveolar hemorrhage in systemic lupus erythematosus. Clin. Rheumatol. 31(5): 841-846.

Shi, M., J. Li, L. Liao, B. Chen, B. Li, L. Chen et al. 2007. Regulation of CXCR4 expression in human mesenchymal stem cells by cytokine treatment: Role in homing efficiency in NOD/SCID mice. Haematologica. 92(7): 897-904.

Shibata, T., K. Naruse, H. Kamiya, M. Kozakae, M. Kondo, Y. Yasuda et al. 2008. Transplantation of bone marrow-derived mesenchymal stem cells improves diabetic polyneuropathy in rats. Diabetes. 57(11): 3099-3107.

Sheng, H., Y. Wang, Y. Jin, Q. Zhang, Y. Zhang, L. Wang et al. 2008. A critical role of IFNgamma in priming MSC-mediated suppression of T cell proliferation through up-regulation of B7-H1. Cell Res. 18(8): 846-857.

Si, Y., Y. Zhao, H. Hao, J. Liu, Y. Guo, Y. Mu et al. 2012. Infusion of mesenchymal stem cells ameliorates hyperglycemia in type 2 diabetic rats: Identification of a novel role in improving insulin sensitivity. Diabetes. 61(6): 1616-1625.

Sobolewski, K., A. Malkowski, E. Bankowski, and S. Jaworski. 2005. Wharton's jelly as a reservoir of peptide growth factors. Placenta. 26(10): 747-752.

Song, Y. S., and J. H. Ku. 2007. Monitoring transplanted human mesenchymal stem cells in rat and rabbit bladders using molecular magnetic resonance imaging. Neurourol. Urodyn. 26(4): 584-593.

Sordi, V., M. L. Malosio, F. Marchesi, A. Mercalli, R. Melzi, T. Giordano et al. 2005. Bone marrow mesenchymal stem cells express a restricted set of functionally active chemokine receptors capable of promoting migration to pancreatic islets. Blood. 106(2): 419-427.

Springer, T. A. 1994. Traffic signals for lymphocyte recirculation and leukocyte emigration: The multistep paradigm. Cell. 76(2): 301-314.

Stamatovic, S. M., R. F. Keep, S. L. Kunkel, and A. V. Andjelkovic. 2003. Potential role of MCP-1 in endothelial cell tight junction 'opening': Signaling via rho and rho kinase. J. Cell. Sci. 116(Pt 22): 4615-4628.

Steingen, C., F. Brenig, L. Baumgartner, J. Schmidt, A. Schmidt, and W. Bloch. 2008. Characterization of key mechanisms in transmigration and invasion of mesenchymal stem cells. J. Mol. Cell. Cardiol. 44(6): 1072-1084.

Stenderup, K., J. Justesen, C. Clausen, and M. Kassem. 2003. Aging is associated with decreased maximal life span and accelerated senescence of bone marrow stromal cells. Bone. 33(6): 919-926.

Stock, P., S. Bruckner, S. Ebensing, M. Hempel, M. M. Dollinger, and B. Christ. 2010. The generation of hepatocytes from mesenchymal stem cells and engraftment into murine liver. Nat. Protoc. 5(4): 617-627.

Sun, L., D. Wang, J. Liang, H. Zhang, X. Feng, H. Wang et al. 2010. Umbilical cord mesenchymal stem cell transplantation in severe and refractory systemic lupus erythematosus. Arthritis Rheum. 62(8): 2467-2475.

Sun, Y., L. Chen, X. G. Hou, W. K. Hou, J. J. Dong, L. Sun et al. 2007. Differentiation of bone marrow-derived mesenchymal stem cells from diabetic patients into insulin-producing cells in vitro. Chin. Med. J. (Engl). 120(9): 771-776.

Takeda, M., M. Yamamoto, K. Isoda, S. Higashiyama, M. Hirose, H. Ohgushi et al. 2005. Availability of bone marrow stromal cells in three-dimensional coculture with hepatocytes and transplantation into liver-damaged mice. J. Biosci. Bioeng. 100(1): 77-81.

Timper, K., D. Seboek, M. Eberhardt, P. Linscheid, M. Christ-Crain, U. Keller et al. 2006. Human adipose tissue-derived mesenchymal stem cells differentiate into insulin, somatostatin, and glucagon expressing cells. Biochem. Biophys. Res. Commun. 341(4): 1135-1140.

Tipnis, S., C. Viswanathan, and A. S. Majumdar. 2010. Immunosuppressive properties of human umbilical cord-derived mesenchymal stem cells: Role of B7-H1 and IDO. Immunol. Cell Biol. 88(8): 795-806.

Tomchuck, S. L., K. J. Zwezdaryk, S. B. Coffelt, R. S. Waterman, E. S. Danka, and A. B. Scandurro. 2008. Toll-like receptors on human mesenchymal stem cells drive their migration and immunomodulating responses. Stem Cells. 26(1): 99-107.

Trounson, A., R. G. Thakar, G. Lomax, and D. Gibbons. 2011. Clinical trials for stem cell therapies. BMC Med. 9: 52-7015-9-52.

Troyer, D. L., and M. L. Weiss. 2008. Wharton's jelly-derived cells are a primitive stromal cell population. Stem Cells. 26(3): 591-599.

Tsagias, N., I. Koliakos, V. Karagiannis, M. Eleftheriadou, and G. G. Koliakos. 2011. Isolation of mesenchymal stem cells using the total length of umbilical cord for transplantation purposes. Transfus. Med. 21(4): 253-261.

Tsai, P. C., T. W. Fu, Y. M. Chen, T. L. Ko, T. H. Chen, Y. H. Shih et al. 2009. The therapeutic potential of human umbilical mesenchymal stem cells from wharton's jelly in the treatment of rat liver fibrosis. Liver Transpl. 15(5): 484-495.

Uccelli, A., A. Laroni, and M. S. Freedman. 2011. Mesenchymal stem cells for the treatment of multiple sclerosis and other neurological diseases. Lancet Neurol. 10(7): 649-656.

Ueno, H., and I. L. Weissman. 2010. The origin and fate of yolk sac hematopoiesis: Application of chimera analyses to developmental studies. Int. J. Dev. Biol. 54(6-7): 1019-1031.

Undale, A. H., J. J. Westendorf, M. J. Yaszemski and S. Khosla. 2009. Mesenchymal stem cells for bone repair and metabolic bone diseases. Mayo Clin Proc. 84(10): 893-902.

Walczak, P., J. Zhang, A. A. Gilad, D. A. Kedziorek, J. Ruiz-Cabello, R. G. Young et al. 2008. Dual-modality monitoring of targeted intraarterial delivery of mesenchymal stem cells after transient ischemia. Stroke. 39(5): 1569-1574.

Wang, B., S. Huang, L. Pan, and S. Jia. 2012. Enhancement of bone formation by genetically engineered human umbilical cord-derived mesenchymal stem cells expressing osterix. Oral Surg. Oral Med. Oral Pathol. Oral Radiol.

Wang, H. S., S. C. Hung, S. T. Peng, C. C. Huang, H. M. Wei, Y. J. Guo et al. 2004. Mesenchymal stem cells in the wharton's jelly of the human umbilical cord. Stem Cells. 22(7): 1330-1337.

Wang, H. W., L. M. Lin, H. Y. He, F. You, W. Z. Li, T. H. Huang et al. 2011. Human umbilical cord mesenchymal stem cells derived from wharton's jelly differentiate into insulin-producing cells in vitro. Chin. Med. J. (Engl). 124(10): 1534-1539.

Wang, L., I. Tran, K. Seshareddy, M. L. Weiss, and M. S. Detamore. 2009a. A comparison of human bone marrow-derived mesenchymal stem cells and human umbilical cord-derived mesenchymal stromal cells for cartilage tissue engineering. Tissue Eng. Part A. 15(8): 2259-2266.

Wang, L., N. H. Dormer, L. F. Bonewald, and M. S. Detamore. 2010. Osteogenic differentiation of human umbilical cord mesenchymal stromal cells in polyglycolic acid scaffolds. Tissue Eng. Part A. 16(6): 1937-1948.

Wang, S. H., S. J. Lin, Y. H. Chen, F. Y. Lin, J. C. Shih, C. C. Wu et al. 2009b. Late outgrowth endothelial cells derived from wharton jelly in human umbilical cord reduce neointimal formation after vascular injury: Involvement of pigment epithelium-derived factor. Arterioscler. Thromb. Vasc. Biol. 29(6): 816-822.

Wang, W., V. Koka, and H. Y. Lan. 2005. Transforming growth factor-beta and smad signalling in kidney diseases. Nephrology (Carlton). 10(1): 48-56.

Wang, X. Y., Y. Lan, W. Y. He, L. Zhang, H. Y. Yao, C. M. Hou et al. 2008a. Identification of mesenchymal stem cells in aorta-gonad-mesonephros and yolk sac of human embryos. Blood. 111(4): 2436-2443.

Wang, Y., Y. Deng, and G. Q. Zhou. 2008b. SDF-1alpha/CXCR4-mediated migration of systemically transplanted bone marrow stromal cells towards ischemic brain lesion in a rat model. Brain Res. 1195: 104-112.

Weiss, M. L., K. E. Mitchell, J. E. Hix, S. Medicetty, S. Z. El-Zarkouny, D. Grieger et al. 2003. Transplantation of porcine umbilical cord matrix cells into the rat brain. Exp. Neurol. 182(2): 288-299.

Weiss, M. L., S. Medicetty, A. R. Bledsoe, R. S. Rachakatla, M. Choi, S. Merchav et al. 2006. Human umbilical cord matrix stem cells: Preliminary characterization and effect of transplantation in a rodent model of parkinson's disease. Stem Cells. 24(3): 781-792.

Weiss, M. L., C. Anderson, S. Medicetty, K. B. Seshareddy, R. J. Weiss, I. VanderWerff et al. 2008. Immune properties of human umbilical cord wharton's jelly-derived cells. Stem Cells. 26(11): 2865-2874.

Williams, A. R., and J. M. Hare. 2011. Mesenchymal stem cells: Biology, pathophysiology, translational findings, and therapeutic implications for cardiac disease. Circ. Res. 109(8): 923-940.

Wilson, T., C. Stark, J. Holmbom, A. Rosling, A. Kuusilehto, T. Tirri et al. 2010. Fate of bone marrow-derived stromal cells after intraperitoneal infusion or implantation into femoral bone defects in the host animal. J. Tissue Eng. 2010: 345806.

Wise, A. F., and S. D. Ricardo. 2012. Mesenchymal stem cells in kidney inflammation and repair. Nephrology (Carlton). 17(1): 1-10.

Wu, J., Z. Sun, H. S. Sun, J. Wu, R. D. Weisel, A. Keating et al. 2008. Intravenously administered bone marrow cells migrate to damaged brain tissue and improve neural function in ischemic rats. Cell Transplant. 16(10): 993-1005.

Wu, K. H., B. Zhou, S. H. Lu, B. Feng, S. G. Yang, W. T. Du et al. 2007a. In vitro and in vivo differentiation of human umbilical cord derived stem cells into endothelial cells. J. Cell. Biochem. 100(3): 608-616.

Wu, K. H., B. Zhou, C. T. Yu, B. Cui, S. H. Lu, Z. C. Han et al. 2007b. Therapeutic potential of human umbilical cord derived stem cells in a rat myocardial infarction model. Ann. Thorac. Surg. 83(4): 1491-1498.

Wu, K. H., S. G. Yang, B. Zhou, W. T. Du, D. S. Gu, P. X. Liu et al. 2007c. Human umbilical cord derived stem cells for the injured heart. Med. Hypotheses. 68(1): 94-97.

Wu, K. H., X. M. Mo, B. Zhou, S. H. Lu, S. G. Yang, Y. L. Liu et al. 2009a. Cardiac potential of stem cells from whole human umbilical cord tissue. J. Cell. Biochem. 107(5): 926-932.

Wu, K. H., C. K. Chan, C. Tsai, Y. H. Chang, M. Sieber, T. H. Chiu et al. 2011. Effective treatment of severe steroid-resistant acute graft-versus-host disease with umbilical cord-derived mesenchymal stem cells. Transplantation. 91(12): 1412-1416.

Wu, L. F., N. N. Wang, Y. S. Liu, and X. Wei. 2009b. Differentiation of wharton's jelly primitive stromal cells into insulin-producing cells in comparison with bone marrow mesenchymal stem cells. Tissue Eng. Part A. 15(10): 2865-2873.

Wu, W., H. Zhao, B. Xie, H. Liu, Y. Chen, G. Jiao et al. 2011. Implanted spike wave electric stimulation promotes survival of the bone marrow mesenchymal stem cells and functional recovery in the spinal cord injured rats. Neurosci. Lett. 491(1): 73-78.

Wynn, R. F., C. A. Hart, C. Corradi-Perini, L. O'Neill, C. A. Evans, J. E. Wraith et al. 2004. A small proportion of mesenchymal stem cells strongly expresses functionally active CXCR4 receptor capable of promoting migration to bone marrow. Blood. 104(9): 2643-2645.

Xiao, Q., S. K. Wang, H. Tian, L. Xin, Z. G. Zou, Y. L. Hu et al. 2012. TNF-alpha increases bone marrow mesenchymal stem cell migration to ischemic tissues. Cell Biochem. Biophys. 62(3): 409-414.

Xiong, N., Z. Zhang, J. Huang, C. Chen, Z. Zhang, M. Jia et al. 2011. VEGF-expressing human umbilical cord mesenchymal stem cells, an improved therapy strategy for parkinson's disease. Gene Ther. 18(4): 394-402.

Yan, Y., W. Xu, H. Qian, Y. Si, W. Zhu, H. Cao et al. 2009. Mesenchymal stem cells from human umbilical cords ameliorate mouse hepatic injury in vivo. Liver Int. 29(3): 356-365.

Yang, X., M. Zhang, Y. Zhang, W. Li, and B. Yang. 2011. Mesenchymal stem cells derived from wharton jelly of the human umbilical cord ameliorate damage to human endometrial stromal cells. Fertil. Steril. 96(4): 1029-1036.

Yannaki, E., E. Athanasiou, A. Xagorari, V. Constantinou, I. Batsis, P. Kaloyannidis et al. 2005. G-CSF-primed hematopoietic stem cells or G-CSF per se accelerate recovery and improve survival after liver injury, predominantly by promoting endogenous repair programs. Exp. Hematol. 33(1): 108-119.

Yoo, K. H., I. K. Jang, M. W. Lee, H. E. Kim, M. S. Yang, Y. Eom et al. 2009. Comparison of immunomodulatory properties of mesenchymal stem cells derived from adult human tissues. Cell. Immunol. 259(2): 150-156.

Yoon, J. H., E. Y. Roh, S. Shin, N. H. Jung, E. Y. Song, J. Y. Chang et al. 2013. Comparison of explant-derived and enzymatic digestion-derived MSCs and the growth factors from wharton's jelly. Biomed. Res. Int. 2013: 428726.

Yu, J., M. Li, Z. Qu, D. Yan, D. Li, and Q. Ruan. 2010. SDF-1/CXCR4-mediated migration of transplanted bone marrow stromal cells toward areas of heart myocardial infarction through activation of PI3K/akt. J. Cardiovasc. Pharmacol. 55(5): 496-505.

Yukawa, H., M. Watanabe, N. Kaji, Y. Okamoto, M. Tokeshi, Y. Miyamoto et al. 2012. Monitoring transplanted adipose tissue-derived stem cells combined with heparin in the liver by fluorescence imaging using quantum dots. Biomaterials. 33(7): 2177-2186.

Zhao, Q., H. Ren, X. Li, Z. Chen, X. Zhang, W. Gong et al. 2009. Differentiation of human umbilical cord mesenchymal stromal cells into low immunogenic hepatocyte-like cells. Cytotherapy. 11(4): 414-426.

Zhao, W., J. J. Li, D. Y. Cao, X. Li, L. Y. Zhang, Y. He et al. 2012. Intravenous injection of mesenchymal stem cells is effective in treating liver fibrosis. World J. Gastroenterol. 18(10): 1048-1058.

Zhao, Z., C. Watt, A. Karystinou, A. J. Roelofs, C. D. McCaig, I. R. Gibson et al. 2011a. Directed migration of human bone marrow mesenchymal stem cells in a physiological direct current electric field. Eur. Cell. Mater. 22: 344-358.

Zhao, Z., Z. Chen, X. Zhao, F. Pan, M. Cai, T. Wang et al. 2011b. Sphingosine-1-phosphate promotes the differentiation of human umbilical cord mesenchymal stem cells into cardiomyocytes under the designated culturing conditions. J. Biomed. Sci. 18: 37-0127-18-37.

Zhang, H. C., X. B. Liu, S. Huang, X. Y. Bi, H. X. Wang, L. X. Xie et al. 2012a. Microvesicles derived from human umbilical cord mesenchymal stem cells stimulated by hypoxia promote angiogenesis both in vitro and in vivo. Stem Cells Dev. 21(18): 3289-3297.

Zhang, L., H. T. Zhang, S. Q. Hong, X. Ma, X. D. Jiang, and R. X. Xu. 2009a. Cografted wharton's jelly cells-derived neurospheres and BDNF promote functional recovery after rat spinal cord transection. Neurochem. Res. 34(11): 2030-2039.

Zhang, S., L. Chen, T. Liu, B. Zhang, D. Xiang, Z. Wang et al. 2012b. Human umbilical cord matrix stem cells efficiently rescue acute liver failure through paracrine effects rather than hepatic differentiation. Tissue Eng. Part A. 18(13-14): 1352-1364.

Zhang, Y. N., P. C. Lie, and X. Wei. 2009b. Differentiation of mesenchymal stromal cells derived from umbilical cord wharton's jelly into hepatocyte-like cells. Cytotherapy. 11(5): 548-558.

Zhang, Z., H. Lin, M. Shi, R. Xu, J. Fu, J. Lv et al. 2012c. Human umbilical cord mesenchymal stem cells improve liver function and ascites in decompensated liver cirrhosis patients. J. Gastroenterol. Hepatol. 27 Suppl 2: 112-120.

Zhou, C., B. Yang, Y. Tian, H. Jiao, W. Zheng, J. Wang et al. 2011. Immunomodulatory effect of human umbilical cord wharton's jelly-derived mesenchymal stem cells on lymphocytes. Cell. Immunol. 272(1): 33-38.

Chapter 2 - Characterization of Pig Umbilical Cord Matrix Stem Cells (PUCs)

Introduction

Mesenchymal stem cells (MSCs) are plastic-adherent and have self-renewal and multi-potential differentiation properties, They express the cell surface markers CD105, CD73 and CD90, and lack expression of CD45, CD34, CD14 or CD11b, CD79alpha or CD19 and HLA-DR (Dominici et al., 2006). A summary of adult human MSCs surface markers from published literature shows that the most commonly detected markers are CD13, CD29, CD44, CD49e, CD51, CD 54, CD59, CD71, CD73, CD90, CD105, CD106, CD146 and CD 166. The most frequently markers that are reported as not detected are CD31, CD34, CD14, CD45, CD11b, CD49d, CD106, CD10 and CD31 (Pa et al., 2011). Adult human MSCs are expected to differentiate in vitro into the three mesodermal lineages: osteogenesis, chondrogenesis and adipogenesis (Kern et al., 2006; Maurer et al., 2011).

MSCs can be derived from both of adult and fetal tissues including bone marrow (Tropel et al., 2004), adipose tissue (Taghi et al., 2012), dental pulp (Perry et al., 2008), synovial membrane (De Bari et al., 2001), skin (Orciani and Di Primio, 2013), peripheral blood (Cao et al., 2005), amniotic fluid (De Coppi et al., 2007), umbilical cord blood and placenta (Barlow et al., 2008). The quantitatively largest source is Wharton's jelly (WJ) of the umbilical cord, a source first described by Mitchell et al. (2003), and reviewed recently by Taghizadeh et al. (2011) and Longo et al. (2012). The in vitro proliferation kinetics of MSCs is important for their applications in cell therapy and tissue engineering. Compared to adult MSCs, MSCs derived from fetal tissues have a higher proliferation capacity (Lee et al., 2006; Baksh et al., 2007; Ramkisoensing et al., 2011) and with longer maintenance of the undifferentiated condition in vitro (Sabapathy et al., 2012) and greater engraftment capacity (Brooke et al., 2008).

MSCs are isolated from WJ the cushioning tissue of umbilical cords. Umbilical cords are discarded and isolation of umbilical cord (UC) MSCs from the WJ matrix is low cost and without ethical issues. UC cells are plastic-adherent and display a high frequency of colony formation (CFU-F) when plated on plastic (Karahuseyinoglu et al., 2007). The cells from human cords express stromal markers (CD29, CD44, CD73, CD90, CD105 and CD106), but they are

negative for hematopoietic markers (CD34 and CD45). In addition, they are capable of mesodermal differentiation (Li et al., 2012).

Porcine umbilical cords matrix stem cells (PUCs) are derived from porcine umbilical cords. Because pig physiology, anatomy, and genetics are closely related to humans, PUCs provide a good biological model for studies such of cell-based therapy and tissue engineering. Pigs are also an important agricultural species and understanding of their biology important in its own right. The objectives of our investigations are to characterize the PUCs derived from porcine WJ explants for their immunophenotypes and mesodermal differentiation. Additionally, growth kinetics of PUCs was investigated to derive estimates of population doubling time (PDT) and gain insights into potential ex vivo expansion of PUCs.

Materials and Methods

PUC isolation

Umbilical cords were collected from newborn pigs at the Kansas State University Swine Research and Teaching Center. Umbilical cords were collected aseptically at birth and placed in storage and transport buffer (STB) consisting of phosphate buffered saline (PBS) supplemented with antimycotic/antibiotic reagent (Gibco, Grand Island, NY, 1:100). The cords were stored at 5º C in STB up to 24 h before WJ was harvested for cell isolation. In the laboratory, each umbilical cord was rinsed with fresh STB and placed in a sterile Petri dish. The cords were opened longitudinally using aseptic techniques. The vein and arteries were removed using hemostats. WJ was scraped from cords with a sterile, medical-grade blade and placed in Petri dishes (150 cm^2) where it was cut into pieces (approximately 1-3 mm^3). The WJ pieces (explants) were allowed to air-dry for 10 minutes to increase attachment and then complete growth medium added. The growth medium consisted of high-glucose Dulbecco's Minimum Essential Medium with HEPES (GlutaMAX™-DMEM-HEPES, Invitrogen, Grand Island, NY) supplemented with fetal bovine serum (20% FBS, Invitrogen), Normocin (100 µg/ml, Invitrogen), Gentamicin Reagent Solution (25 µg/ml Gentamicin, Invitrogen) and 2-mercaptoethanol (55 µmol/ml, Sigma). Culture dishes were incubated at 38.5°C with 5% CO_2 and saturated humidity. The tissues explants were removed from culture when PUCs migrated out from WJ explants and attached on the dish after incubation for 5-7 days. PUCs were harvested by dissociation with 0.1% trypsin (Gibco) + 1.0 mM EDTA in PBS. Harvested cells were re-suspended in Recovery Cell Culture Freezing Medium (Gibco) and cryopreserved in liquid nitrogen.

Mesodermal differentiation potential of PUCs

The adipogenic potential of PUCs was tested using the StemPro® Adipogenesis Differentiation Kit (Gibco) containing StemPro® Adipocyte Differentiation Basal Medium and StemPro® Adipogenesis Supplement. Early PUCs (P3) were plated in tissue culture flasks ($1x10^4$cells/cm^2). They were cultured in complete growth medium at 38.5°C in a humidified atmosphere of 5% CO_2 until they reached 80-90% confluence. The complete growth medium was replaced by adipogenesis differentiation medium prepared according to the kit instructions.

PUCs were cultured continuously under the differentiation medium for 21 days by replacing new differentiation medium every 3 days.

After 21 days, cultured PUCs were washed 3 times with PBS and fixed with 4% paraformaldehyde solution for 30 minutes at room temperature. The fixed cells were rinsed twice with PBS and LipidTOX™ Red (diluted 1:100) (Invitrogen) added to dye the neutral lipid droplets red (fluorescence excitation/emission maxima as 577/609 nm) and incubated for 30 minutes at room temperature. Cell nuclei were counterstained with green-fluorescent nucleic stain, Syto®16 (Invitrogen) (0.05 μM) (maximum excitation/emission 448/518) for 8 minutes at room temperature. Cells were mounted on slides with cover slips using glycerol solution (Fisher Bioreagents®). Intracellular stained neutral lipid droplets were observed under an inverted Zeiss LSM 700 confocal microscope (LSM 700, Carl Zeiss). The 40x/1.30 Oil M27 EC Plan-Neofluar objective lens with a pinhole opened 30 μm was used to visualize within a field of view of 266.5 × 266.5 μm. Image size and dynamic range were 1024x1024 and 8 bit. Scanning speed number, mode of scanning and average number of signal/noise ratio were 6, line mode and 4, respectively. Sequential excitation was at 2% of 488 nm and 2% of 555 was provided by argon and helium-neon gas lasers. Emission filters BP 520-580 nm and LP 630 nm were used for collecting green and red in channels one and two with the master gain of each channel as 428 and 360, respectively. After sequential excitation, green and red fluorescent images of the same cell were saved and analyzed by Zeiss Zen 2010 software.

To determine an adipogenic potential, PUCs were incubated in adipogenic differentiation medium for 21 days then harvested (0.1% trypsin + 1.0 mM EDTA in PBS) and washed 3 times with PBS. Cells were fixed (4% paraformaldehyde for 30 minutes at room temperature) then washed twice with PBS to remove residual paraformaldehyde. Fixed cells were stained with LipidTOX™ Red (diluted 1:100) (Invitrogen) for 30 minutes at room temperature and they were analyzed for the emission of red fluorescence through the PM3 channel of a microcapillary cytometer (Guava EasyCyte Plus, Millipore). PUCs cultured in complete growth medium were stained by LipidTOX™ Red and used as a negative control.

For chondrogenic differentiation, PUCs were cultured in chondrogenesis differentiation medium (StemPro® Chondrogenesis Differentiation Kit; Gibco®) according to the kit instructions. PUCs suspended in complete growth medium at 1.6×10^7 viable cells/ml were seeded in a 5 μl droplet in the center of wells of a multi-well plate to generate micromass

cultures. After cultivating micromass cultures for 6 h at 38.5°C in a humidified atmosphere of 5% CO_2, 3 ml of warmed chondrogenesis differentiation medium was added and the plate was incubated for 21 days at 38.5°C in a humidified atmosphere of 5% CO_2. Differentiation medium was removed and the cells were washed 3 times with PBS. Then, cells were fixed with 4% paraformaldehyde solution for 30 minutes at room temperature, rinsed twice with PBS and stained 30 minutes with 1% (w/v) Alcian Blue solution prepared in 0.1 N HCl. The stained cells were rinsed 3 times with 0.1N HCl and distilled water added to neutralize the acidity. The blue color-stained cells indicated the synthesis of proteoglycans by chondrocytes.

Osteogenic differentiation of PUCs was investigated using the StemPro® Osteogenesis Differentiation Kit (Gibco). Early passage (P3) PUCs were seeded in culture wells at $5x10^3$cells/cm^2 and cultured in complete growth medium at 38.5°C until they reached 80-90% confluence. The medium was replaced with pre-warmed osteogenesis differentiation medium prepared according to the kit instructions. PUCs were cultured continuously under the differentiation medium for 21 days with replacement every 3 days. After 21 days, the PUCs were washed 3 times with PBS, fixed (4% paraformaldehyde for 30 minutes at room temperature). The fixed cells were rinsed twice with PBS before 2% (w/v) Alizarin Red S solution (pH 4.2) prepared in distilled water) was added and incubated 3 minutes. The stained cells were rinsed 3 times with distilled water and visualized under a light microscope. Cultured cells undergoing osteogenesis differentiation showed increased mineral deposition and were stained red color by Alizarin Red S dye.

Cell surface marker staining and flow cytometry

Early passages of PUCs were analyzed to determine surface phenotype. Mouse monoclonal antibodies to porcine CD31 (LCI-4): IgG1- RPE, CD45 (K252-1E4): IgG1-FITC and SLA class II DR (2E9/13): IgG2b-FITC (AbD Serotec, Bio-Rad, Hercules, CA), porcine CD105 (MEM-229): IgG2a-FITC and CD90 (5E10): IgG1-FITC (Abcam, Cambridge, MA) and porcine CD44 (MEM-263): IgG1-FITC (Thermo Scientific, Middletown, VA). All isotype control antibodies derived from mice (IgG1-FITC, IgG1-RPE, IgG2a-FITC and IgG2b-FITC) were purchased from Invitrogen (Carlsbad, CA). Cultures were washed twice with PBS, and cells detached by enzymatic treatment (0.05% trypsin/EDTA in PBS) for 7 minutes at room temperature. Culture medium was added to inactivate trypsin and cells were washed twice with

PBS before adjusting to 1×10^7 cells /ml in PBS. Cell suspensions (100 µl) were incubated with 5-10 µl of antibodies or isotype controls (to provide a final concentration of 3µg/ml) for 45 minutes at 4°C in the dark. Fluorescence emission of cells was analyzed using a microcapillary cytometer (Guava EasyCyte Plus, Millipore). Nonspecific background was evaluated by parallel staining with isotype-matched IgG1-FITC, IgG1-RPE, IgG2a-FITC and IgG2b-FITC. The cell population was gated separately from the cell debris using a side scatter/forward scatter dot plot and, then was applied to the histograms for green, yellow, and red fluorescence. The number and percent positive cells was generated by CytosoftTM software, Guava ExpressPro assay (Millipore).

In vitro doubling time for PUCs

PUCs (P3) were plated (10^4 cells/cm^2) in a 75 cm^2 tissue culture flask and cultured with complete culture medium until >90% confluent. PUCs were synchronized to the resting phase, washed 3 times with PBS and were incubated with StemPro® basal medium with no serum (Invitrogen) for 6 days with medium replacement every 2 days. Cells cycle stage was determined by Guava® Cell Cycle Reagent (Millipore) and microcapillary cytometer (Guava EasyCyte Plus, Millipore). Briefly, harvested PUCs ($1x10^5$ cells) were washed 3 times with PBS and fixed in 10 ml of ice-cold 70% ethanol 1-12 hours prior to staining. Fixed cells were centrifuged and supernatant was discarded. Then, cells were washed 1 time with PBS for 1 minute at room temperature. The washed cells were centrifuged and the supernatant was removed. Ethanol-fixed cells were resuspended in 200 µl Guava® Cell Cycle Reagent and incubated at room temperature for 30 minutes with shielding from light. The stained cells were transferred to a 1.5 ml microcentrifuge tube before acquiring the data from the PM2 (red) channel. To generate growth curves, PUCs in resting phase were plated (10^4 cells/cm^2) in 6-well plate. The viable cell numbers were determined at 12, 24, 36, 48, 60, 72, 84, 96 and 108 hours after plating. Determination of cells number was performed in triplicate. The cell doubling time of PUCs was calculated using the Patterson formula: Td = Tlog2/logN1-logN0 (Td = doubling time, T = log phase time, N1 = cell number at the end of the log phase, N0 = cell number at the beginning of the log phase).

Results

PUCs isolation

Wharton's jelly explants attached to the dish within 1 day after plating. Cells were seen migrating from the explants after culturing 2-3 days (Fig 2.1A). The migrating cells had a heterogeneous shape, including fibroblast-like cells with short and long processes and small round cells with a highly reflective appearance (Fig 2.1B). Cells grew to 80% or more confluent in 7-10 days and the interval between the explant plating and the first passage was about 2 weeks. Approximately, 1.2 x 10^7 cells were harvested at first passage with viability greater than 90%.

Mesodermal differentiation potential of PUCs

After 14-21 days, PUCs cultured in the differentiation induction media demonstrated adipogenic, osteogenic and chondrogenic differentiation as assessed by appropriate staining. For adipogenic supplementation, differentiation was apparent after 3 weeks of induction. Morphologically PUCs changed from fibroblastic to spherical and intracellular lipid droplets appeared. The accumulated lipid vacuoles were visualized by LipidTOX™ Red neutral lipid stain (Figure 2.2A-C). The non-treated PUCs cultured in complete growth medium showed no lipid droplets or staining with with LipidTOX™ Red (Fig 2.2D). Flow cytometry revealed 5.84% of PUCs displayed staining indicative of adipogenesis (Figure 2.3).

Osteogenic differentiation conditions for 21 days resulted in matrix calcification as identified by Alizarin red staining. The dye-calcium complexes with extracellular calcium deposits exhibited a bright orange-red color (Figure 2.4).

Chondrogenic differentiation potential of PUCs in chondrogenesis differentiation medium for 21days resulted in cell pellets within 3 days and the pellet size increased over a period of 2 to 3 weeks. After 3 weeks, pellets stained with Alcian blue dye were positive indicated the presence of sulfated proteoglycan, a matrix component of mature chondrocyte cultures (Figure 2.5).

Immunophenotypic analysis of PUCs

Flow cytometry results showed that early passage of PUCs (P5) shared most of their immunophenotype with mesenchymal stem cells by uniformly positive expression (> 90%) for stromal markers (CD44, CD90 and CD105), but lack of expression (< 2%) for hematopoietic markers (CD45, CD31 and HLA-DR) as shown in Table2.1 and Figure2.6.

In vitro doubling time for PUCs

PUCs were culture for 5 days in 2% FBS culture medium to induce cell cycle synchronisation at resting (G0/G1) phase before determination of cell doubling time. Almost all (92.5%) PUCs were at G0/G1 phase after starvation for 6 days (Fig 2.7 and Table 2.2). The viability of synchronized PUCs was 77.1%. Complete growth medium containing 20% FBS was added to the cells and PUCs were harvested at 12, 24, 36, 48, 60, 72, 84, 96 and 108 hours after plating (Table 2.3). Viability of harvested PUCs was between 88-93%. The growth curves displayed an initial lag phase of 24 hours, a log phase at exponential rate from 24 to 84 hours, and a plateau phase. According to the Patterson formula, the doubling time in the log phase of PUCs was 13.8 hours (Fig 2.8).

Discussion

Migrating cells from WJ explants initially contained a heterogeneous population of cells with fibloblast-like and small round cell morphologies. They were observed around the explants after incubation for approximately 5 days. Similarly, human umbilical cord matrix stem cells isolated by the enzymatic method comprised a heterogeneous population, mesenchymal-like cells and small round cells with a high nuclear to cytoplasm ratio (Weiss et al., 2006). The small round cell population exhibited rapid proliferation and low population doubling time (PDT) (Christodoulou et al., 2013). Also, the subpopulation of high reflective small round cells was found in isolated bone marrow mesenchymal stem cells and they were called the rapid self-renewal (RS) cells. They are reportedly the precursor of the mature fibroblast-like cells and exhibited multilineage differentiation potential (Colter et al., 2000; Colter et al., 2001).

Cells isolated from WJ derived from human (Abu Kasim et al., 2012), canine (Lee et al., 2013), bovine (Cardoso et al., 2012), equine (Hoynowski et al., 2007), and rat (Ganta et al., 2009) umbilical cords are positive for MSCs markers (CD44, CD90, CD73 and CD105) and lack markers for the hematopoietic lineage (CD34 and CD45). Cells isolated from porcine WJ cell are consistent with this pattern. Greater than 90% of early passage PUCs expressed CD90, CD44 and CD105, but not CD 31, CD45 and SLA-DR. We did not evaluate CD 73 and CD34, two of the indicated standard CD markers for MSCs, because we did not have antibodies for these porcine antigens. Moreover, monoclonal antibodies against human CD73 and CD34 do not cross react with porcine CD73 and CD34 (Noort et al., 2012; Rozemuller et al., 2010). Monoclonal antibody against CD31 antigen specific to platelet, leukocytes and endothelial cells and used to characterize MSCs (Peister et al., 2004) was performed to characterize cells isolated from porcine Wharton's jelly instead of employing CD34.

Mesenchymal stem cells isolated from WJ of miniature pigs were positive for CD44, CD90, SLA class I and negative for CD31, CD45, SLA class II-DR, SLA class II-DQ (Cho et al., 2008; Kang et al., 2013). Using an explant isolation method, MSCs isolated from WJ of postnatal miniature pig showed expression of CD29, CD44 and CD90 (98%, 83.3% and 84.7%, respectively). Additionally, they were negative for CD45 (0%) and had low expression of SLA class II-DR (4%) (Kang et al., 2013).

Expression levels of CD markers of MSCs isolated from the same source may differ due to the isolation method, the procedure of fixation and staining, the concentration of monoclonal antibodies, the passage number or other factors.

Here, we demonstrated that cells isolated from porcine WJ contained MSCs capable of mesodermal lineage differentiation. Adipocyte, osteocyte, and chondrocyte differentiation in vitro was shown. Under adipogenic differentiation conditions, PUCs changed into a cuboidal shape and contained tiny intracellular lipid droplets. The multilocular cells could be considered as early adipocytes and the spindle shape cells in the absence of detectable lipid droplets have been identified as preadipocytes (Zhang et al., 2012). MSCs isolated from bone marrow showed high potential for adipogenic differentiation in that they formed large homogeneous intracellular lipid droplets after culturing in adipogenic differentiation medium (Sekiya et al., 2004). Sekiya et al. (2004) and Chang et al. (2006) have reported that MSCs isolated from umbilical cords-related tissues expressed lower potency of adipogenic differentiation than bone marrow mesenchymal stem cells. Flow cytometry illustrated that low numbers of WJ-derived cells were able to differentiate to adipocytes. This could be because the improper ingredients in adipogenic induction medium were not optimal (Scott et al., 2011), inadequate incubation time or an unsuitable oxygenic condition (Valorani et al., 2010). It could also be that the more primitive WJ-cells are less capable of adipogenesis (Ragni et al., 2013).

For kinetic analyses of cell cycle progression it is desirable to synchronize the cells in G1/G0. This can be achieved by growing the culture to confluence followed by serum deprivation (Schorl and Sedivy, 2007). Perinatal MSCs derived from WJ have shorter doubling times than adult MSCs derived from adipose tissues (Christodoulou et al., 2013) and there was no difference of proliferation kinetics of WJ-derived MSCs cultured in passage 1 and 7 with lag and log phase as 72 and 48 hours respectively (Zhou et al., 2011). Qiao et al. (2008) have shown that early passage human umbilical cord matrix stem cells had population doubling time (PDT) of 26 hours and it was as fast as that of human bone marrow MSCs (Qiao et al., 2008).

Here, the growth curve of early passage of cells isolated from porcine WJ was generated after synchronizing cells into resting (G0/G1) phase. According to the growth cure, proliferating cells exhibited a lag phase, a log phase and doubling time (24, 60 and 13.8 hours respectively). The doubling time is considerably shorter than reported for other MSCs including WJ cells. A shorter doubling time is an advantage for expanding WJ cells for use in experiments and

therapies. Understanding the growth kinetic of MSCs after synchronizing cells into the resting phase may also be useful information for increasing gene transfer efficiency using viral transduction. Viruses have specific transduction character into different host cell stages. High efficiency for retroviral transduction was observed in cells resting in G0/G1 (Chen et al., 2012). However, adeno-associated virus preferentially transduced proliferating cells (Russell et al., 1994).

References

Abu Kasim, N. H., V. Govindasamy, N. Gnanasegaran, S. Musa, P. J. Pradeep, T. C. Srijaya et al. 2012. Unique molecular signatures influencing the biological function and fate of post-natal stem cells isolated from different sources. J. Tissue Eng. Regen. Med.

Baksh, D., R. Yao, and R. S. Tuan. 2007. Comparison of proliferative and multilineage differentiation potential of human mesenchymal stem cells derived from umbilical cord and bone marrow. Stem Cells. 25(6): 1384-1392.

Barlow, S., G. Brooke, K. Chatterjee, G. Price, R. Pelekanos, T. Rossetti et al. 2008. Comparison of human placenta- and bone marrow-derived multipotent mesenchymal stem cells. Stem Cells Dev. 17(6): 1095-1107.

Brooke, G., H. Tong, J. P. Levesque, and K. Atkinson. 2008. Molecular trafficking mechanisms of multipotent mesenchymal stem cells derived from human bone marrow and placenta. Stem Cells Dev. 17(5): 929-940.

Cao, C., Y. Dong, and Y. Dong. 2005. Study on culture and in vitro osteogenesis of blood-derived human mesenchymal stem cells. Zhongguo Xiu Fu Chong Jian Wai Ke Za Zhi. 19(8): 642-647.

Cardoso, T. C., H. F. Ferrari, A. F. Garcia, J. B. Novais, C. Silva-Frade, M. C. Ferrarezi et al. 2012. Isolation and characterization of wharton's jelly-derived multipotent mesenchymal stromal cells obtained from bovine umbilical cord and maintained in a defined serum-free three-dimensional system. BMC Biotechnol. 12: 18-6750-12-18.

Chang, Y. J., D. T. Shih, C. P. Tseng, T. B. Hsieh, D. C. Lee, and S. M. Hwang. 2006. Disparate mesenchyme-lineage tendencies in mesenchymal stem cells from human bone marrow and umbilical cord blood. Stem Cells. 24(3): 679-685.

Chen, M., J. Huang, X. Yang, B. Liu, W. Zhang, L. Huang et al. 2012. Serum starvation induced cell cycle synchronization facilitates human somatic cells reprogramming. PLoS One. 7(4): e28203.

Cho, P. S., D. J. Messina, E. L. Hirsh, N. Chi, S. N. Goldman, D. P. Lo et al. 2008b. Immunogenicity of umbilical cord tissue derived cells. Blood. 111(1): 430-438.

Christodoulou, I., F. N. Kolisis, D. Papaevangeliou, and V. Zoumpourlis. 2013. Comparative evaluation of human mesenchymal stem cells of fetal (wharton's jelly) and adult (adipose tissue) origin during prolonged in vitro expansion: Considerations for cytotherapy. Stem Cells Int. 2013: 246134.

Colter, D. C., R. Class, C. M. DiGirolamo, and D. J. Prockop. 2000. Rapid expansion of recycling stem cells in cultures of plastic-adherent cells from human bone marrow. Proc. Natl. Acad. Sci. U. S. A. 97(7): 3213-3218.

Colter, D. C., I. Sekiya, and D. J. Prockop. 2001. Identification of a subpopulation of rapidly self-renewing and multipotential adult stem cells in colonies of human marrow stromal cells. Proc. Natl. Acad. Sci. U. S. A. 98(14): 7841-7845.

De Bari, C., F. Dell'Accio, P. Tylzanowski, and F. P. Luyten. 2001. Multipotent mesenchymal stem cells from adult human synovial membrane. Arthritis Rheum. 44(8): 1928-1942.

De Coppi, P., G. Bartsch Jr, M. M. Siddiqui, T. Xu, C. C. Santos, L. Perin et al. 2007. Isolation of amniotic stem cell lines with potential for therapy. Nat. Biotechnol. 25(1): 100-106.

Dominici, M., K. Le Blanc, I. Mueller, I. Slaper-Cortenbach, F. Marini, D. Krause et al. 2006. Minimal criteria for defining multipotent mesenchymal stromal cells. the international society for cellular therapy position statement. Cytotherapy. 8(4): 315-317.

Ganta, C., D. Chiyo, R. Ayuzawa, R. Rachakatla, M. Pyle, G. Andrews et al. 2009. Rat umbilical cord stem cells completely abolish rat mammary carcinomas with no evidence of metastasis or recurrence 100 days post-tumor cell inoculation. Cancer Res. 69(5): 1815-1820.

Hoynowski, S. M., M. M. Fry, B. M. Gardner, M. T. Leming, J. R. Tucker, L. Black et al. 2007. Characterization and differentiation of equine umbilical cord-derived matrix cells. Biochem. Biophys. Res. Commun. 362(2): 347-353.

Kang, E. J., Y. H. Lee, M. J. Kim, Y. M. Lee, B. M. Kumar, B. G. Jeon et al. 2013. Transplantation of porcine umbilical cord matrix mesenchymal stem cells in a mouse model of parkinson's disease. J. Tissue Eng. Regen. Med. 7(3): 169-182.

Karahuseyinoglu, S., O. Cinar, E. Kilic, F. Kara, G. G. Akay, D. O. Demiralp et al. 2007. Biology of stem cells in human umbilical cord stroma: In situ and in vitro surveys. Stem Cells. 25(2): 319-331.

Kern, S., H. Eichler, J. Stoeve, H. Kluter, and K. Bieback. 2006. Comparative analysis of mesenchymal stem cells from bone marrow, umbilical cord blood, or adipose tissue. Stem Cells. 24(5): 1294-1301.

Lee, C. C., F. Ye, and A. F. Tarantal. 2006. Comparison of growth and differentiation of fetal and adult rhesus monkey mesenchymal stem cells. Stem Cells Dev. 15(2): 209-220.

Lee, K. S., J. J. Nah, B. C. Lee, H. T. Lee, H. S. Lee, B. J. So et al. 2013. Maintenance and characterization of multipotent mesenchymal stem cells isolated from canine umbilical cord matrix by collagenase digestion. Res. Vet. Sci. 94(1): 144-151.

Li, J., D. Li, X. Liu, S. Tang, and F. Wei. 2012. Human umbilical cord mesenchymal stem cells reduce systemic inflammation and attenuate LPS-induced acute lung injury in rats. J. Inflamm. (Lond). 9(1): 33-9255-9-33.

Longo, U. G., M. Loppini, A. Berton, L. La Verde, W. S. Khan, and V. Denaro. 2012. Stem cells from umbilical cord and placenta for musculoskeletal tissue engineering. Curr. Stem Cell. Res. Ther. 7(4): 272-281.

Maurer, M. H. 2011. Proteomic definitions of mesenchymal stem cells. Stem Cells Int. 2011: 704256.

Mitchell, K. E., M. L. Weiss, B. M. Mitchell, P. Martin, D. Davis, L. Morales et al. 2003. Matrix cells from wharton's jelly form neurons and glia. Stem Cells. 21(1): 50-60

Noort, W. A., M. I. Oerlemans, H. Rozemuller, D. Feyen, S. Jaksani, D. Stecher et al. 2012. Human versus porcine mesenchymal stromal cells: Phenotype, differentiation potential, immunomodulation and cardiac improvement after transplantation. J. Cell. Mol. Med. 16(8): 1827-1839.

Orciani, M., and R. Di Primio. 2013. Skin-derived mesenchymal stem cells: Isolation, culture, and characterization. Methods Mol. Biol. 989: 275-283.

Pa, M., H. S, M. R, G. M, and S. K. W. 2011. Adult mesenchymal stem cells and cell surface characterization - a systematic review of the literature. Open Orthop. J. 5(Suppl 2): 253-260.

Peister, A., J. A. Mellad, B. L. Larson, B. M. Hall, L. F. Gibson, and D. J. Prockop. 2004. Adult stem cells from bone marrow (MSCs) isolated from different strains of inbred mice vary in surface epitopes, rates of proliferation, and differentiation potential. Blood. 103(5): 1662-1668.

Perry, B. C., D. Zhou, X. Wu, F. C. Yang, M. A. Byers, T. M. Chu et al. 2008. Collection, cryopreservation, and characterization of human dental pulp-derived mesenchymal stem cells for banking and clinical use. Tissue Eng. Part C. Methods. 14(2): 149-156.

Qiao, C., W. Xu, W. Zhu, J. Hu, H. Qian, Q. Yin et al. 2008. Human mesenchymal stem cells isolated from the umbilical cord. Cell Biol. Int. 32(1): 8-15.

Ragni, E., M. Vigano, V. Parazzi, T. Montemurro, E. Montelatici, C. Lavazza, S. Budelli, A. Vecchini, P. Rebulla, R. Giordano and L. Lazzari. 2013. Adipogenic potential in human mesenchymal stem cells strictly depends on adult or foetal tissue harvest. Int J Biochem Cell Biol. 45(11): 2456-2466.

Ramkisoensing, A. A., D. A. Pijnappels, S. F. Askar, R. Passier, J. Swildens, M. J. Goumans et al. 2011. Human embryonic and fetal mesenchymal stem cells differentiate toward three different cardiac lineages in contrast to their adult counterparts. PLoS One. 6(9): e24164.

Rozemuller, H., H. J. Prins, B. Naaijkens, J. Staal, H. J. Buhring, and A. C. Martens. 2010. Prospective isolation of mesenchymal stem cells from multiple mammalian species using cross-reacting anti-human monoclonal antibodies. Stem Cells Dev. 19(12): 1911-1921.

Russell, D. W., A. D. Miller and I. E. Alexander. 1994. Adeno-associated virus vectors preferentially transduce cells in S phase. Proc Natl Acad Sci U S A. 91(19): 8915-8519.

Sabapathy, V., S. Ravi, V. Srivastava, A. Srivastava, and S. Kumar. 2012. Long-term cultured human term placenta-derived mesenchymal stem cells of maternal origin displays plasticity. Stem Cells Int. 2012: 174328.

Schorl, C., and J. M. Sedivy. 2007. Analysis of cell cycle phases and progression in cultured mammalian cells. Methods. 41(2): 143-150.

Scott, M. A., V. T. Nguyen, B. Levi, and A. W. James. 2011. Current methods of adipogenic differentiation of mesenchymal stem cells. Stem Cells Dev. 20(10): 1793- 1804.

Sekiya, I., B. L. Larson, J. T. Vuoristo, J. G. Cui, and D. J. Prockop. 2004. Adipogenic differentiation of human adult stem cells from bone marrow stroma (MSCs). J. Bone Miner. Res. 19(2): 256-264.

Taghi, G. M., H. Ghasem Kashani Maryam, L. Taghi, H. Leili, and M. Leyla. 2012. Characterization of in vitro cultured bone marrow and adipose tissue-derived mesenchymal stem cells and their ability to express neurotrophic factors. Cell Biol. Int. 36(12): 1239-1249.

Taghizadeh, R. R., K. J. Cetrulo, and C. L. Cetrulo. 2011. Wharton's jelly stem cells: Future clinical applications. Placenta. 32 Suppl 4: S311-5.

Tropel, P., D. Noel, N. Platet, P. Legrand, A. L. Benabid, and F. Berger. 2004. Isolation and characterisation of mesenchymal stem cells from adult mouse bone marrow. Exp. Cell Res. 295(2): 395-406.

Valorani, M. G., A. Germani, W. R. Otto, L. Harper, A. Biddle, C. P. Khoo et al. 2010. Hypoxia increases sca-1/CD44 co-expression in murine mesenchymal stem cells and enhances their adipogenic differentiation potential. Cell Tissue Res. 341(1): 111-120.

Weiss, M. L., S. Medicetty, A. R. Bledsoe, R. S. Rachakatla, M. Choi, S. Merchav et al. 2006. Human umbilical cord matrix stem cells: Preliminary characterization and effect of transplantation in a rodent model of parkinson's disease. Stem Cells. 24(3): 781-792.

Zhang, Y., D. Khan, J. Delling, and E. Tobiasch. 2012. Mechanisms underlying the osteo- and adipo-differentiation of human mesenchymal stem cells. ScientificWorldJournal. 2012: 793823.

Zhou, C., B. Yang, Y. Tian, H. Jiao, W. Zheng, J. Wang et al. 2011. Immunomodulatory effect of human umbilical cord wharton's jelly-derived mesenchymal stem cells on lymphocytes. Cell. Immunol. 272(1): 33-38.

Figure 2.1 Isolation of PUCs from Wharton's jelly of umbilical cord.

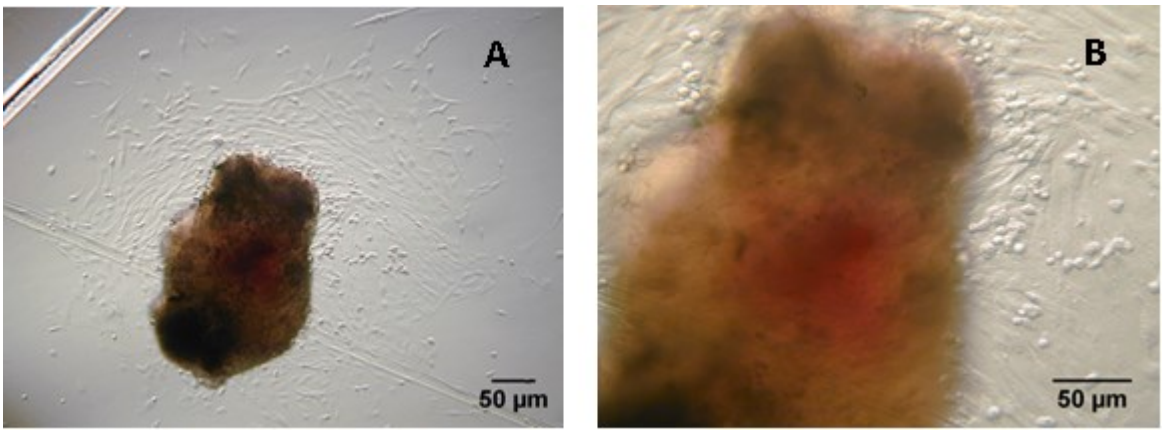

Migration of heterogeneous cells from a Wharton's jelly explant was observed with 4x magnification bright field microscopy after incubation in complete medium for 5 days (A) With 10x magnification, migrating cells displayed two type of morphology as spindle and round shapes (B).

Figure 2.2 Adipogenic differentiation potential of PUCs

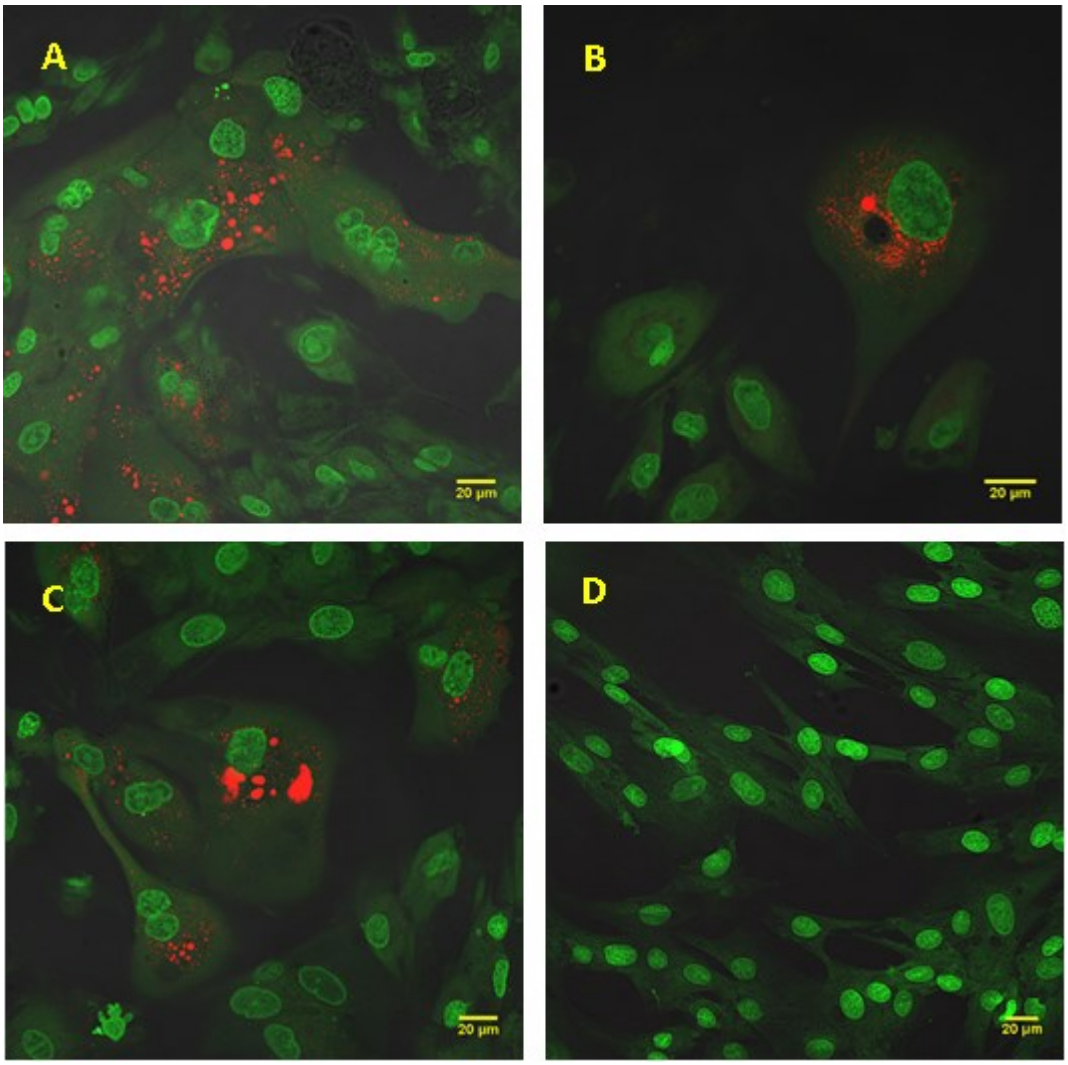

Adipogenesis-induced PUCs undergo a morphological change from spindle to enlarged spherical shape with intracellular lipid droplets (red spots) stained with neutral lipid- specific dye, LipidTOX™ Red (A-C). As a negative control, PUCs cultured in growth culture medium displayed fibroblast-like morphology without expression of stained lipid droplets (D). Cell nuclei counterstained with Syto®16 showed green. Image were taken at 40x magnification with 0.6x digital zoom (A-B), 0.8x digital zoom (C) and 0.5x digital zoom (D) on a Zeiss 710 confocal microscope

Figure 2.3 Flow cytometry analysis for adipogenic differentiation of PUCs.

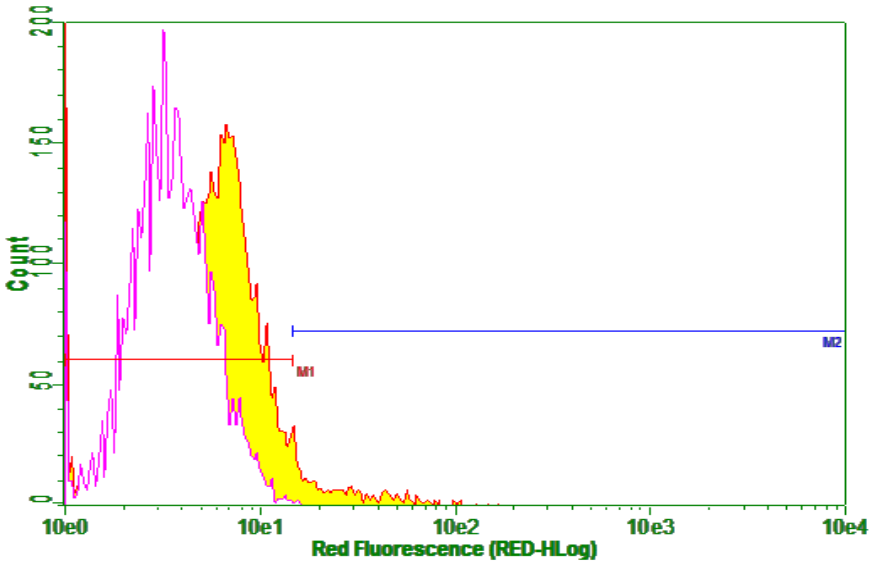

Histogram illustrates the result of adipogenic differentiation of PUCs after staining with LipidTOX™ Red neutral lipid stain. Gate M1, an open area, is representative of non-induced PUCs cultured in complete growth medium. PUCs undergone the adipogenic differentiation are in gate M2, a yellow area.

Figure 2.4 Osteogenic differentiation potential of PUCs.

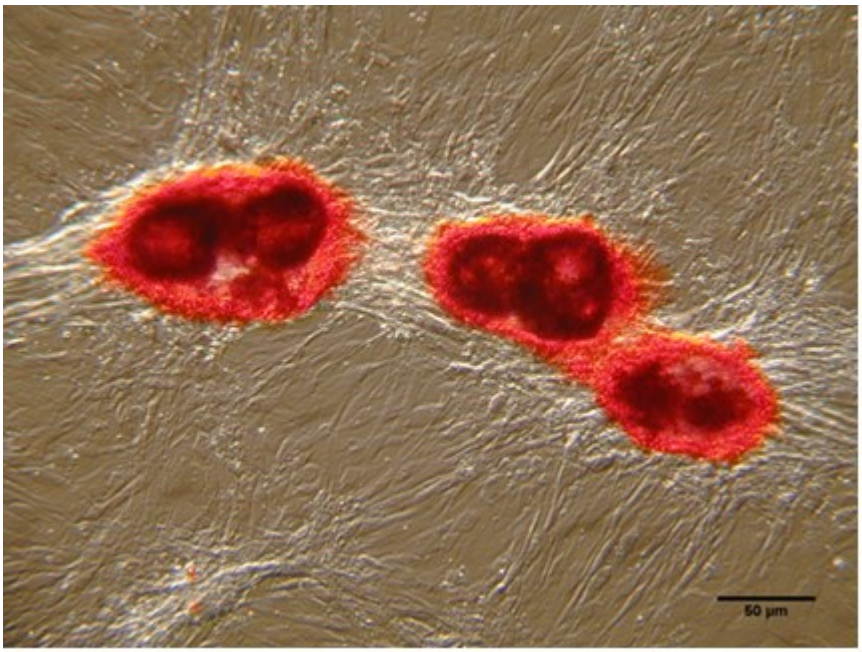

PUCs cultured in osteogenic differentiation medium showed extracellular calcium deposits that stained bright orange-red when stained with Alizarin red dye. The image was taken by inverted-phase contrast microscope (Nikon Diaphot-300) with 4x magnification.

Figure 2.5 Chondrogenic differentiation potential of PUCs.

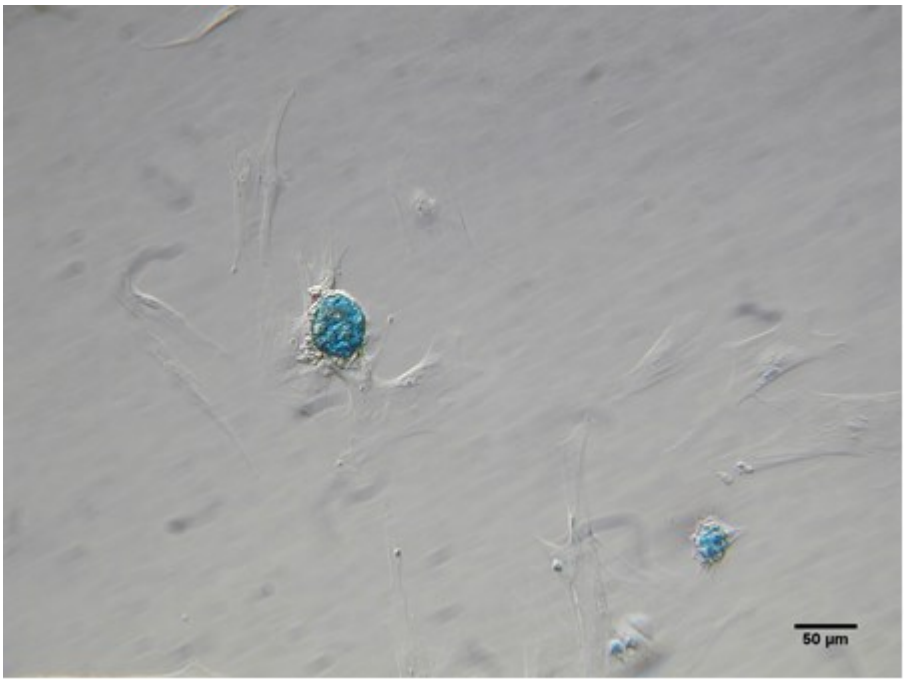

Induction of chondrogenesis in PUCs. Micromass culture was established as described in Materials and Methods. Cell pellets stained positively with Alcian Blue indicating the presence of proteoglycans a component of the matrix. The image was taken with inverted-phase contrast microscope (Nikon Diaphot-300) with 10x magnification.

Figure 2.6 Flow cytometric analysis of surface marker expression by PUCs.

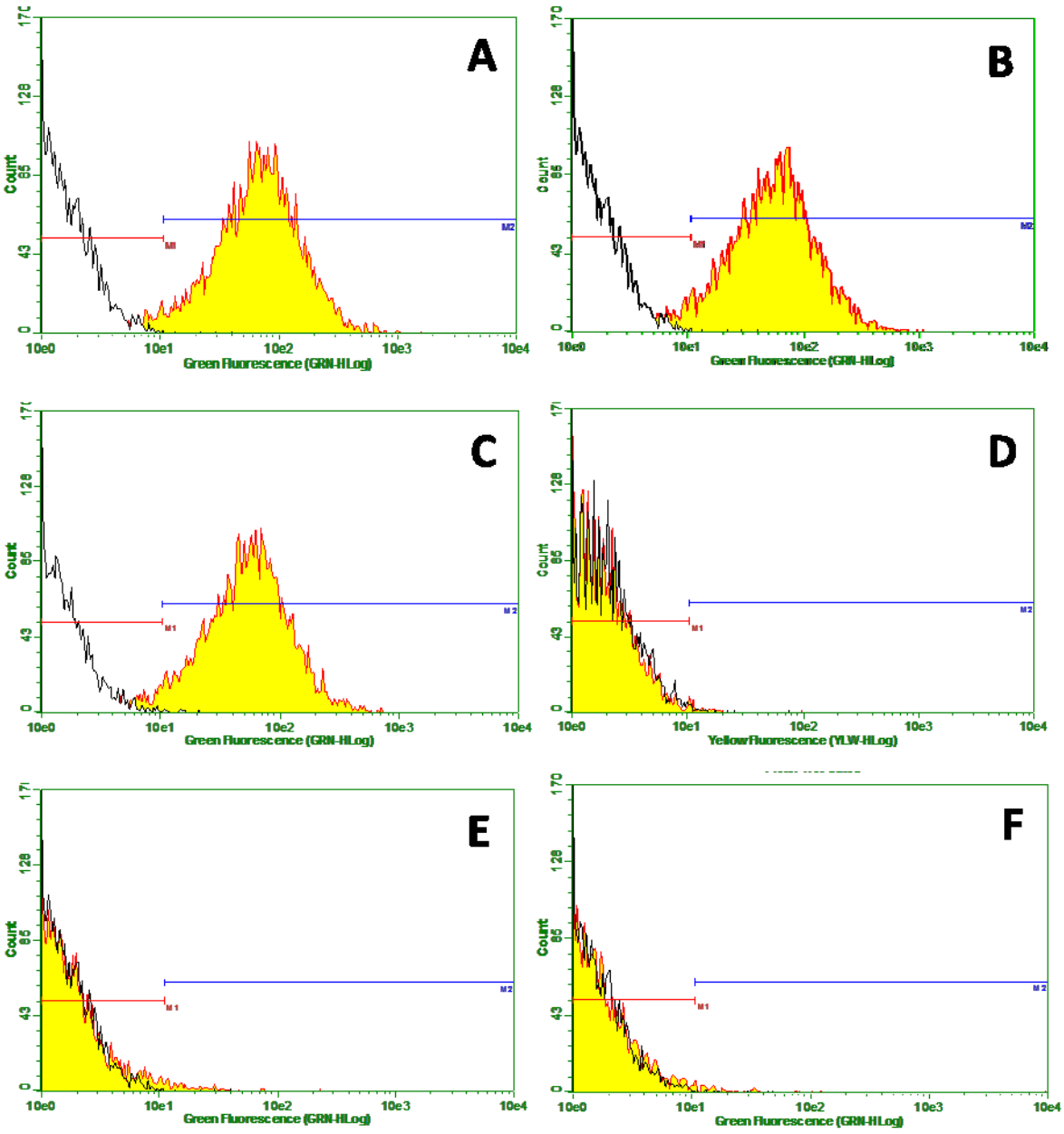

Cell suspensions obtained from 4 different cell lines of PUCs were stained with specific mouse anti-porcine monoclonal antibodies indicated in filled histograms: CD 90 (A), CD 44 (B), CD 105 (C), CD 31 (D), CD 45 (E), SLA-DR (F). The empty histogram is the respective IgG isotype control. The data shown are representative of those obtained in 4 different experiments.

Figure 2.7 Flow cytometry for DNA content illustrating the synchronization of PUCs in G0/G1 phase.

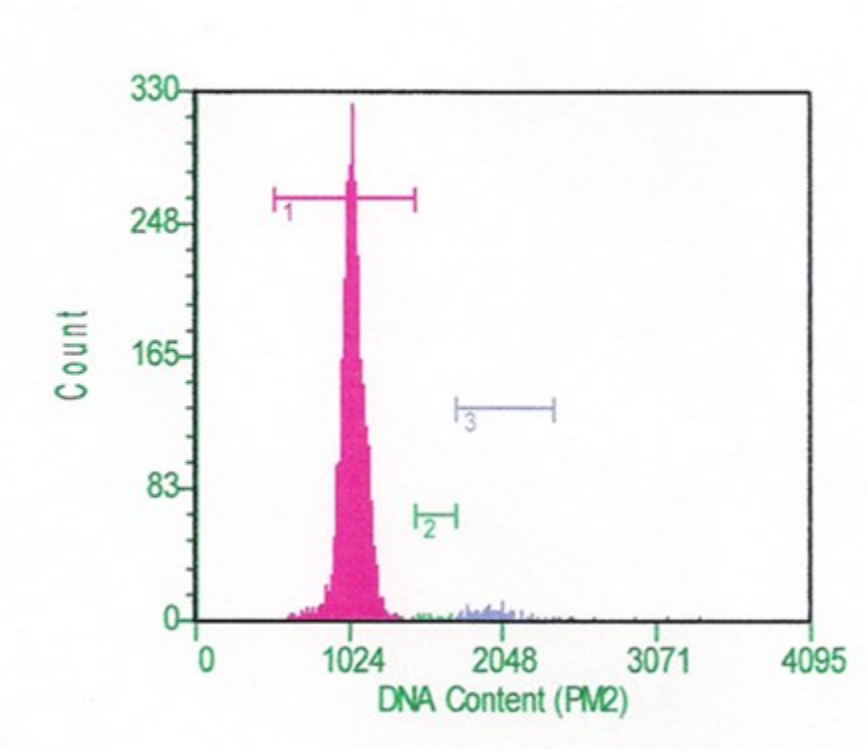

Histogram indicates the distribution of DNA content of PUCs (P3) synchronized into resting phase by culturing in the absence of serum. The pink, green and blue filled areas are representative of the number of cells within G0/G1, S and G2/M phase respectively.

Figure 2.8 The growth curve of PUCs at passage 3 (P3).

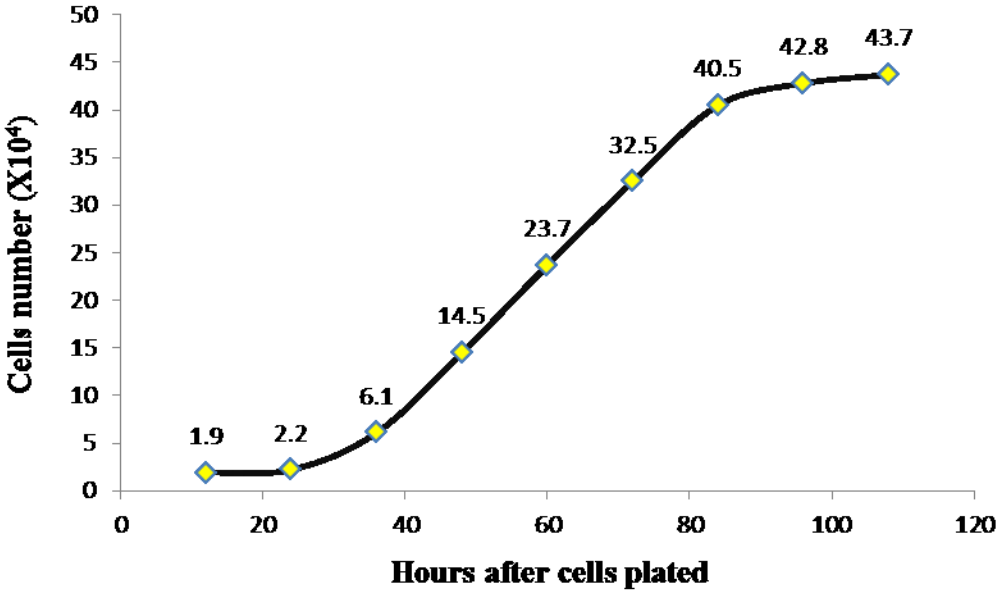

The growth kinetics of early passage (P3) PUCs: The average growth kinetics of PUCs was measured by determining triplicates cell count number every 12 hours in culture.

Table 2.1 Phenotype characterization of PUCs cultured in passage 3.

Phenotype characterization (%)	PUCs (10^6 cells)					
	1	2	3	4	Mean	SE
CD 90	94.1	93.8	92.6	90.5	92.7	0.82
CD 44	91.5	90.7	93.1	92.1	91.9	0.51
CD 105	92.8	90.5	94.2	91.3	92.2	0.82
CD 31	0.84	0.64	0.72	0.85	0.76	0.05
CD 45	1.74	1.92	1.54	1.32	1.63	0.13
SLA-DR	1.32	1.64	1.33	1.24	1.38	0.09

Table 2.2 Percentage of viability and G0/G1 phase of PUCs passage 3 (P3) after culturing in serum-deprived medium

PUCs (P3)	G0/G1 Phase	Viability
1	92.8	77.5
2	91.5	76.8
3	93.4	77.2
Mean	92.5	77.1
SE	0.56	0.20

Table 2.3 Triplicate collection data of viable PUCs (P3) in 12-108 hours after plating in complete growth medium.

Hours after plating PUCs	Cells numbers ($x10^4$)			
	1	2	3	Mean±SE
12	1.8	2	1.85	1.9±0.06
24	2.3	2.3	1.95	2.2±0.12
36	6.1	5.9	6.2	6.1±0.09
48	14	15	14.5	14.5±0.29
60	23	24	24	23.7±0.33
72	33	32	32.5	32.5±0.29
84	41	40.5	40	40.5±0.29
96	42	43.5	43	42.8±0.44
108	44	44.2	43	43.7±0.37

Chapter 3 - Engraftment Potential of PUCs Transplanted to Allogeneic Neonatal Pigs

Introduction

Regenerative medicine is focused on the application of stem-cell technologies to repair, replace, or regenerate cells, tissues or organs to restore impaired function that results from any cause (Daar and Greenwood, 2007). As this central objective has developed other potentials of some stem-cell populations have been identified. Thus the use of stem cells as delivery vehicles for various therapeutics has been demonstrated (eg. Rachakatla et al., 2007). Another emerging field is the potential trophic, protective, or otherwise beneficial effects of mesenchymal stem cells (MSCs) in therapies (Caplan, 2007; Prockop, 2009). MSCs isolated from many adult and fetal tissues are a major advance for transplantation therapy. MSCs can be cultured and proliferate to high numbers in vitro with the capacity for self-renewal and the potential to differentiate into one or more types of specialized cells (Mimeault and Batra, 2008). Evaluation of the appropriate route of cell administration is an essential prerequisite for the success of cell engraftment for organ repair (Strauer and Kornowski, 2003) and for the other therapeutic objectives. High cell concentrations within the areas of inflammation and infarct and minimizing homing of transplanted cells into other non-target tissues are desirable. Therefore, regional and targeted administration of cells may be preferable unless systemic administration is required. Infusion of cells directly into the blood circulation via intravenous routes is the most frequently used transplantation method. Arterial and venous thromboses are potential complications and may cause morbidity and mortality in recipients transplanted intravenously (Kansu, 2012).

The intraperitoneal (IP) route is commonly used for therapies such as paracentesis, peritoneal dialysis, and chemotherapeutic drug administration (Chua et al., 2009). The advantage of IP injection is the large absorbent surface of the peritoneum that allows quick local/systemic diffusion (Esquivel, 2009). Stachowska-Pietka et al. (2006) demonstrated that 20–40% of the fluid that flows into the tissue from the peritoneal cavity is absorbed by the lymphatics, whereas the larger (60–80%) volume of the fluid is absorbed by the blood capillaries. Cells transplanted by intraperitoneal injection have been employed mainly prenatally (Flake et al., 1986; Shaaban et

al., 1999). The possibility of using the IP route for postnatal systemic cell delivery has been suggested (Di Campli et al., 2004; Piscaglia et al., 2005).

Oral administration is generally not considered for cells because they would be exposed to harsh conditions, including digestive enzymes and acidic conditions of the stomach and small intestine and if absorbed into the portal system would still be potentially metabolized at the liver (Turner et al., 2011). Intestine contains two independent lymphatic networks located in lamina propria and muscularis mucosa. Both finally drain the lymph into a common collecting lymph vessel found in submucosa layer. Then, the lymph is drained into the thoracic duct prior to circulating systematically. It is likely that cells which cross the intestinal epithelium would reach the systemic circulation using this route (Miller et al., 2010). Gastrointestinal tracts of neonates have pH conditions near neutrality and a low activity of digestive enzymes (Sangild et al., 2000). Previously we administered PUCs orally into pre-nursing porcine neonates and detected them the in lamina propria of the intestine 8 hours after feeding (Miller et al., 2012). However, allogeneic PUCs administered orally were not found in other organs at 8 hours after oral administration.

The aim of this study was to evaluate the ability of allogeneic PUCs injected peritoneally and given orally to healthy neonatal pigs for systemic migration and potential engraftment into various tissues. PUCs are porcine umbilical cord matrix stem cells (UMCs) that are generally collected perinatally. UMCs have intermediate characteristic between embryonic and adult stem cells (Pappa and Anagnou, 2009). Unlike postnatal MSCs, UMCs consistently express embryonic stem cell markers and Oct-4, Sox-2, and Nanog are expressed in PUCs (Carlin et al., 2006). Human UMCs also express markers of pluripotency, such as SSEA-4 and Tra-1-60 (Jo et al., 2008). Importantly, these cells also demonstrate characteristics of immunoprivilege, and do not form tumor after transplantation. UMCs possessing broader multipotent plasticity and proliferate faster than adult MSCs (Weiss et al., 2006; Fong et al., 2011).

Moreover, because umbilical cords are normally discarded after birth, these stem cells could be isolated without ethical concerns (Marcus and Woodbury, 2008). In xenograft models using immunocompromised mice, human UMCs transplanted intravenously migrate to tumor sites (Rachakatla et al., 2007; Maurya et al., 2010; Ganta et al., 2009) and distribute to various tissues of healthy mice after intravenous injection (Maurya et al., 2011). To evaluate the potential for allogeneic transplantation we conducted a series of experiments using neonatal pigs administered PUCs by oral and IP routes.

Materials and Methods

Animal

Pigs used for these experiments were provided by the Swine Teaching and Research Center, Kansas State University. All animal procedures were approved by the Institutional Animal Care and Use Committee.

Fluorescent dye staining of PUCs and neonatal fibroblasts

PUCs were labeled with the lipophilic fluorescent dyes PKH26GL (Sigma-Aldrich) or CellVue®NIR815 (LI-COR Biosciences, Lincoln, NE). The fibroblasts derived from ears of neonatal pigs also were labeled with PKH26GL. The maximum excitation/emission wavelengths of PKH26GL and CellVue®NIR815 are 551/567 nm and 786/814 nm. Expanded adherent PUCs were harvested from tissue culture flasks using trypsin/EDTA and as a single cell suspensions. Approximately, $1x10^7$ cells were washed with serum free medium, and centrifuged (400 x g). The supernatant was aspirated and the cells were resuspended and dispersed with 1 ml of Diluent C provided by the manufacturer. Immediately prior to staining, $4x10^{-6}$ M of either PKH26GL or CellVue®NIR815 dye solution was prepared by adding 4 µl of $1x10^{-3}$ M dye stock in ethanol into 1 ml of Diluent C in a polypropylene centrifuge tube and mixing to disperse. The 1 ml of cell suspension was added rapidly to 1 ml of dye solution and incubated 25°C for 5 minutes. The staining reaction was stopped by adding an equal volume of serum and incubated for 1 minute. The serum-stopped sample was diluted with an equal volume of complete medium. The stained cells were centrifuge (400 x g) for 10 minutes 25°C and the supernatant removed. The stained cells were washed twice with serum free medium to eliminate excess dye and resuspended in high-glucose Dulbecco's Minimum Essential Medium with HEPES (GlutaMAX™-DMEM-HEPES, Invitrogen) at a concentration of $1x10^7$cells/ml.

To verify cell staining and viability, PKH26GL stained cells were stained with 0.05 µM of cell-impermeant cyanine dye, SYTOX® Green dye (Invitrogen), with excitation and emission maxima of 504 nm and 523 nm. Double fluorescent dye stained-PUCs were detected by the emitted red and green fluorescence in PM3 and PM2 channels of a microcapillary cytometer (Guava EasyCyte Plus, Millipore). PUCs stained with CellVue®NIR815 were verified by plating $2x10^5$ cells (approximately) in a well of a 96 black-well plate before using IVIS Lumina II imaging system (Caliper Life Sciences) with 745 nm excitation laser line and BP 810-875 nm

filter for detection of fluorescence emission. Viability of CellVue®NIR815-stained cells was evaluated by the dye exclusion method using 0.4% trypan blue dye (Gibco®).

Cell administration to pigs

The fluorescence-dye labeled PUCs were administrated to pre-nursed and nursed newborn pigs by oral feeding. They also were injected intraperitoneally into neonatal, 1-day, 1 week, 2-week and 3-week old pigs. Fibroblasts stained with PKH26 were injected intraperitoneally into post-colostral newborn pigs. Pigs were weighed and ear tagged before administration of labeled PUCs. Subsequently pigs were ear notched to provide two means of identification. For oral feeding, sows were observed during farrowing and newborn pigs were not allowed to nurse until cells were fed (<1 h following birth). Oral feeding of nursed pigs was also evaluated in newborn pigs allowed to nurse and about 1 hour after birth. Feeding of the labeled cells was by a modified 12 French feeding tube (Kendall Healthcare, Marietta, Georgia), cut to 187 mm in length. The feeding tube was placed behind the tongue and labeled PUCs suspended in 3 ml of complete medium were administered with a 5 ml syringe. The pig was observed to swallow the labeled cell suspension during feeding and the feeding tube was flushed with PBS (1 ml) to wash any the residual cells through the tube. The treated pigs were returned to the farrowing crate for ad libitum nursing until sacrifice. For IP injections, pigs were restrained by holding the rear legs with the head down before injection. The labeled PUCs were injected in 3 ml of serum free medium into the peritoneal cavity using an 18 gauge 1-1/2" needle placed on the right side lateral to the teat line and between the first and the second pairs of nipples. The pigs were returned to the sow and observed for 30 minutes.

Pig Sacrifice

Pigs were sacrificed by first anesthetizing by inhalation of Isoflurane (1-5% in O_2) administered to effect via a cone placed over the nose. Once pigs reached to a deep surgical plane with no palpebral or pedal reflex, they were sacrificed by intracardiac injection of a saturated solution of potassium chloride to induce cardiac arrest.

Blood and tissues collection

Blood samples (10 ml) from each treated and control pig were collected directly from the heart prior to KCl injection and transferred into evacuated blood collection tubes containing

sodium heparin. Blood was refrigerated until processing. Following sacrifice, the pig was positioned dorsally and the trunk opened longitudinally. Tissues were collected from the heart, lung, pancreas, liver, kidney, omentum, stomach, intestine, uterine horn, ovary, muscle and bone marrow. The whole intestine was opened longitudinally and intestinal lumen washed with tap water. The duodenum, jejunum, ileum, cecum and colon were separated and kept in ice cold 1X HBSS containing Ca^{2+} and Mg^{2+}. All parts of intestines were scanned to locate fluorescent positive area using IVIS Lumina II imaging system (Caliper Life Sciences). All pieces of collected organs including fluorescent positive and negative areas of all parts of intestines were collected and preserved in DMSO/EDTA/Saturated NaCl buffer (DESS) buffer and 4% paraformaldehyde solution (16%, Thermo Scientific) for cryosection and DNA isolation.

Cell isolation from blood and bone marrow

Femurs of sacrificed pigs were removed, cleaned of all connective tissues and placed in ice-cold PBS containing antimycotic/antibiotic reagent (Gibco, 1:100). The ends of femurs were cut to expose the marrow. To prevent clotting, the marrow was flushed from both ends with DMEM containing 5 mM EDTA using a 3 ml syringe with an 18-g needle. Isolated cells were centrifuged (400 x g) for 8 minutes and suspended in 5 ml of red blood cell lysis buffer (Sigma) for 5 minutes. Cells were again pelleted by centrifugation (400 x g) for 8 minutes and washed 2 times with PBS. Bone marrow cells were suspended in PBS and evaluated by flow cytometry or were cultured with complete growth medium in tissue culture flasks (25 cm^2) until they reached 85-90% confluence. Cultured cells were harvested and their chromosomal DNA was isolated to determine the presence of the Y-chromosome gene, SRY gene, by PCR. Blood of female recipients was diluted 1:1 with PBS before centrifugation (400 x g) for 8 minutes. The cell pellet was suspended in 10 ml of red blood cell lysis buffer for 10 minutes followed by washing 2 times with PBS. The isolated blood cells were suspended in 200 µl of PBS before they were evaluated by flow cytometry or PCR. Chromosomal DNA of cells derived from female recipient blood was isolated and used as a template to detect SRY gene of engrafted male donor cells by PCR. Cells isolated from blood and bone marrow of female recipients were suspended with 200 µl of PBS. Expression of transplanted PKH26- labeled male PUCs in cell suspensions were detected by a microcapillary cytometer (Guava EasyCyte Plus, Millipore) using the red filter channel, PM3.

DNA isolation

Collected tissues (25 mg) preserved in DMSO/EDTA/sodium chloride solution (DESS) were placed in a dish with water for a few minutes to remove any salt or DESS that might be attached. The washed tissue was transferred to a microcentrifuge tube and homogenized using a pellet pestle (Sigma). Total DNA was isolated from homogenized tissues using DNeasy Kits (Qiagen) according to the manufacturer's instructions. Briefly, the disrupted tissue was lysed by tissue lysis buffer and proteinase K. Tissue lysates were treated with RNase and cell lysis buffer. Cell lysates were mixed with molecular-grade ethanol and transferred into DNeasy spin columns. Total genomic DNA was eluted from spin columns and quantified using the NanoDrop ND-1000 spectrophotometer (NanoDrop Technologies, Wilmington, DE).

Polymerase chain reaction (PCR)

Two micrograms of total genomic DNA was used as the template for 50 µl PCR reactions. The PCR reaction was carried out using the HotStar Taq DNA Polymerase Kit (Qiagen) which included 10X PCR buffer (15 mM Mg^{2+} plus), 25 mM MgCl2, 5X Q solution and 5 U/µl HotStar Taq DNA polymerase. Each PCR reaction contained 1X PCR buffer, 2.0 mM $MgCl_2$, 0.8mM dNTP (Advantage Ultrapure Nucleotide, Clonetech), 1X Q solution, 0.05 U/µl of HotStar Taq DNA polymerase, and 0.28 µM specific porcine SRY forward and reverse primers (Forward: 5'-GGCTTTCTGTTCCTGAGCAC-3', Reverse: 5'-CTGGGATGCAAGTGGAAAAT-3', product size: 247 bp) and porcine-specific beta-actin genes forward and reverse primer (Forward: 5'-GTCATCACCATCGGCAATGA-3', Reverse: 5'-CGTGAATGCCGCAGGATT-3', product size: 183 bp). PCR conditions were 1 cycle of 15 min at 95 °C, followed by 35 cycles of 30 sec at 95°C, 30 sec at 59°C, and 30 sec at 72°C, and finishing with 7 min incubation at 72°C. PCR reaction products stained with ethidium bromide were visualized by agarose gel electrophoresis.

Agarose gel electrophoresis

The agarose gel (2.5%) was prepared in 1X TBE and ethidium bromide (250 ng/µl). Loading dye (6x; 5µl) was added to the PCR reactions (25 µl) and mixed prior to loading into wells of agarose gel. Agarose gels were run at 100 volts for approximately 1 hour. A DNA ladder (100 bp) was included and the DNA was visualized under UV on a transilluminator and photographed with a Polaroid camera.

Digoxigenin (DIG) labeled DNA probes synthesis

Based on PCR reaction, 377 bp of dsDNA probes specific to porcine Y chromosome, SRY, was synthesized and labeled with digoxigenin (DIG) using a PCR DIG Probe Synthesis Kit (Roche). The kit was comprised of PCR buffer with 15 mM MgCl2 (10X), PCR DIG Probe synthesis Mix (10X) and enzyme mix. Synthesis of DIG-labeled DNA probes followed the manufacturer's instructions. Briefly, 50 ng of male genomic DNA isolated from male PUCs was added to 50 µl PCR reaction contained with 1X PCR buffer with 1.5 mM MgCl2, 1X PCR DIG Probe Synthesis Mix containing dNTPs and DIG-11-dUTP, 0.75 µl of enzyme mix and 0.25 µM of specific porcine SRY forward and reverse primers (Forward: 5'-AATCCACCATACCTCATGGACC-3', Reverse: 5'-TTTCTCCTGTATCCTCCTGC-3', product size: 377 bp). PCR conditions were 1 cycle of 2 min at 95 °C, followed by 35 cycles of 15 sec at 95°C, 60 sec at 60°C, and 15 sec at 72°C, and finishing with 7 min incubation at 72°C. Digoxigenin (DIG) labeled DNA probes were isolated and purified from PCR reactions using QIAquick PCR Purification Kit (Qiagen) according to the manufacturer' instructions. PCR reactions were treated with high chaotropic salts buffer and ethanol to facilitate precipitated DNA probe to bind to a silica membrane of QIAquick PCR Purification spin columns before the purified DNA probes were eluted with elution buffer. Size and purity of eluted DIG-labeled dsDNA probes were determined by staining with ethidium bromide and visualized by agarose gel electrophoresis. The DIG-labeled dsDNA probes were approximately quantified according to the density of ethidium bromide-stained 100 bp DNA ladder.

Re-culture of intestinal transplanted PUCs

Pieces of the exposed and cleaned intestines (15-20 cm) were collected in ice-cold serum free culture medium until processing for cell isolation. The collected pieces of inverted intestines were incubated in 1 mM EDTA mixed with 1mM dithiothreitol (DTT) in PBS without Ca^{2+} and Mg^{2+} for 7 minutes at 37°C to remove mucus and intestinal epithelial cells. The pieces of intestines were washed 5 minutes twice in PBS without Ca^{2+} and Mg^{2+} at room temperature, then, placed incubated in enzymatic digestion solution (100 ml) with shaking (low speed) at 37°C for 45 minutes. The enzymatic solution was comprised of collagenase type 3 (220 u/ml), neutral protease (0.5 u/ml) and deoxyribonuclease type 1 (50 u/ml) (all enzymes were from Worthington) in complete growth medium. The pieces of intestine were removed and the

enzymatic reaction inactivated by incubating at 4°C for 5 minutes. The isolated cell suspension was filtered (Steriflip® 60 µm pore size; EMD Millipore), then centrifuged (500 x g for 10 minutes at 4°C). The cell pellet was washed twice with PBS (room temperature). Recovered cells were plated on chamber slides (Lab-Tek® II Slide) and a tissue culture flask (75 cm^2) for detection of transplanted PUCs engrafted in intestines using FISH and PCR methods.

Slide preparation for fluorescent in situ hybridization (FISH)

Intestinal cells isolated from small intestines using the enzymatic digestion procedure were cultured in complete growth medium at 38.5°C for 7-10 days with the medium replaced every 3 days. After culture the medium was removed and the slides were washed 3 times with PBS, fixed with cold methanol: glacial acetic acid (3:1) for 10 minutes. The cells were washed in PBS for 5 minutes, 3 times before the fixed cells were incubated in 10 mM sodium citrate (pH 6.0) at 96 °C for 15 minutes. Slides were air-dried at room temperature (5 minutes) and washed 2 times (5 minutes each) in 2X SSC solution at room temperature. Subsequently, the slides were treated with 200 µl of 100 µg/ml of RNase A (Sigma) in 2X SSC for 1 hour at 37 °C and washed 2 times, 5 minutes in 2X SSC solution at room temperature. Then, the slides were rinsed with 10 mM HCl for 2 minutes and treated with 200 µl of 40 U/ml of pepsin (Sigma) in 10 mM HCl for 10 minutes at 37 °C. The enzyme-treated slides were rinsed with distilled water and washed 2 times for 5 minutes in 2X SSC solution at room temperature. The slides were dehydrated by passing through a series of ethanol concentrations (70%; 85%; 100%) and air-dried. Chromosome denaturation was carried out in 70% (v/v) formamide/2X SSC solution at 75 °C for 5 minutes. The slides were dehydrated by passing through a series of ethanol concentrations (70%; 85%; 100%) and air-dried.

Fluorescent in situ hybridization and detection

HybriwellTM (Sigma), a slide sealing system, was installed over the slide. One hundred and fifty microliters of a hybridization mixture containing 24 µl of purified DIG-labeled DNA probe solution derived from 2 PCR reactions and 126 µl of hybridization buffer was prepared. The HybriwellTM was filled with hybridization mixture before it was sealed with adhesive plastic. The slide was incubated (75°C for 5 minutes) to denature DIG-labeled DNA probes and then incubated in a dark moist chamber at 37°C (24 hours) for probe hybridization. The post-hybridization steps started when the HybriwellTM was removed from the slide and excessive

DIG-labeled DNA probes were washed out by incubating the slide two times for 5 minutes in 2X SSC buffer at room temperature. Then the slide was placed in 50% formamide/2X SSC solution for 2 minutes at 42°C. Subsequently, the slide was passed through in 3 wash steps, 2 times in 2X SSC buffer for 15 minutes at 42°C, 2 times in 1X SCC buffer for 15 minutes at 42°C and two times in 0.5X SSC buffer for 10 minutes at room temperature.

After the post-hybridization washing steps the slide was washed 3 times in PBS for 5 minutes at room temperature and then blocked for non-specific binding by incubating in 1% normal goat serum and 0.1% Triton X-100 in PBS for 30 minutes at room temperature. The blocking solution was poured off and the slide was incubated with 200 µl of conjugation buffer containing 1:15 of conjugate stock solution and blocking solution for 12 hours at 4°C. The slide was washed three times in PBS for 5 minutes at room temperature and rinsed two times with distill water. Cell nuclei were counterstained with 200 µl of 0.05 µM green-fluorescent nucleic stain, Syto®16 (Invitrogen) contained maximum excitation/emission as 448/518 for 8 minutes at room temperature. The slide was mounted with glycerol and fluorescence evaluated using confocal microscopy. Detection of DIG-labeled DNA hybridized probes was performed by direct fluorescence detection. Fab fragments from an anti-digoxigenin (DIG) antibody conjugated with 5-carboxy-tetramethyl-rhodamine-N-hydroxy-succinimide ester (TAMRA) (Roche) with maximum excitation/emission as 555/580 bound directly and specifically to DIG-labeled DNA probes.

Confocal microscopy

Slides were examined using an inverted Zeiss LSM 700 confocal microscope (LSM 700, Carl Zeiss). The 20x/0.50 and 40x/1.30 Oil M27 EC Plan-Neofluar objectives with a pinhole opened 33 µm were used to visualize cells within a field of view of 266.5 x 266.5 and 319.8 x 319.8 µm, respectively. Image size and dynamic range were 1024 x 1024 and 8 bit. Scanning speed number, mode of scanning and averaging number of signal/noise ratio were 6, line mode and 4, respectively. Sequential excitation at 2% of 488 nm and 2% of 555 was provided by argon and helium-neon gas lasers. To scan of cells labeled with TAMRA and Syto®16, emission filters BP 500-530 and LP 580 were used for collecting green and red in channels one and two with the master gain of each channel at 400-450 and 670-715 respectively Emission filters BP 490-535 and LP 568 were used for collecting green and red in channels one and two with the master gain

of each channel as 400-450 and 670-715 respectively to scan cells labeled with PKH26 and Syto®16. After sequential excitation, green and red fluorescent images of the same cell were saved and analyzed by Zeiss Zen 2010 software.

Cryosection

The 4% paraformaldehyde fixed tissues obtained from sacrificed pigs were washed 3 times (10 minutes each) with PBS and subsequently incubated in 30% sucrose (w/v) in PBS for 24 hours at 4°C. Tissues were treated with cryoprotectant and submerged in cryomolds (Tissue-Tek®) containing embedding medium (Tissue-Tek®) and frozen in liquid nitrogen for 5 minutes. The frozen tissues were stored at –70°C until cryosectioning. The frozen tissues were kept in the cryostat chamber at -20°C for 1 hour prior to cryosectioning. The tissue specimen block was removed from the cryomold, placed on the chilled cryostage and sectioned at 12 µm thickness with a cold razor blade and anti-roll plate. Then, each tissue section was gently transferred and melted on Probe On™ Plus Microscope Slides (Fisher Scientific). The section was allowed to adhere to the slide at room temperature for at least 2 h and kept at -20°C until processing to visualize with the confocal microscope.

Results

Labeling PUCs with fluorescent dye

After staining with PKH26, early passage of PUCs and neonatal fibroblasts (P2-P3) emitted bright red fluorescence (Fig 3.1A) and were nearly all (98%) stained (Fig 3.1B) 78.6% of PKH26 labeled PUCs were viable (3.2B) comparable to 78.8% viability of unstained PUCs (Fig 3.2A). PKH26 labeled fibroblast viability was 85% viability after evaluating by the trypan blue exclusion method. PUCs were also stained with lipophilic near infrared fluorescent dye, CellVue® NIR 815 with the same method as for PKH26 staining and they illustrated high emitted fluorescence (Fig 3.3). Viability of CellVue® NIR 815-labeled cells was evaluated by the trypan blue exclusion method that indicated 80-85% viability of stained cells.

Transplantation of fluorescent stained PUCs orally and by intraperitoneal injection

Initially, the PUCs were transplanted in medium with serum (20% FBS) and 2 recipients (2 weeks old female pigs) of 16 recipients transplanted intraperitoneally showed symptoms of anaphylaxis with labored breathing, vomiting and pale skin within 5-10 minutes. Both appeared to recover within one hour but one died within 24 hours and the other recoverd with no further symptoms. Subsequent IP transplantations in 3 recipients were in medium without serum and these symptoms were not observed. There were also no indications of reactions when the PUCs were given orally into 6 recipients with serum in the transplant medium.

Tissues collection and intestine screening

The processed fresh whole intestine was approximately 350-430 cm long and was scanned under red and near infrared filters of the IVIS imaging system to indicate the areas of potential PKH26 and NIR815-labeled donor cells engraftment. Emitted red fluorescing areas were found for small and large intestines of female recipients transplanted by PKH26-labeled donor cells after scanning. However, there were fluorescent areas also in intestines of untransplanted control female pigs. The presence of autofluorescence complicates the use of IVIS scanning to detect areas of engrafted cells. Positive and negative fluorescent areas of intestines of recipients were collected to detect engrafted male PUCs and neonatal fibroblasts. Scanning the fresh whole intestine of female transplanted with NIR815-labeled male PUCs and

untreated control female pigs showed no fluorescing areas. Because the labeled cells were not found with these scans random collection of small and large intestine tissues was performed.

Detection of transplanted male PUCs in female recipients

Nursed-newborn female piglets transplanted with donor cells by intraperitoneal route were sacrificed post transplantation for 6 hours (n=2) and 24 hours (n=2) and tissues (n=3 per tissue) collected. DNA isolated from all tissues except blood and bone marrow was analyzed for expression of the male gene, SRY. PCR analysis indicated that allogeneic male PUCs were present in all tissues. At the earliest sacrifice (6 h), transplanted male PUCs were found in the omentum and diaphragm in relatively large amounts (Fig 3.4A) and 24 h (Fig 3.4B) post-injection. The lowest detection of PUCs was in the mesenteric lymph nodes (Table A.1). Cells isolated from blood were negative for emitted red fluorescent detection analyzed by flow cytometry. Blood cells were not checked for expression of the SRY gene by PCR.

Using PCR to detect the SRY gene, male PUCs transplanted orally into pre-nursed pigs were found broadly in the gastrointestinal tract, liver, spleen, mesenteric lymph nodes, pancreas and omentum at 1 week post-administration. A lower incidence of PUCs was seen in heart, lung, kidney and bone marrow (Fig 3.5A). There was no SRY gene expression for cells in the blood (Table A.2). Tissues were not collected from nursed female recipients fed PKH26 labeled male PUCs for PCR-based SRY detection. Blood collected from these recipients was absent of red-fluorescent donor cells as indicated by flow cytometry analysis.

When intraperitoneal injection was used to administer PUCs, all tissues, including cells from bone marrow (but not the blood) were positive for the SRY gene in female recipients of all ages (Fig 3.5-3.8**).** Incidence of detected PUCs was low for the mesenteric lymph nodes of all ages. Two- and three-week old female recipients showed the presence of allogeneic male PUCs one week post transplantation in tissues derived from uterine horns, urinary bladder, and muscle (semimembranosus). There was no positive signal for the SRY gene from cells isolated from blood at sacrifice for any recipients of any age (Table A.2).

Cryosection of intestines and organs collected from newborn pig recipients transplanted with PKH26-labeled PUCs and fibroblasts were visualized with confocal microscopy. Dispersion of red fluorescent labeled cells was found in intestinal mucosal layer of pre-colostral and post-colostral newborn pigs administered orally and intraperitoneally respectively. PUCs were mostly

detected in the base of villi and the areas around the intestinal crypts of small (Fig 3.9B, 3.9C and 3.9D) and large intestines (Fig 3.10B and 3.10D). Also, they were detected in cryosections of spleen (Fig 3.11B), kidney (Fig 3.11D) and stomach (Fig 3.12B). Compared to PUCs engrafted in the recipient intestines, PKH26 labeled-fibroblasts given by IP injection were found similar sites (Fig 3.10A). There were no cells containing red fluorescent spots in cryosections obtained from non-transplanted recipients (Fig 3.9A, 3.10C, 3.11A, 3.11C and 3.12A). Tissue cryosections derived from nursed newborn pigs fed with PKH26 labeled PUCs did not have red-fluorescent donor cells.

Intestinal cells from all transplantation ages of orally and intraperitoneally transplanted recipients were isolated by enzymatic digestion and cultured in vitro. After plating, attachment of isolated intestinal cells was observed in two days and colonies formed within ten days. Fluorescent in situ hybridization (FISH) analysis with DNA probes specific to SRY gene performed after two weeks culture revealed transplanted male PUCs derived from the intestines of recipients orally and intraperitoneally transplanted PUCs (Table A.3 and Fig 3.13A). Colonies of donor male PUCs also were detected by FISH when intestinal cells were plated at low cell density (Figure 3.13B). PCR confirmed the presence of the SRY gene in these cultured intestinal cells (Figure 3.14).

Discussion

The ability of transplanted cells to engraft and survive in the host is an important consideration for the application of stem-cell therapy. Migration and engraftment of MSCs after local and systemic transplantation has been the subject of several reports. Allogeneic transplantations have also been studied for adult MSCs such as BM-MSCs and adipose tissue derived MSCs. These cells are reported to migrate to and engraft into sites of infact and injured areas after intravenous and intraperitoneal administration (Wang et al., 2011; Castelo-Branco et al., 2012; Wise et al., 2012). There also have been reports that BM-MSCs distribute into various organs after systemic delivery with low frequencies (Devine et al., 2003).

Xenogeneic and allogeneic fetal MSCs derived from placenta and amniotic fluid showed engraftment in various normal tissues of fetal and neonatal rats after in utero and IP transplantation (Chen et al., 2009). IP injection of human fetal MSCs into osteogenesis imperfect neonatal mice resulted in engraftment in the injured tissues (Jones et al., 2012).

Wharton's jelly-derived MSCs are potentially useful for various medical therapies. They are simple to harvest, abundant, mutipotent, highly proliferative and have low immunogenicity (Cho et al., 2008). Specifically relevant to the work reported here, migration and engraftment of human umbilical cord matrix stem cells (hUCMS) in immune deficient mice after intravenous injection has been studied. The cells were found non-randomly engrafted in various normal tissues (Maurya et al., 2011).

We reported that allogeneic PUCs were capable of trans-epithelial trafficking and incorporation into deep layers of intestine of pre-colostral neonatal pigs when given orally (Miller et al., 2012). The present report expands on this observation and extends it by including intraperiotoneal administration. Moreover, the isolation and re-culture of transplantated PUCs from the intestinal mucosa indicates the cells are viable and mitotically competent after 7 days.

PUCs migrated from both the intestinal lumen and the peritoneal cavity, and engrafted in multiple tissues and persisted for at least 7d, the longest time studied in the current investigation. Their recovery from the stromal layer of the intestine and re-culture with the formation of colonies indicates that at least in these characteristics they have retained their mesenchymal phenotype. Further work will be required to fully characterize the recovered cells. In addition to the potential of MSCs to differentiate and contribute to tissue regeneration, they are also reported

to contribute supportive and protective effects. In this regard maintenance of mesenchymal phenotype and residence in the stromal compartment of tissues is an important ability.

Using sex mismatched donor cells with PCR and FISH to detect the Y-chromosome gene, SRY, was a key method for this work. As reported in our earlier work the oral feeding of allogeneic PUCs into non-nursed newborn pigs is a safe and effective procedure. Oral delivery of allogeneic donor cells resulted in migration and engraftment into a variety of distant organs. However, the requirement for administering the cells before the pig nurses is inconvenient and limits the recipient age that can be studied. It is expected that the harsh condition of gut that is established after nursing would be lethal for the PUCs and our preliminary studies confirmed that no transplanted cells were detected when they were fed after the recipient had nursed (Miller et al., 2012). The formed milk curds that form in the stomach after nursing probably trap the orally administered cells and and create an inhospitable environment for survival and trans-epithelial trafficking.

Before nursing the physiological conditions of gastrointestinal tracts of newborn pigs are close to neutral pH with low digestive enzyme activity. Moreover, culture medium administered orally with PUCs contains high buffer capacity that may prevents rapid change in pH. It is likely that oral-fed PUCsat a size of 8-20 μm (Majore et al., 2009) are able to penetrate through incompletely formed intercellular junctions of the intestinal epithelium of pre-colostral neonatal pigs and this may be the same mechanism used by colostral lymphoid cells as they are absorbed from digestive track into immune system of newborn pigs (Tuboly et al., 1988).

The gastrointestinal tract and internal organs of the abdominal compartment were the major sites for transplanted PUC with 75-100% of these organs containing PUCs 1 week after oral administration. PUCs were detected in the heart, lung, kidney and bone marrow but less frequently (37.5-50%).

Likely, allogeneic PUCs migrate from mucosa layer of intestines to mesenteric lymph nodes via the lymphatic system similar to the migration pattern of colostral leukocytes (Williams, 1993). However, they do not appear to reach the general circulation in large numbers or according to the pattern reported for colostral leukocytes. The portal venous system drains the venous blood from the visceral organs of the stomach, intestines, spleen, pancreas, omentum to liver by veins. Zhou et al (2000) reported the accumulated maternal leukocytes were found at a perisinusoidal capillary region of the neonatal liver of mice after foster nursing on a GFP

transgenic mother (Zhou et al., 2000). It is probable that incompletely developed venous valves of newborn pigs allow migration of male PUCs from intestines to reach multiple tissues linked by the portal system. Then, the donor cells possibly moved from portal system by the hepatic vein into inferior vena cava and engrafted in heart, lung and bone marrow.

IP injection is a convenient and simple method for administer PUCs to neonatal pigs. The peritoneal cavity is a space surrounding the viscera in the abdomen. Its large surface with abundant vascularization provides a portal of entry to the general circulation. Water, solutes and cells can be transported across the mesothelium lining of peritoneal cavity to the blood stream via the lymphatic system (Flessner, 1991). Fluid, macromolecules and cells from the peritoneal cavity are drained into the diaphragmatic lymph system through mesothelial stomata prior to passing through mesenteric, retroperitoneal channels and associated lymph nodes. Then, the lymph is passed into the thoracic duct before entering the blood circulation (Abu-Hijleh et al., 1995). Mesothelial stoma overlying milky spots in the omentum is also an entrance route for cells migrating from peritoneal cavity into lymphatic system (Mironov et al., 1979).

Neonatal fibroblasts were also detected in intestinal mucosa layer of newborn pigs after IP injection. Fibroblasts have phenotypic and functional resemblance with MSCs and global gene and micro RNA expression profiles of MSCs and fibroblasts have shown them to be similar (Bae et al., 2009). This could be consistent with the finding MSCs and fibroblast in the same regions after transplantation. However, the two cell types differ markedly in that genes functioning in cell plasticity are highly expressed in MSCs compared to fibroblasts (Bae et al., 2009). The study of Pereira et al (2011) in rat model of Parkinson's disease (PD) demonstrated that fibroblast engraftment was not promising treatment as cell-based therapy due to their absence of immunomodulatory properties. Fibroblasts have also been observed to cause scar formation after transplantation which further limits their usefulness.

There are concerns about intravenous cell transplantation resulting in cell emboli that block blood vessels and causing death when large numbers of cells are transplanted, at least in mice (Plock et al., 2013). Moreover, cells administered by intravenous injection could be trapped in the lung capillaries in a phenomenon known as "transpulmonary first-pass attenuation" (Strauer and Kornowski., 2003). Intraperitoneal delivery of human umbilical cord blood cells in a rodent model showed migration and engraftment in different organs such as bone marrow, liver and spleen. These transplanted cells could reduce liver damage in an immunocompetent rat

model of toxic liver injury. The homing ability of stem cells to injured organ after intraperitoneal injection was directly related to severity of the organ damage (Piscaglia et al., 2005).

In the current study, the earliest observation were at 6 hours after IP injection with the PUCs detected in the diaphragm and omentum in all samples examined at 6 and 24 hours after injection. In contrast, lower frequency of PUCs (<50%) was found in other tissues at 6 hours compared to detection in most tissues at 24 hours. It appears that the omentum and diaphragm are the major sites of entrance for the donor cells.

It is somewhat surprising that the IP-administered PUCs were detected at a high incidence in all the regions of the small intestine. Confocal imaging showed that they were located around base of villi and intestinal crypts. There have been reports illustrating that BM-MSCs transplanted systemically into irradiated animals could migrate to engraft in the lamina propria and pericryptal intestinal mucosal layer (Brittan et al., 2002; Zhang et al., 2008) and PUCs given IP showed a similar ability. The intestinal mucosal layer is a loose connective tissue with abundant capillary networks and lymphatic vessel including lacteals. The intestinal lymphatic system found in the mucosa layer is the initial lymphatic network comprising of blind-end vessels without smooth muscle and valves. Initial lymphatic vessels are formed by a single layer of endothelial cells that attach to intestinal connective tissues and drain the lymph following the force generated by intestinal peristalsis (Miller et al., 2010). Overlapping flaps at the borders of oak leaf-shaped endothelial cells of the initial lymphatic vessels open during vessel expansion due to extrinsic force. The openings allow the entrance of lymph from interstitial space and leukocytes (Baluk et al., 2007). Possibly, PUCs in the intestinal mucosa use the intestinal lymphatic network for migration through the entire intestines.

Weiss et al. (2003) reported that PKH26 labeled UMCs administered intravenously migrated and engrafted in the parenchyma of the recipients kidney. The present study also found the labeled PUCs in spleen, stomach and kidney after IP injection. It is possible that PUCs injected intraperitoneally were able to migrate and engraft to organs through the recipient blood circulation.

Blood collected from female recipients one week after oral and IP injection was negative for expression of SRY using PCR. Because PCR is highly sensitive, these results suggested that donor PUCs were not in the circulation at that time, although they may have been earlier. Flow cytometry analyses for PKH26 labeled PUCs in blood collected at 6 hours and 1 day after IP

administration also were negative however PCR was not used for these samples. Therefore a low concentration of donor PUCs, if it occurred, could have gone undetected. Therefore the route of migration of PUCs is unresolved.

A novel aspect of the current work is the recovery of transplanted PUCs from the mucosa of recipients. Cultured intestinal cells were positive for SRY gene after analysis by PCR and FISH identifying donor male PUCs in the cultured cells. The donor male PUCs attached to culture flasks and had fibroblast-like morphology. Moreover, these re-cultured male PUCs were proliferating as they formed colonies. Therefore engrafted male PUCs were able to survive and express self-renewal after recovery from the host small intestines after oral and intraperitoneal transplantation.

Earlier we found that PKH26-labeled PUCs were found in the bright spot detected by IVIS Lumina II imaging. Here we found that freshly washed intestine obtained from non-transplanted control as well as recipient pigs transplanted with PKH26-labeled donor male PUCs showed fluorescent positive areas. Positive and negative fluorescent areas of recipient intestines transplanted with PKH26-labeled donor PUCs were checked for expression of SRY by PCR and the frequency of positive signal was similar. Residual intestinal contents emitted at the same wavelength as PKH26 dye and were probably the cause of false fluorescent positive areas. To avoid auto-fluorescent background, the near infrared dye (NIR 815), which has been used for noninvasive real-time cell tracking in small animal models (Armentero et al., 2013) was used to label donor PUCs before intraperitoneal transplantation. There were no fluorescent positive areas detected on both non-transplanted control and recipient intestines transplanted with NIR 815-labeled donor PUCs following screening with IVIS Lumina II imaging system set at the line/filter wavelength of 745/BP810-875 nm, however, randomly collected fluorescent negative areas of intestines showed positive for SRY gene after using PCR for detection. The NIR 815 labeled donor PUCs in the recipient intestines probably emitted too low a fluorescent signal to be detected.

In conclusion, allogeneic donor PUCs administered orally into pre-nursed piglets and intraperitoneally into neonatal to weaning pigs were found in the intestines and several other organs both in intra-peritoneal (i.e. gut, liver, spleen) and extra-peritoneal (i.e. kidneys, bladder, uterus) organs. Also, they were able to incorporate in muscle and thoracic organs including heart and lung. Distribution of PUCs to various organs could be related to the proximity of the

abdominal organs to delivery site and cell migration toward the tissues might occur both via lymphatic drainage and the blood, but also directly through the serosa. The presence of PUCs in organs was observed 6 hours after IP injection and the donor PUCs were able to persist in the organs at least 1 week. Donor PUCs implanted in small intestines for 1 week were viable and exhibited self-renewal after re-culturing in vitro. In light of these results, the IP and oral administration of stem cells are potential routes for cell therapy in pediatric disorders.

In the future, the persistence and differentiation of PUCs could be explored perhaps by using genetically modified PUCs expressing exogenous near infrared fluorescent or bioluminescent genes. Moreover, migration and engraftment of either genetically modified PUCs to up-regulate homing receptor or normal PUCs transplanted via intraperitoneal injection to local and systemic tissue damage as in irradiated animals, intestinal ischemic model or intestinal inflammation model would be intriguing studies.

References

Abu-Hijleh, M. F., O. A. Habbal, and S. T. Moqattash. 1995. The role of the diaphragm in lymphatic absorption from the peritoneal cavity. J. Anat. 186(3): 453-467.

Ai, H., H. Bai, C. B. Wang, J. F. Ou, Q. Zhao, X. Han. 2011. Expression characteristics of SDF-1 receptor CXCR4 in mesenchymal stem cells derived from human umbilical cord tissue. Zhongguo Shi Yan Xue Ye Xue Za Zhi. 19(1): 169-173.

Armentero, M. T., P. Bossolasco, and L. Cova. 2013. Labeling and tracking of human mesenchymal stem cells using near-infrared technology. Methods Mol. Biol.

Bae, S., J. H. Ahn, C. W. Park, H. K. Son, K. S. Kim, N. K. Lim et al. 2009. Gene and microRNA expression signatures of human mesenchymal stromal cells in comparison to fibroblasts. Cell Tissue Res. 335(3): 565-573.

Baluk, P., J. Fuxe, H. Hashizume, T. Romano, E. Lashnits, S. Butz et al. 2007. Functionally specialized junctions between endothelial cells of lymphatic vessels. J. Exp. Med. 204(10): 2349-2362.

Brittan, M., T. Hunt, R. Jeffery, R. Poulsom, S. J. Forbes, K. Hodivala-Dilke et al. 2002. Bone marrow derivation of pericryptal myofibroblasts in the mouse and human small intestine and colon. Gut. 50(6): 752-757.

Caplan A. I. 2007. Adult mesenchymal stem cells for tissue engineering versus regenerative medicine. J Cell Physiol. 21(3): 341-347.

Carlin, R., D. Davis, M. Weiss, B. Schultz, and D. Troyer. 2006. Expression of early transcription factors oct-4, sox-2 and nanog by porcine umbilical cord (PUC) matrix cells. Reprod. Biol. Endocrinol. 4: 8.

Castelo-Branco, M. T., I. D. Soares, D. V. Lopes, F. Buongusto, C. A. Martinusso, A. do Rosario Jr et al. 2012. Intraperitoneal but not intravenous cryopreserved mesenchymal stromal cells home to the inflamed colon and ameliorate experimental colitis. PLoS One. 7(3): e33360.

Chen, C. P., S. H. Liu, J. P. Huang, J. D. Aplin, Y. H. Wu, P. C. Chen et al. 2009. Engraftment potential of human placenta-derived mesenchymal stem cells after in utero transplantation in rats. Hum. Reprod. 24(1): 154-165.

Cho, P. S., D. J. Messina, E. L. Hirsh, N. Chi, S. N. Goldman, D. P. Lo et al. 2008. Immunogenicity of umbilical cord tissue derived cells. Blood. 111(1): 430-438.

Chua, T. C., T. D. Yan, J. Zhao, and D. L. Morris. 2009. Peritoneal carcinomatosis and liver metastases from colorectal cancer treated with cytoreductive surgery perioperative intraperitoneal chemotherapy and liver resection. Eur. J. Surg. Oncol. 35(12): 1299-1305.

Daar, A. S., and H. L. Greenwood. 2007. A proposed definition of regenerative medicine. J. Tissue Eng. Regen. Med. 1(3): 179-184.

Devine, S. M., C. Cobbs, M. Jennings, A. Bartholomew, and R. Hoffman. 2003. Mesenchymal stem cells distribute to a wide range of tissues following systemic infusion into nonhuman primates. Blood. 101(8): 2999-3001.

Di Campli, C., A. C. Piscaglia, L. Pierelli, S. Rutella, G. Bonanno, M. R. Alison et al. 2004. A human umbilical cord stem cell rescue therapy in a murine model of toxic liver injury. Dig. Liver Dis. 36(9): 603-613.

Esquivel, J. 2009. Technology of hyperthermic intraperitoneal chemotherapy in the united states, europe, china, japan, and korea. Cancer J. 15(3): 249-254.

Flake, A. W., M. R. Harrison, N. S. Adzick, and E. D. Zanjani. 1986. Transplantation of fetal hematopoietic stem cells in utero: The creation of hematopoietic chimeras. Science. 233(4765): 776-778.

Flessner, M. F. 1991. Peritoneal transport physiology: Insights from basic research. J. Am. Soc. Nephrol. 2(2): 122-135.

Fong, C. Y., L. L. Chak, A. Biswas, J. H. Tan, K. Gauthaman, W. K. Chan et al. 2011. Human wharton's jelly stem cells have unique transcriptome profiles compared to human embryonic stem cells and other mesenchymal stem cells. Stem Cell. Rev. 7(1): 1-16.

Ganta, C., D. Chiyo, R. Ayuzawa, R. Rachakatla, M. Pyle, G. Andrews et al. 2009. Rat umbilical cord stem cells completely abolish rat mammary carcinomas with no evidence of metastasis or recurrence 100 days post-tumor cell inoculation. Cancer Res. 69(5): 1815-1820.

Ghadge, S. K., S. Mühlstedt S, C. Ozcelik and M. Bader. 2011. SDF-1α as a therapeutic stem cell homing factor in myocardial infarction. Pharmacol Ther. 129(1): 97-108.

Jo, C. H., O. S. Kim, E. Y. Park, B. J. Kim, J. H. Lee, S. B. Kang et al. 2008. Fetal mesenchymal stem cells derived from human umbilical cord sustain primitive characteristics during extensive expansion. Cell Tissue Res. 334(3): 423-433.

Jones, G. N., D. Moschidou, K. Lay, H. Abdulrazzak, M. Vanleene, S. J. Shefelbine et al. 2012. Upregulating CXCR4 in human fetal mesenchymal stem cells enhances engraftment and bone mechanics in a mouse model of osteogenesis imperfecta. Stem Cells Transl. Med. 1(1): 70-78.

Kansu, E. 2012. Thrombosis in stem cell transplantation. Hematology. 17 Suppl 1: S159-62.

Karp, J. M., and G. S. Leng Teo. 2009. Mesenchymal stem cell homing: The devil is in the details. Cell. Stem Cell. 4(3): 206-216.

Majore, I., P. Moretti, R. Hass, and C. Kasper. 2009. Identification of subpopulations in mesenchymal stem cell-like cultures from human umbilical cord. Cell. Commun. Signal. 7: 6-811X-7-6.

Marcus, A. J., and D. Woodbury. 2008. Fetal stem cells from extra-embryonic tissues: Do not discard. J. Cell. Mol. Med. 12(3): 730-742.

Maurya, D. K., C. Doi, A. Kawabata, M. M. Pyle, C. King, Z. Wu et al. 2010. Therapy with un-engineered naive rat umbilical cord matrix stem cells markedly inhibits growth of murine lung adenocarcinoma. BMC Cancer. 10: 590-2407-10-590.

Maurya, D. K., C. Doi, M. Pyle, R. S. Rachakatla, D. Davis, M. Tamura et al. 2011. Non-random tissue distribution of human naive umbilical cord matrix stem cells. World J. Stem Cells. 3(4): 34-42.

Miller, D., K. Packthongsuk, T. Rathbun, D. Boyle, D. Troyer, and D. L. Davis. 2012. Confocal imaging of trans-epithelial trafficking by immune and umbilical cord stem cells in the neonatal porcine intestine. Anat. Histol. Embryol. 41(6): 461-468.

Miller, M. J., J. R. McDole, and R. D. Newberry. 2010. Microanatomy of the intestinal lymphatic system. Ann. N. Y. Acad. Sci. 1207 Suppl 1: E21-8.

Mimeault, M., and S. K. Batra. 2008. Recent progress on tissue-resident adult stem cell biology and their therapeutic implications. Stem Cell. Rev. 4(1): 27-49.

Mironov, V. A., S. A. Gusev, and A. F. Baradi. 1979. Mesothelial stomata overlying omental milky spots: Scanning electron microscopic study. Cell Tissue Res. 201(2): 327-330.

Pappa, K. I., and N. P. Anagnou. 2009. Novel sources of fetal stem cells: Where do they fit on the developmental continuum? Regen. Med. 4(3): 423-433.

Pereira, M. C., M. Secco, D. E. Suzuki, L. Janjoppi, C. O. Rodini, L. B. Torres et al. 2011. Contamination of mesenchymal stem-cells with fibroblasts accelerates neurodegeneration in an experimental model of parkinson's disease. Stem Cell. Rev. 7(4): 1006-1017.

Pie, S., J. P. Lalles, F. Blazy, J. Laffitte, B. Seve, and I. P. Oswald. 2004. Weaning is associated with an upregulation of expression of inflammatory cytokines in the intestine of piglets. J. Nutr. 134(3): 641-647.

Piscaglia, A. C., C. Di Campli, M. A. Zocco, G. Di Gioacchino, M. Novi, S. Rutella et al. 2005. Human cordonal stem cell intraperitoneal injection can represent a rescue therapy after an acute hepatic damage in immunocompetent rats. Transplant. Proc. 37(6): 2711-2714.

Plock, J. A., J. T. Schnider, R. Schweizer, and V. S. Gorantla. 2013. Are cultured mesenchymal stromal cells an option for immunomodulation in transplantation? Front. Immunol. 4: 41.

Prockop, D. J. 2009. Repair of tissues by adult stem/progenitor cells (MSCs): controversies, myths and changing paradigms. Mol Ther. 17(6): 939-946.

Rachakatla, R. S., F. Marini, M. L. Weiss, M. Tamura, and D. Troyer. 2007. Development of human umbilical cord matrix stem cell-based gene therapy for experimental lung tumors. Cancer Gene Ther. 14(10): 828-835.

Rempel, S. A., S. Dudas, S. Ge, and J. A. Gutierrez. 2000. Identification and localization of the cytokine SDF1 and its receptor, CXC chemokine receptor 4, to regions of necrosis and angiogenesis in human glioblastoma. Clin. Cancer Res. 6(1): 102-111.

Ries, C., V. Egea, M. Karow, H. Kolb, M. Jochum, and P. Neth. 2007. MMP-2, MT1-MMP, and TIMP-2 are essential for the invasive capacity of human mesenchymal stem cells: Differential regulation by inflammatory cytokines. Blood. 109(9): 4055-4063.

Sangild, P. T., A. L. Fowden., J. F. Trahair. 2000. How does the foetal gastrointestinal tract develop in preparation for enteral nutrition after birth?. Livest Prod Sci. 66: 141-150.

Shaaban, A. F., H. B. Kim, R. Milner, and A. W. Flake. 1999. A kinetic model for the homing and migration of prenatally transplanted marrow. Blood. 94(9): 3251-3257.

Stachowska-Pietka, J., J. Waniewski, M. F. Flessner, and B. Lindholm. 2006. Distributed model of peritoneal fluid absorption. Am. J. Physiol. Heart Circ. Physiol. 291(4): H1862-74.

Strauer, B.E., R. Kornowski. 2003. Stem cell therapy in perspective. Circulation. 107(7): 929-934.

Tuboly, S., S. Bernath, R. Glavits, and I. Medveczky. 1988. Intestinal absorption of colostral lymphoid cells in newborn piglets. Vet. Immunol. Immunopathol. 20(1): 75-85.

Turner, P. V., T. Brabb, C. Pekow, and M. A. Vasbinder. 2011. Administration of substances to laboratory animals: Routes of administration and factors to consider. J. Am. Assoc. Lab. Anim. Sci. 50(5): 600-613.

Wang, W., Q. Jiang, H. Zhang, P. Jin, X. Yuan, Y. Wei et al. 2011. Intravenous administration of bone marrow mesenchymal stromal cells is safe for the lung in a chronic myocardial infarction model. Regen. Med. 6(2): 179-190.

Weiss, M. L., K. E. Mitchell, J. E. Hix, S. Medicetty, S. Z. El-Zarkouny, D. Grieger et al. 2003. Transplantation of porcine umbilical cord matrix cells into the rat brain. Exp. Neurol. 182(2): 288-299.

Weiss, M. L., S. Medicetty, A. R. Bledsoe, R. S. Rachakatla, M. Choi, S. Merchav et al. 2006. Human umbilical cord matrix stem cells: Preliminary characterization and effect of transplantation in a rodent model of parkinson's disease. Stem Cells. 24(3): 781-792.

Williams, P. P. 1993. Immunomodulating effects of intestinal absorbed maternal colostral leukocytes by neonatal pigs. Can. J. Vet. Res. 57(1): 1-8.

Wise, A. F., and S. D. Ricardo. 2012. Mesenchymal stem cells in kidney inflammation and repair. Nephrology (Carlton). 17(1): 1-10.

Zhang, J., J. F. Gong, W. Zhang, W. M. Zhu, and J. S. Li. 2008. Effects of transplanted bone marrow mesenchymal stem cells on the irradiated intestine of mice. J. Biomed. Sci. 15(5): 585-594.

Zhou, L., Y. Yoshimura, Y. Huang, R. Suzuki, M. Yokoyama, M. Okabe et al. 2000. Two independent pathways of maternal cell transmission to offspring: Through placenta during pregnancy and by breast-feeding after birth. Immunology. 101(4): 570-580.

Figure 3.1 Labeling of PUCs with lipophilic fluorescent dye.

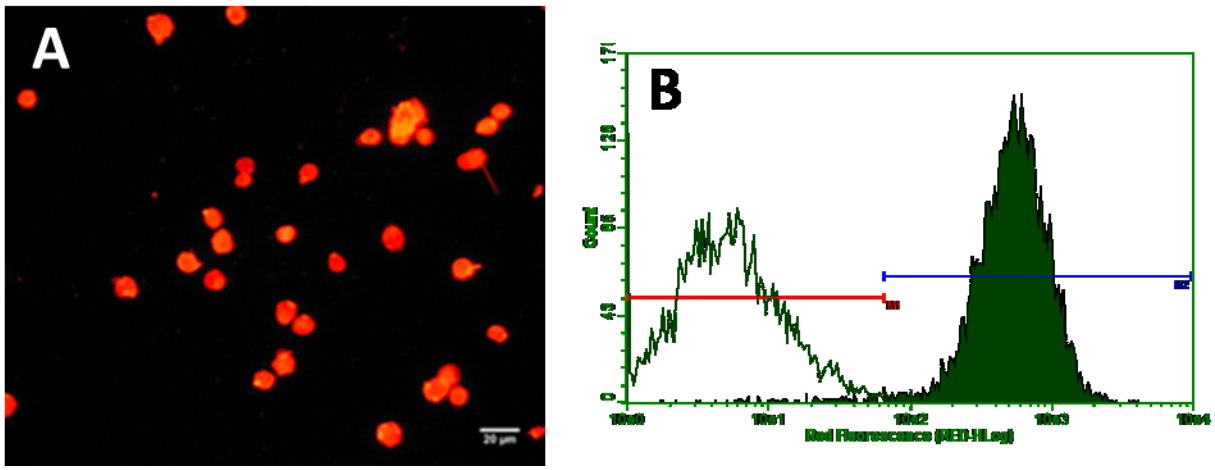

Early passage of PUCs labeled with the lipophilic fluorescent dye, PKH26, showed bright red round cells when observed with 20x magnification and fluorescence microscopy (A). Flow cytometry illustrates unstained PUCs control (open histogram) and PKH-26-stained PUCs (filled histogram) (B). Y axis represents counted cells and X axis represents red fluorescent intensity in log scale.

Figure 3.2 Flow cytometry evaluation of viable PUCs stained with PKH26.

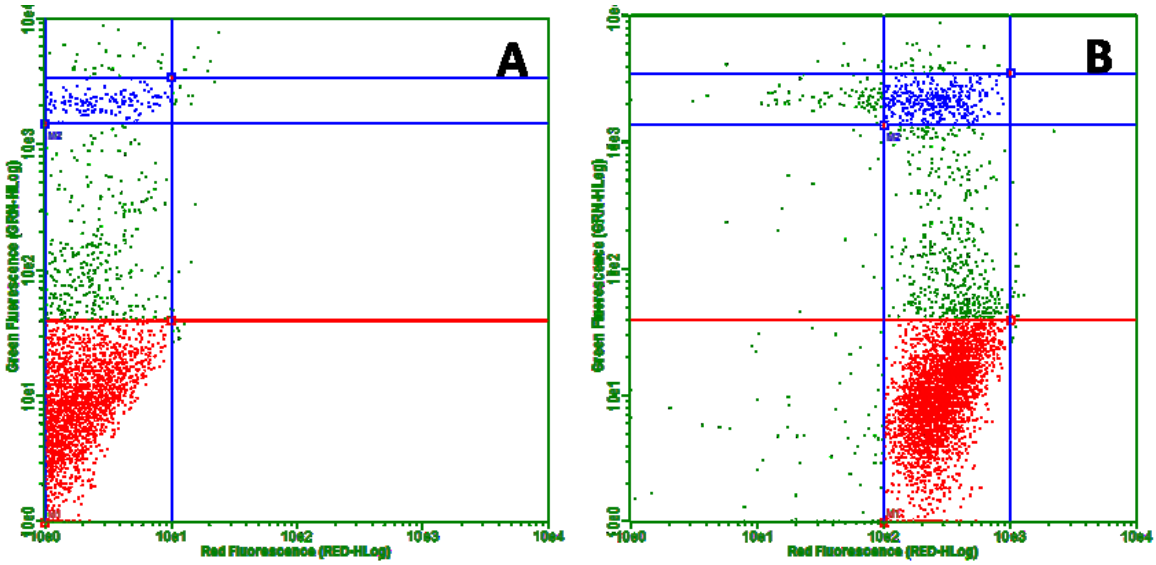

Dot-plot of PUCs stained with SYTOX® Green under the red fluorescent (x-axis) and green fluorescent (y-axis) channels were gated as a control of the viable-unstained PUCs. The red dot population represents unstained viable PUCs (A). With the same gating, a population of viable PKH26-labeled PUCs indicated as the red population was determined after staining with SYTOX® Green (B).

Figure 3.3 Fluorescent emission scanning of PUCs labeled with the near infrared fluorescent dye, CellVue® NIR815 by the IVIS imaging system.

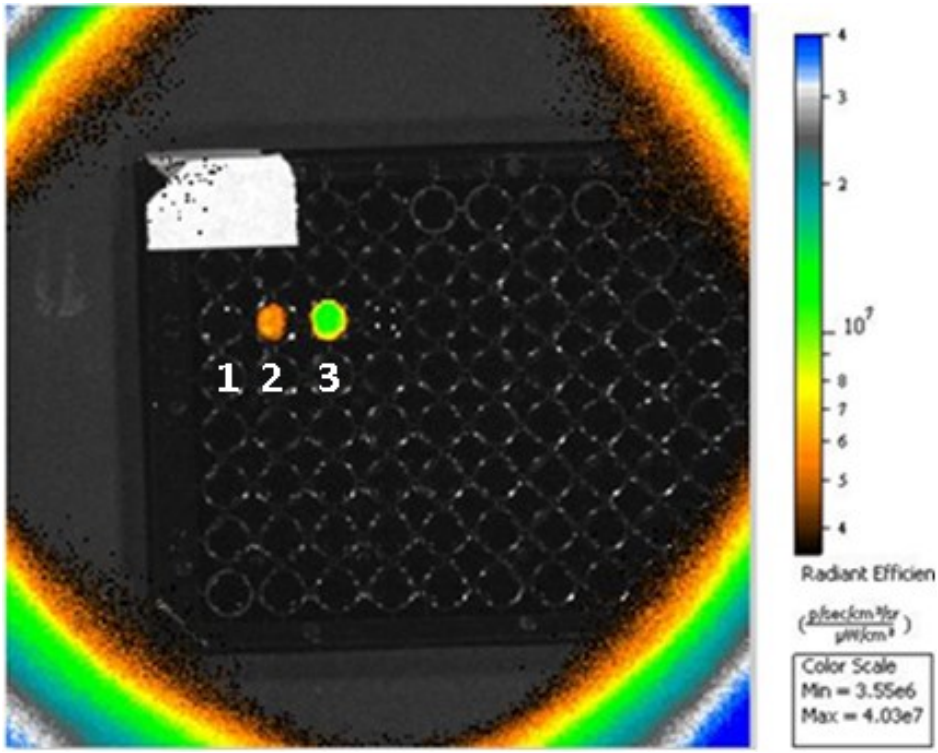

Fluorescent intensity images of PUCs (2 x 10^5 cells) loaded in a 96- well black plate after staining with lipophilic near infrared fluorescent (CellVue® NIR815) (3) and the stained PUCs (2 x 10^5 cells) cultured in vitro for 1 week after staining (2). Unstained PUCs (control) showed no fluorescent emitted (1). Right bar of the figure shows high (top) and low (bottom) intensity of emitted fluorescent.

Figure 3.4 Percentage of samples with detected PUCs collected from female recipients given male PUCs at birth by IP transplantation and sacrifice 6 or 24 hours later.

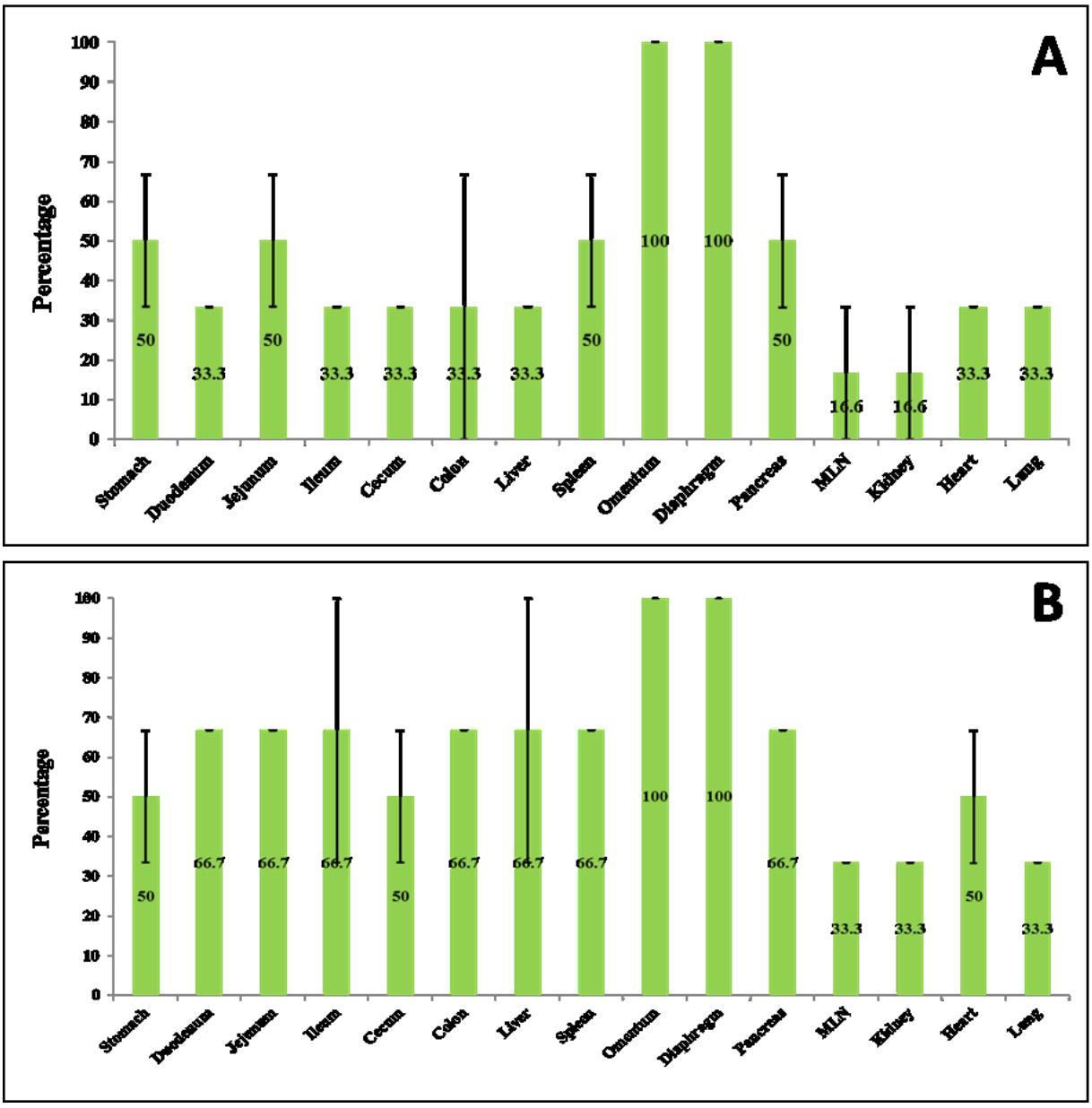

Female recipients injected intraperitoneally with male PUCs and were sacrificed after 6 hours (n=2) (A) and 24 hours (n=2) (B) after administration. Each bar represents the number of samples (n=3/tissue) that were found to be positive for SRY expression. Results are shown as the mean; error bars indicate standard error.

Figure 3.5 Percentage of samples of various organs collected 1 week after oral or IP transplantation to newborn female recipients for which male PUCs were detected.

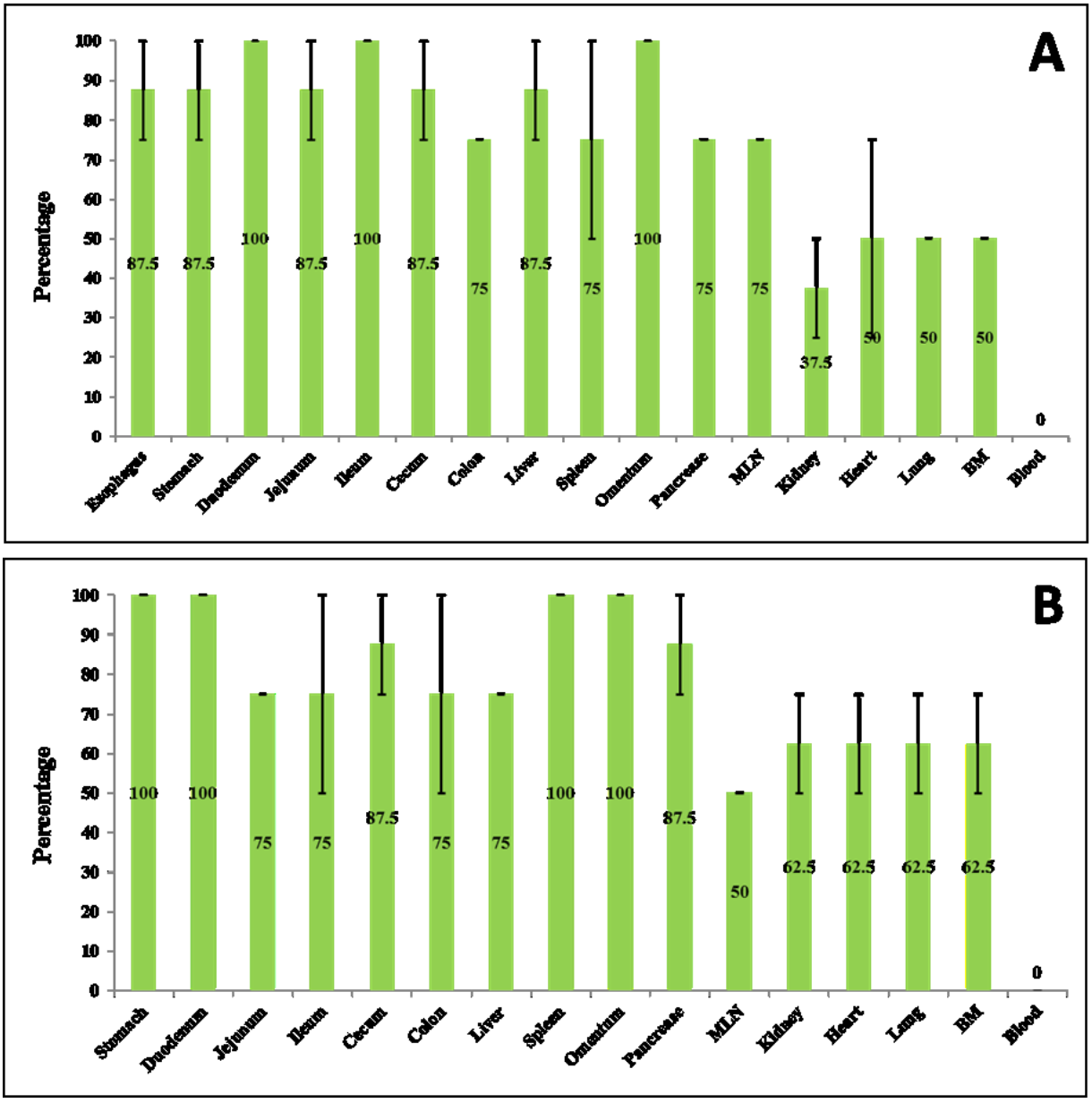

(A) Pre-colostral female newborn pigs (n=2) fed male PUCs were sacrificed 1 week after administration. Tissues (n=4) were collected from each organ to determine the presence of male PUCs using PCR to detect the Y-chromosome gene, SRY, (B). Newborn pig (n=2) injected intraperitoneally with male PUCs were sacrificed 1 week post-injection. Tissues (n=4) were collected from each organ to determine the presence of male PUCs using PCR to detect SRY expression. Results are shown as the mean; error bars indicate standard error.

Figure 3.6 PCR screening for the SRY gene in neonatal porcine tissues after allogeneic transplantation.

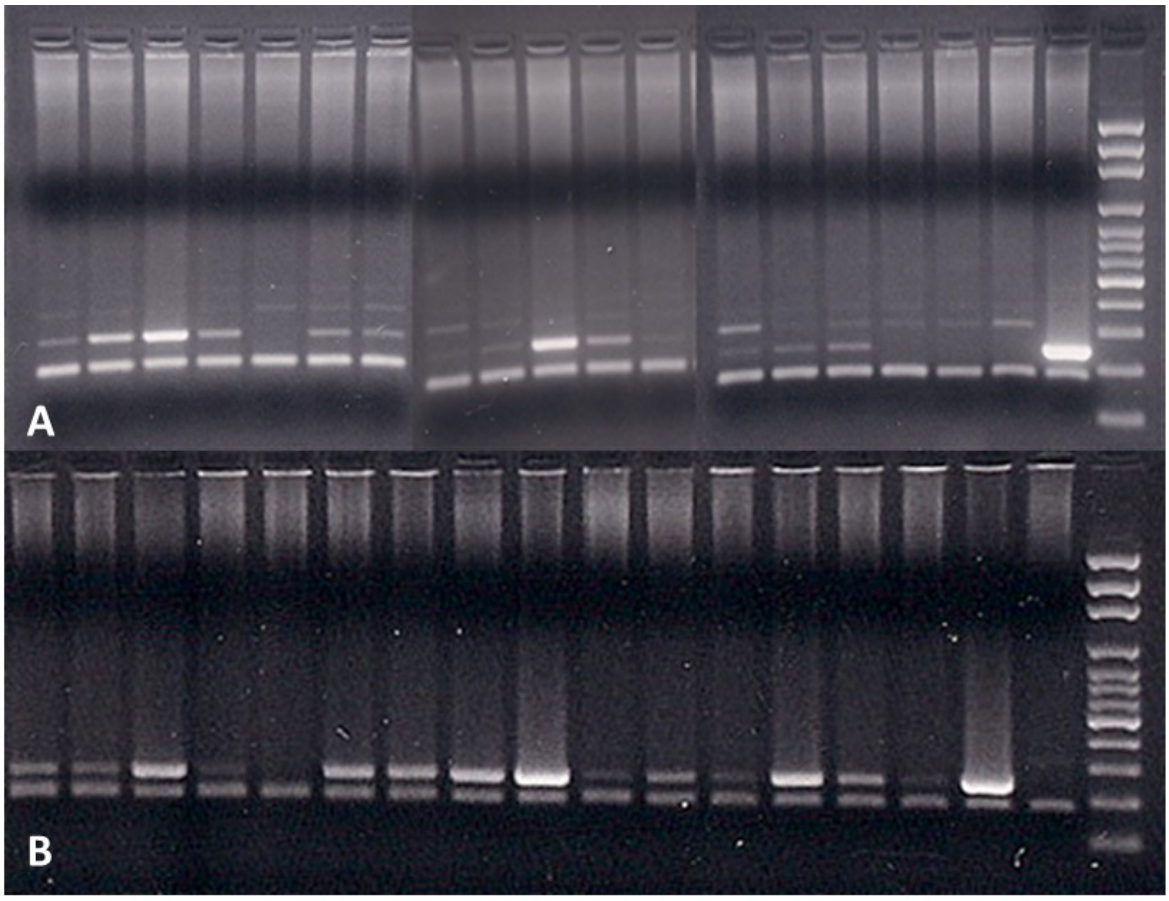

Gels representative of samples from two pigs transplanted intraperitoneally with PUCs at birth (A) and 1 week (B) of age followed by tissues collection 1 week after transplantation. Size of the SRY and porcine-specific beta-actin genes productes are 247 and 183 bp, respectively. Right lane is a molecular size marker (100 base pair).

(A) Left to right: Duodenum, Jejunum, Ileum, Cecum, Colon, Stomach, Liver, Spleen, Omen, Kidney, Pancreas, Mesenteric lymph node, Heart, Lung, Bone marrow, Male control, Female control, DNA ladder.

(B) Left to right: Duodenum, Jejunum, Ileum, Cecum, Colon, Esophagus, Stomach, Liver, Spleen, Omen, Kidney, Pancreas, Mesenteric lymph node, Heart, Lung, Bone marrow, Blood, Female control, Male control, DNA ladder.

Figure 3.7 Percentage of samples of various organs collected 1 week after IP transplantation to 1-day and 7-day old female recipients.

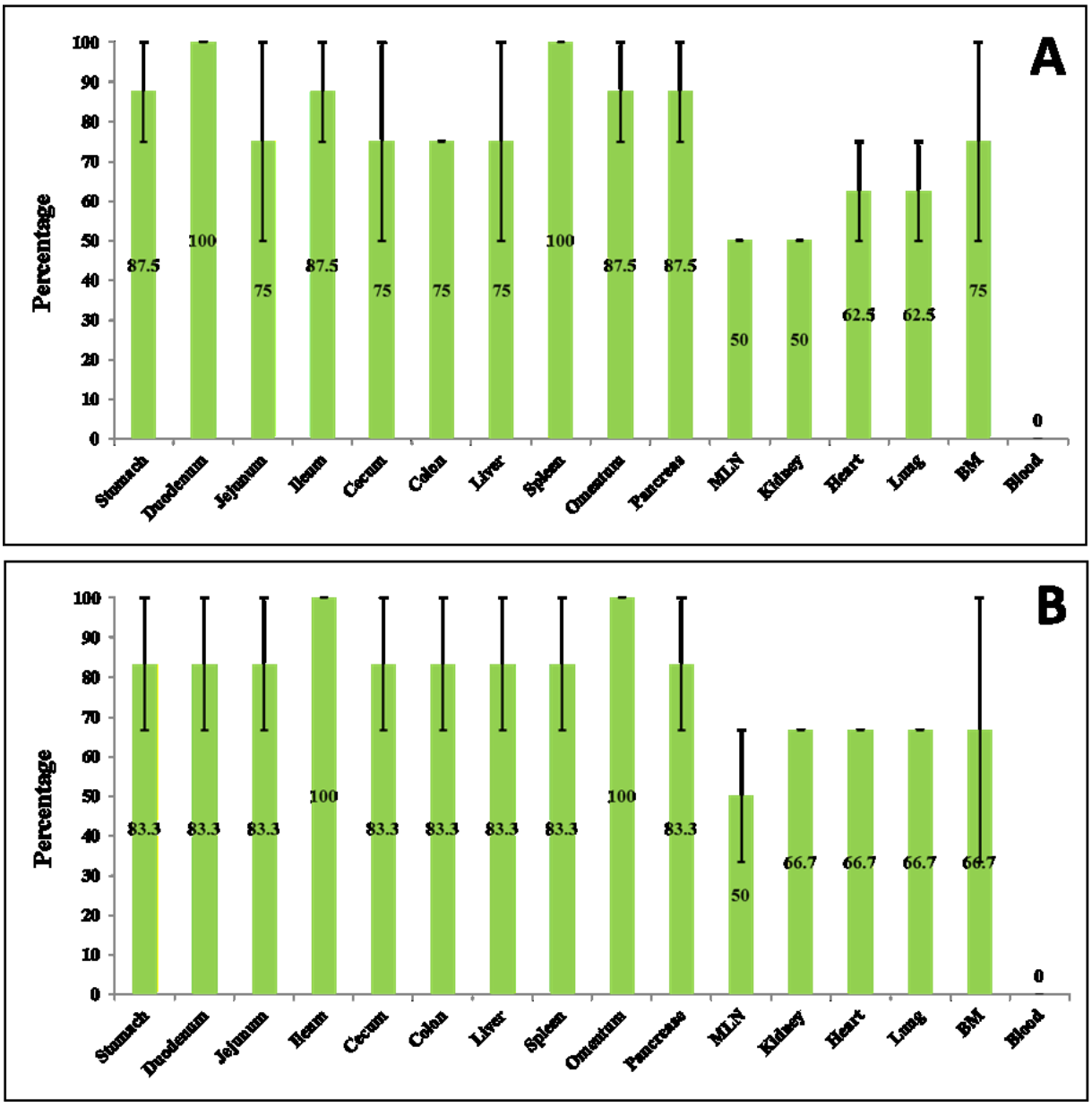

1 day-old (n=2) and 1 week-old (n=2) female recipients were injected IP with male PUCs and were sacrificed 1 week after administration. Sample (n=4/tissue) were collected from each organ of 1 day-old recipients (A) and 1 week-old recipients (n=3/tissue). Presence of male PUCs was detected as SRY expression (B). Results are shown as the mean; error bars indicate standard error.

Figure 3.8 Percentage of samples of various organs of recipients that were collected 1 week after IP transplantation to 2-week and 3-week old (n=2/age) female pigs.

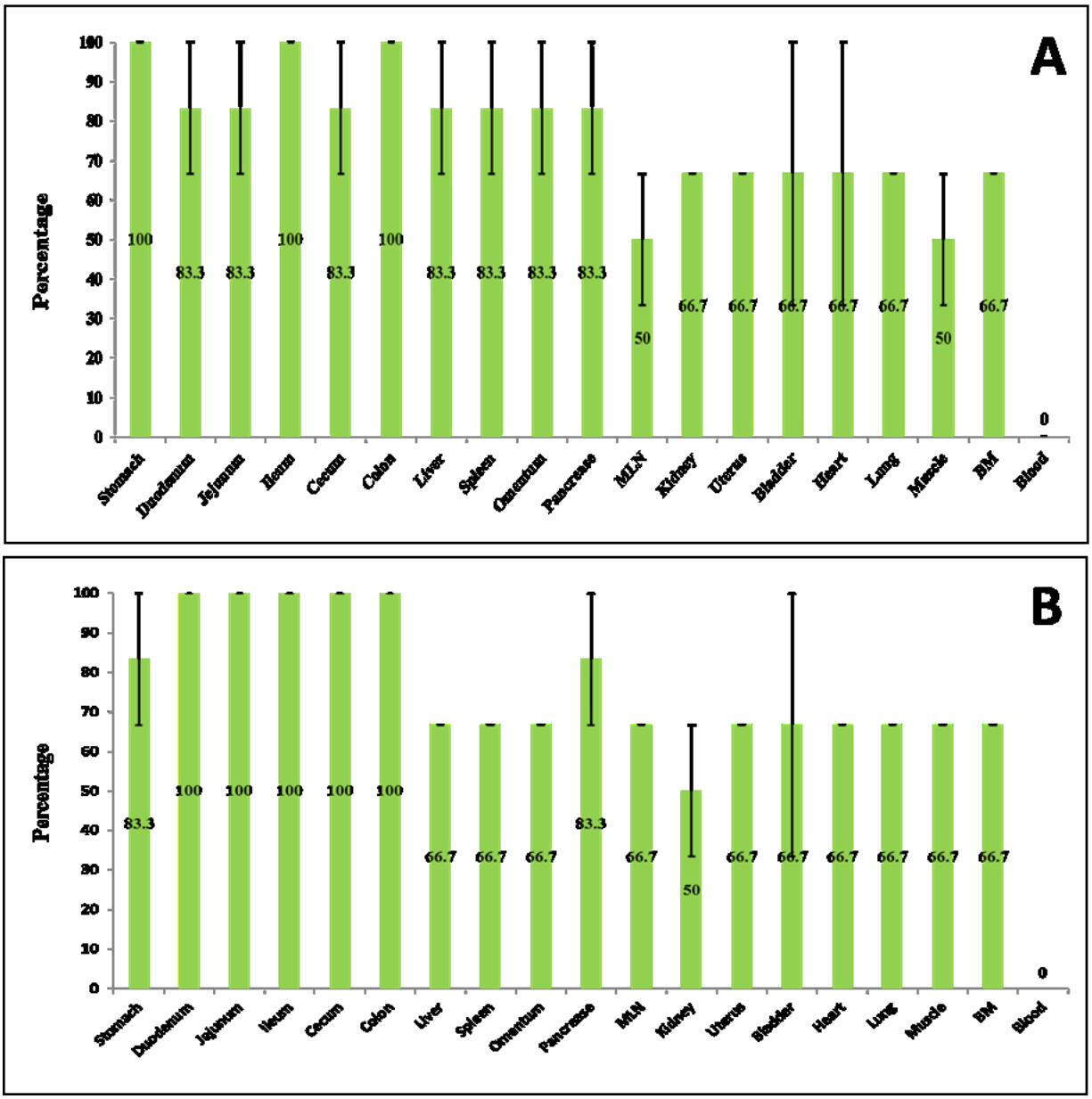

2 week-old (n=2) and 3 week-old (n=2) female recipients were sacrificed 1 week after IP administration of male PUCs. Samples (n=3/organ) were collected from 2 week-old recipients (A) and 3 week-old recipients (B). Results are shown as the mean; error bars indicate standard error.

Figure 3.9 Confocal microscopic images illustrating intestine cryosections 1 week after transplantation.

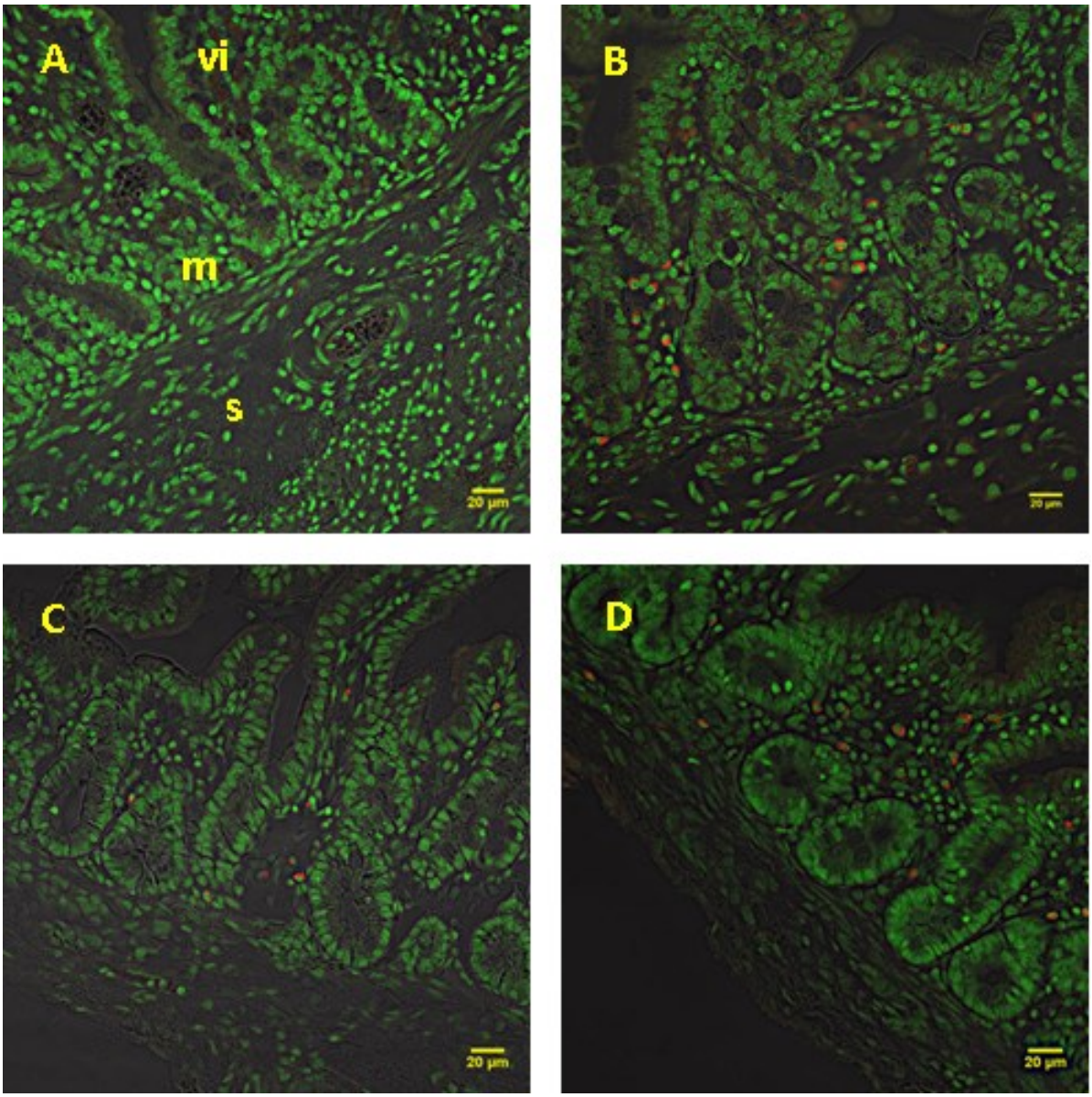

(A) Duodenum cryosection from a control (non-transplanted) pig (m: mucosal layer, s: submucosal layer and vi: villus). Cryosections from the duodenum of pigs sacrificed 1 week after transplantation of PKH26-labeled PUCs by IP injection (B). Duodenum (C) and jejunum (D) cryosections of pigs fed with PKH26 labeled PUCs before consuming colostrum. Green and red spots indicate cell nuclei labeled with the counterstain, Syto®-16, and PKH26-labeled PUCs.

Figure 3.10 Confocal microscopic images of ileal and cecal cryosections from recipients 1 week after transplantation.

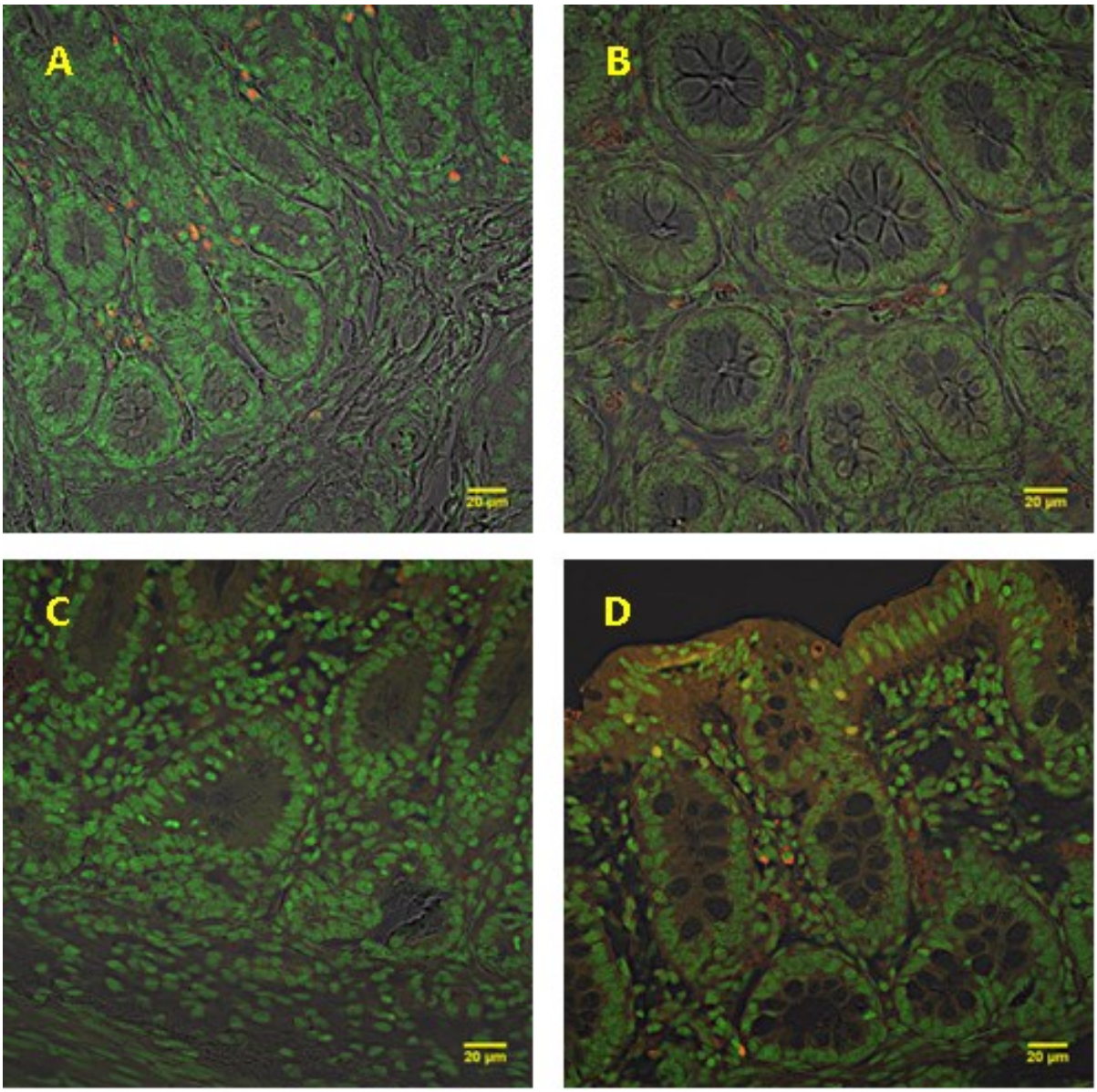

Ileum cryosection of 1-week old pig transplanted with PKH26 labeled neonatal fibroblasts at birth (A). Cross section of cecum of 1-week old pig transplanted intraperitoneally at birth with PKH26 labeled PUCs (B). Non-transplanted colon (C) and colon of 1-week old pig (D) after IP injection of PKH26 labeled PUCs at birth.

Figure 3.11 Confocal microscopic images illustrating organ cryosections of control and transplanted pigs.

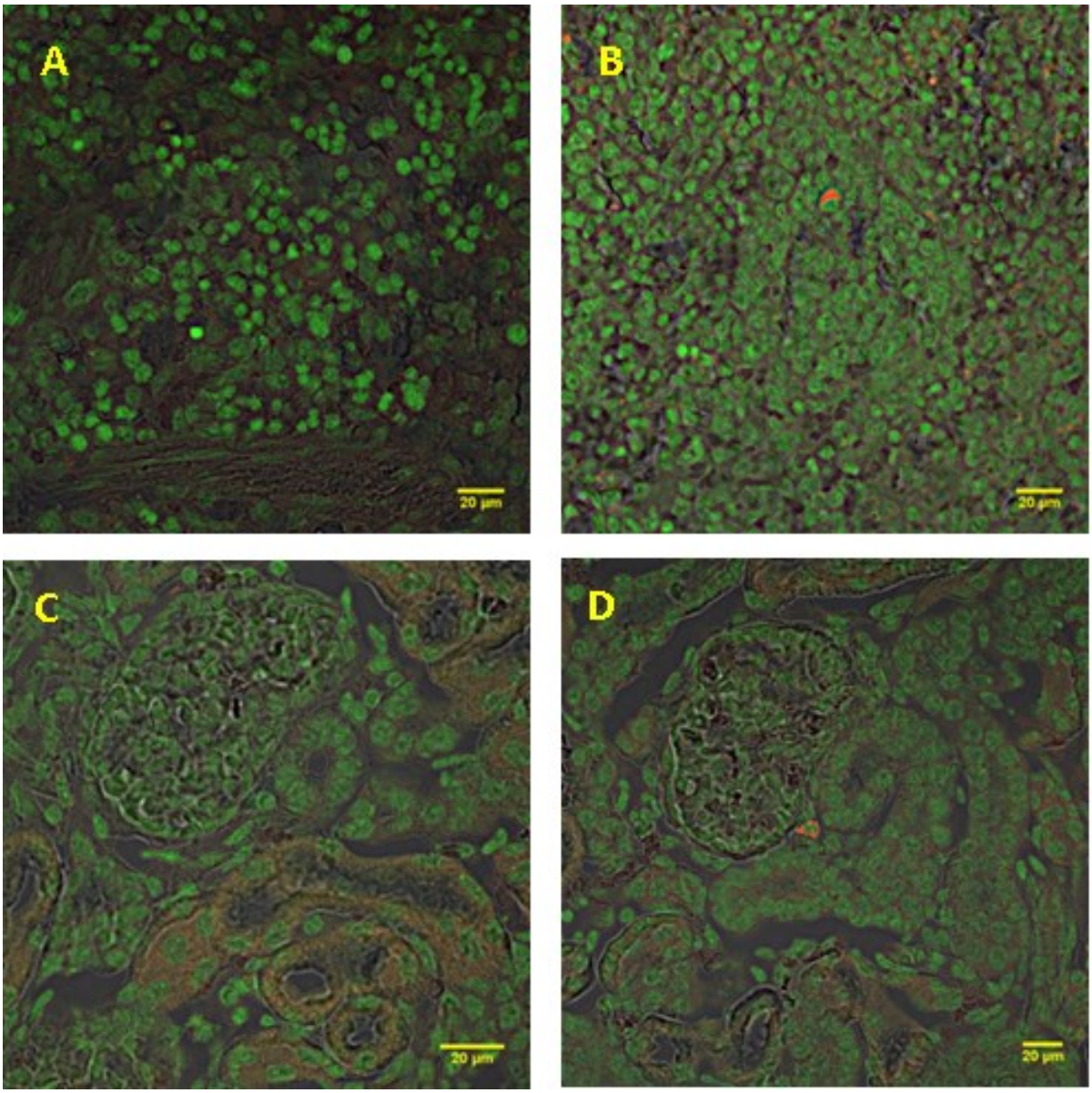

(A) Spleen cryosection of non-transplanted newborn pig recipient. (B) Spleen cryosection of newborn pig transplanted intraperitoneally with PKH26 labeled PUCs. (C) Kidney cryosection of non-transplanted newborn pig recipient. (D) Kidney cryosection of newborn pig transplanted intraperitoneally with PKH26 labeled PUCs.

Figure 3.12 Confocal microscopic images of stomach cryosections of control and transplanted pigs.

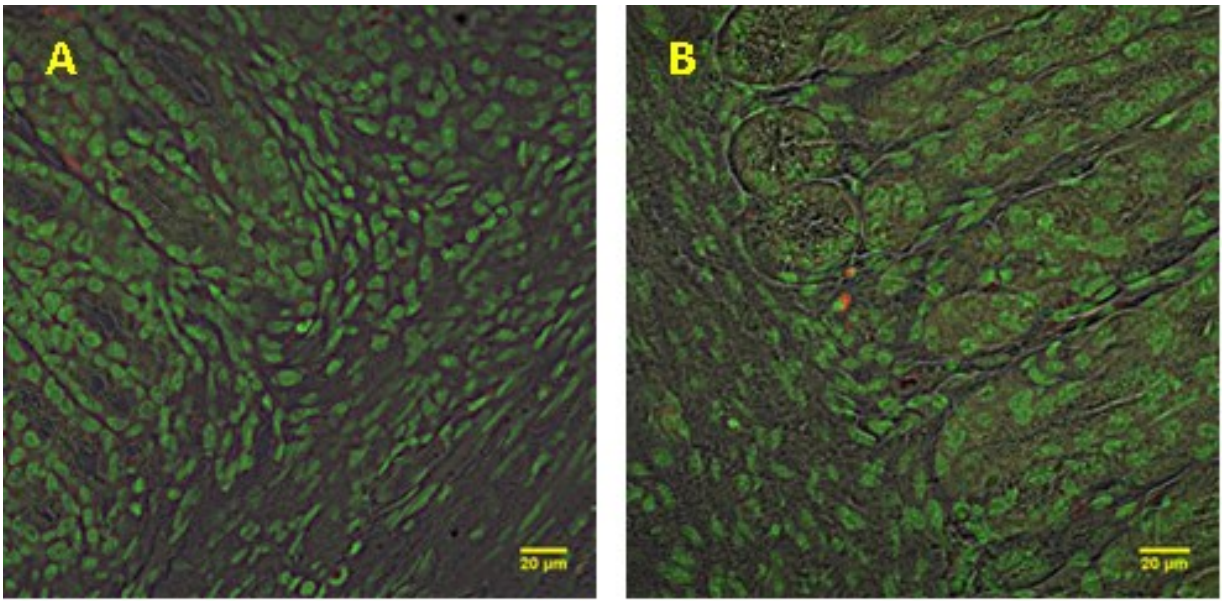

(A) Stomach cryosection of non-transplanted newborn pig recipient. (B) Stomach cryosection of a 1-week old pig transplanted intraperitoneally with PKH26 labeled PUCs at birth.

Figure 3.13 Confocal microscopic images of cultured male PUCs isolated from intestines of female recipients and detected using FISH analysis.

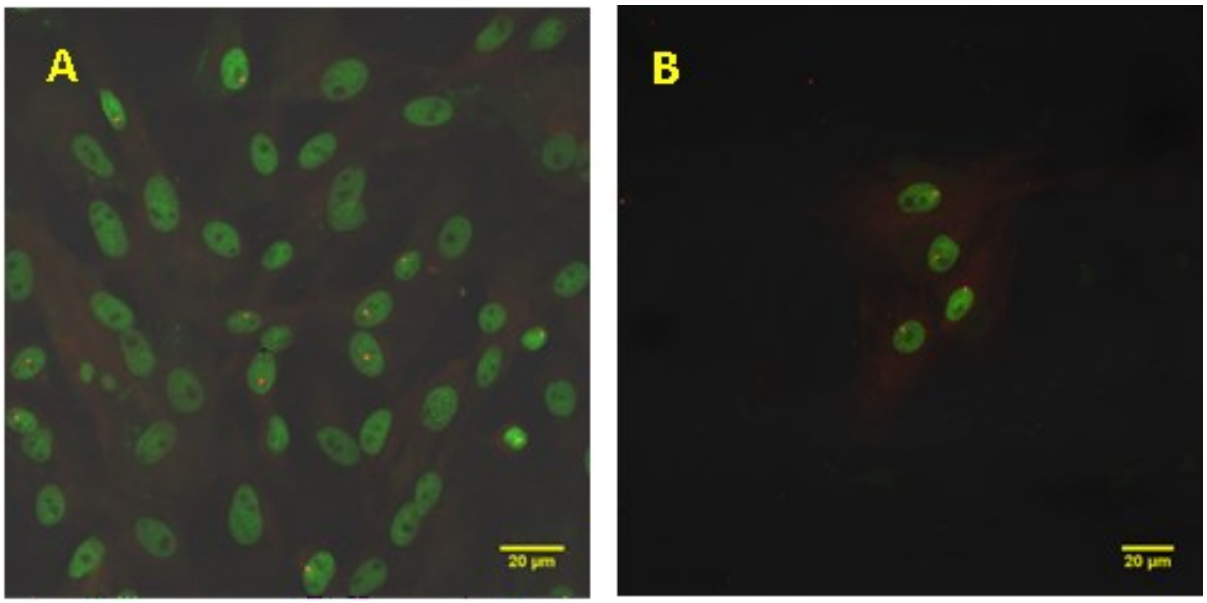

Green areas show Syto®16 staining of nuclei of enzymatically isolated intestinal cells. Re-cultured PUCs are detected with a yellow spot labeling the SRY gene on Y chromosomes; 20x magnification with 1.2x digital zoom (A). Colony formation of isolated allogeneic male PUCs was observed after re-culturing; 40x magnification with 0.6 x digital zoom (B).

Figure 3.14 PCR detection of the SRY gene of re-cultured cells derived from intestines of female recipients.

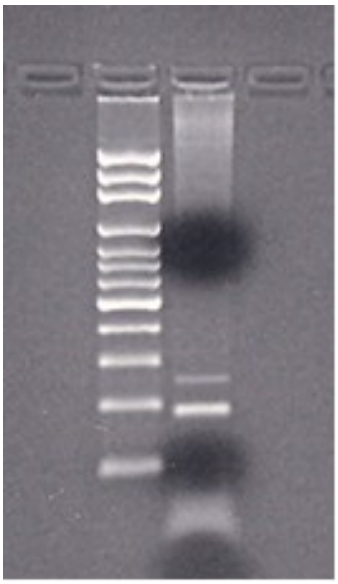

Agarose gel electrophoresis showed a PCR product of the SRY gene (247 bp) of engrafted male PUCs re-cultured from the ileum of 2-week old female porcine recipients 1 week after intraperitoneal transplantation. A lower PCR product (183 bp) is the porcine-specific beta actin gene an internal control. The left lane is a 100 bp DNA ladder.

Appendix A - Transplantation experiments

Table A.1 Number of SRY positive samples derived from organs of each newborn female recipient after intraperitoneal transplantation for 6 hours and 1 day

Collective tissues	Time after intraperitoneal injection	
	6 Hours (n=2)	1 Day (n=2)
No. of samples evaluated/organ	3	3
Organ	Samples with detected Sry DNA	
Du - Duodenum	1,1[a]	2,2
Je - Jejunum	1,2	2,2
Il - Ileum	1,1	3,2
Ce - Cecum	1,1	2,1
Co - Colon	2,0	2,2
St - Stomach	2,1	2.1
Li - Liver	1,1	2,3
Sp - Spleen	1,2	2,2
Dia - Diaphragm	3,3	3,3
Om - Omentum	3,3	3,3
Ki - Kidney	0,1	1,1
Pa - Pancreas	2,1	2,2
ML – Mesenteric lympnodes	0,1	1,1
He - Heart	1,1	1,2
Lu - Lung	1.1	1,1
BM - Bone marrow (n=2)	ND	ND
Bl - Blood (n=2)	ND	ND

ND = Not done

[a]No. of positive samples for each recipient

Table A.2 Number of SRY positive tissue samples derived from each female recipient after transplantation for 1 week.

Collective tissues	Ages of recipient female pigs at transplantation					
	Newborn		1 Day old (n=2)	1 Week old (n=2)	2 Weeks ol (n=2)	3 Weeks old (n=2)
	Oral feeding (n=2)	Intraperitoneal injection (n=2)	Intraperitoneal injection	Intraperitoneal injection	Intraperitoneal injection	Intraperitoneal injection
No. of samples evaluated/organ	4	4	4	3	3	3
Organ	Samples with detected Sry DNA					
Duodenum	4,4[a]	4,4	4,4	3,2	2,3	3,3
Jejunum	4,3	3,3	4,2	3,2	2,3	3,3
Ileum	4,4	2,4	3,4	3,3	3,3	3,3
Cecum	3,4	4,3	2,4	2,3	3,2	3,3
Colon	3,3	2,4	3,3	2,3	3,3	3,3
Esophagus	4,3	ND	ND	ND	ND	ND
St - Stomach	4,3	4,4	4,3	3,2	3,3	3,2
Li - Liver	3,4	3,3	4,2	2,3	2,3	2,2
Sp - Spleen	2,4	4,4	4,4	2,3	3,2	2,2
Om - Omentum	4,4	4,4	3,4	3,3	2,3	2,2
Ki - Kidney	2,1	2,3	2,2	2,2	2,2	2,1
Pa - Pancreas	3,3	3,4	3,4	2,3	3,2	3,2
ML – Mesenteric lymph	3,3	2,2	2.2	2,1	1,2	2,2
He - Heart	1,3	3,2	3,2	2,2	3,1	2,2
Lu - Lung	2,2	2,3	2,3	2,2	2,2	2,2
Ut - Horn of uterus	ND	ND	ND	ND	2,2	2,2
Ub - Urinary bladder	ND	ND	ND	ND	1,3	1,3
Mu - Muscle (Semimembranosus)	ND	ND	ND	ND	ND	2,2
BM - Bone marrow	2,2	3,2	2,4	2,3	2,2	2,2
Bl - Blood	0	0	0	0	0	0

ND = Not done

[a]No. of positive samples for each recipient

Table A.3 Number of re-cultured cell samples isolated from small intestines of female porcine recipients positive to SRY gene after transplantation for 1 week.

Detection methods	Ages of recipient female pigs at transplantation					
	Newborn (n=2)		1 Day old (n=2)	1 Week old (n=2)	2 Week old (n=2)	3 Week old (n=2)
	Oral feeding	Intraperitoneal injection	Intraperitoneal injection	Intraperitoneal injection	Intraperitoneal injection	Intraperitoneal injection
Samples with detected Sry DNA						
PCR	1,1[a]	1,1	1,1	1,1	1,1	1,1
Samples with detected Sry probes						
Fluorescent *in situ* hybridization (FISH)	1,1	1,1	ND	1,Cont	1,1	1,1

Cont = Microbial contamination

ND = Not done

[a]No. of positive samples for each recipient

Table A.4 Details of the transplantation experiments[a]

Transplantation /recipient	Pig number	Dye/donor cells	Collected tissues performed by detection methods	Detection methods	Transplantation time	Collected Tissues/ organ
Oral/pre-nursed newborn pig	N=2	PKH26/PUCs	Organs/Blood	CM/FC	1 week	N=4
	N=2	NIR815/PUCs	Organs, Blood, BM/Intestine	PCR/(PCR&FISH)		N=4
Oral/nursed newborn pig	N=2	PKH26/PUCs	Organs/blood	CM/FC	1 week	N=4
IP/newborn pig	N=2	PKH26/PUCs	Organs/blood	CM/FC	1 week	N=4
	N=2	NIR815/PUCs	Organs, Blood, BM/Intestine	PCR/(PCR&FISH)	1 week	N=4
IP/newborn pig	N=2	PKH26/ FIBs	Organs/Blood	CM/FC	1 week	N=4
IP/newborn pig	N=2	PKH26/PUCs	Organs/Blood	PCR/FC	6hr	N=3
IP/newborn pig	N=2	PKH26/PUCs	Organs/Blood	PCR/FC	24hr	N=3
IP/1-day pig	N=2	PKH26/PUCs	Organ,BM,Blood/Blood/Organs/intestine	PCR/FC/CM/PCR	1 week	N=4
IP/1week pig	N=2	NIR815/PUCs	Organs, Blood, BM/Intestine	PCR/PCR&FISH	1 week	N=3
IP/2week pig	N=2	NIR815/PUCs	Organs, Blood, BM/Intestine	PCR/PCR&FISH	1 week	N=3
IP/3week pig	N=2	NIR815/PUCs	Organs, Blood, BM/Intestine	PCR/PCR&FISH	1 week	N=3

[a]Abbreviation: BM: Bone marrow, CM: Confocal microscopy, FC: Flow cytometry, FISH: Fluorescent in situ hybridization